1-1-2012

Hyperbranched And Polydimethylsiloxane Based Membranes For CO2 Capture

Willie Wesley Wells

HYPERBRANCHED AND POLYDIMETHYLSILOXANE BASED MEMBRANES FOR CO_2 CAPTURE

by

Willie Wesley Wells
Bachelors of Science, San Jose State University, 2009

A Thesis
Submitted to the Graduate Faculty

Of the

University of North Dakota

In partial fulfillment of the requirements

For the degree of

Master of Science

Grand Forks, North Dakota
December
2012

This thesis, submitted by Willie Wesley Wells in partial fulfillment of the requirements for the Degree of Master of Science from the University of North Dakota, has been read by the Faculty Advisory Committee under whom the work has been done and is hereby approved.

_____
Brian Tande

_____
Steven Benson

_____
Edward Kolodka

This thesis meets the standards for appearance, conforms to the style and format requirements of the Graduate School of the University of North Dakota, and is hereby approved.

_____
Wayne Swisher
Dean of the Graduate School

_____
November 29, 2012

PERMISSION

Title Hyperbranched and Polydimethylsiloxane based membranes for CO_2 capture

Department Chemical Engineering

Degree Master of Science

In presenting this thesis in partial fulfillment of the requirements for a graduate degree from the University of North Dakota, I agree that the library of this University shall make it freely available for inspection. I further agree that permission for extensive copying for scholarly purposes may be granted by the professor who supervised my thesis work or, in his absence, by the chairperson of the department or the dean of the Graduate School. It is understood that any copying or publication or other use of this thesis or part thereof for financial gain shall not be allowed without my written permission. It is also understood that due recognition shall be given to me and to the University of North Dakota in any scholarly use which may be made of any material in my thesis.

Willie Wesley Wells
November 29, 2012

TABLE OF CONTENTS

LIST OF FIGURES

Table Page

LIST OF TABLES

Table Page

ACKNOWLEDGEMENTS

I am forever grateful to the Department of Chemical Engineering at UND for the opportunity to conduct this research. First and foremost a special thanks to my advisor Dr. Brian Tande. It has truly been a privilege to learn from him and grow from his wisdom these past years. I appreciated all of his input, ideas, jokes, words of encouragement and funding which has allowed me to conduct and complete my research. I am also grateful to my research committee members, Dr. Steven Benson and Dr. Edward Kolodka for their guidance in reviewing my thesis.

I would also like to take the time to thank my group members Zain Abbas, Xuefei Zhang, Tom Hilpisch and Alireza Pesaran for offering input and collaboration throughout the project. A special thanks to Sarita Kolhatkar, Robert Mota and Adam Garret-Clark for helping me during the final stretch of completing this document.

I would also like to thank North Dakota State University (NDSU) in particular Dean Webster and Jon Netfield for providing me with test samples to carry out parts of my research. I would also like to thank Mr. David Hirschmann, Mr. Joe Miller, Mr. Dennis Sisq and Mr. Harry Feilen for helping me with the experimental setup because the research would have been inconceivable without all their efforts.

This degree would definitely not be possible without the love, encouragement and spirit I receive daily from my dad, Willie Clifford Wells and mother, Valarie Denise

Dandridge. They have been my strength, life and motivation to make it and continue striving to become greater. A special thanks goes to my sister, Lashawnda Rhonda Wells, and all my nieces and nephews who I love very much. A very special thank you goes to Mike Hopperstad and the Hopperstad family which has treated me with much love and kindness during my adventures here in the Midwest. Thank You.

ABSTRACT

As we continue to come to terms with a warming planet created, in part, by our dependence on fossil fueled power plants, there is a great and urgent need for cost effective methods of isolating and capturing greenhouse gasses. Among the many methods currently being explored for CO_2 separation, membranes have proven to be a promising solution. This thesis examines three types of possible membranes: composite layer membranes, hyperbranched membranes and dense film membranes. In addition to examining the permeance of each type, the study explored various membrane formation techniques and how that affects the permeability of specific membrane types.

The results showed that solvent selection and polymer/solvent contact angle has the greatest effect of creating thin film layers in composite layer membranes. Also hyperbranched polymers included in a membrane matrix increased permeability. Lastly sol-gel coating of polymers has led to increased permeability in membranes.

CHAPTER I

INTRODUCTION

The future of the world's energy production is dependent upon developing new technologies to prevent CO_2 emissions from continuing to cause harm to the environment. Post combustion CO_2 capture technologies are the easiest to retrofit to current power plants in operation, but the problem with these prevailing technologies is that they require large amounts of energy.

Polymer based membranes for CO_2 separation hold an advantage over its counterparts because of its low energy requirements. Membranes have lower energy cost compared to other technologies and also have lower maintenance costs.

To use polymer membranes as an effective form of CO_2 separation the membranes must be thermally, chemically and mechanically stable under various conditions. This thesis examines various membranes in different setups to understand their potential for CO_2 separation.

Membranes are used as a selective barrier to isolate chemicals within a liquid or gas solution [1]. Membrane filtering techniques have progressed from simple designs using animal bladders to polymer composite membranes made in facilities that can control a wide range of factors in proper membrane design.

In the U.S. alone, the industry has grown and continues to show significant signs of growth for years to come. The combined U.S. market for membranes used for liquid and gas separation is estimated at $1.7 billion in 2010 and is forecast to grow at a compound annual growth rate of 6.9% during a five year forecast from 2010 to 2015 to reach 2.3 billion [2]. These figures suggest a trend that would benefit from further study and research in the field.

My research involved the design and operation of an apparatus to measure the gas permeation of carbon dioxide (CO_2) through three types of membranes: hyperbranched polymer membranes (HBP), composite polydimethylsiloxane membranes (PDMS) and 3-methacryloxypropyltrimethoxysilane cross-linked membranes (3-MPS) also called dense film membranes.

The HBP membranes were studied using a mass spectrometer (MS). The 3-MPS membranes and PDMS membranes were examined by the use of a gas chromatograph (GC). The PDMS membranes were also analyzed by a CO_2 analyzer to monitor the CO_2 flux during the pervaporation process.

Chapter 2 gives a brief background on carbon capture and separation technologies, membrane science, gas permeation, pervaporation, HBPs and discussion of the various methods that have been developed to separate CO_2 from flue gas streams using membranes and solvent solutions.

Chapter 3 describes a study of PDMS membranes. Currently, the majority of CO_2 capture methods use a chemical absorption process with monoethanolamine (MEA) as a solvent. This process allows flue gas to have contact with an MEA solution in an absorber. The MEA selectively absorbs CO_2 and is then sent to a stripper. In the stripper, CO_2-rich solvent is heated to release almost pure CO_2 and the lean MEA solution is recycled back to the absorber. Challenges to this technology include heating costs related to releasing the CO_2 from the CO_2-rich solvent and large equipment requirements for the stripping process.

My research aims to reduce the challenges associated with this technology by replacing the stripper column with a membrane separation process. By using composite membranes that consists of a thin film selective layer supported by a porous substrate the aim is to lower the energy penalties, increase the contact area with smaller equipment and lower the operation and capital cost to the facility. This research began by investigating potential porous supports and attempting to cast PDMS thin films on the porous supports. Effects of thickness of the PDMS layer on various substrates were examined in these membranes. The membranes were created then characterized by SEM imaging performed at NDSU and ran in an experimental setup where the CO_2 flux was monitored in different setups. The setups used gas separation and pervaporation systems to analyze CO_2 flux behavior. Steady state behavior was observed and recorded for each system.

Chapters 4 and 5 include work done in partnership with North Dakota State University (NDSU). This work consisted of investigating the behavior of polymers blended with HBPs and silane groups to determine how these changes affect CO_2 permeability in an ideal gas separation system. The regulation of greenhouse gases in power-plants requires equipment that can be retrofitted to existing plants or built into new plants with 90% capture of CO_2. Membranes in post-combustion processes have the potential to be a viable technology for CO_2 separation, but detailed investigation into potential membrane materials is required to develop the best membranes for these processes. The research in chapter 4 and 5 looks at different membrane materials and casting methods to evaluate their permeability to CO_2.The membranes were created at NDSU and tested at UND. The flux of CO_2 was analyzed through MS or a GC setup and compared for different series of membranes.

The appendices include detailed information about experimental setups, calculation and analysis. Appendix A includes sample permeability calculations; appendix B provides procedure examples for use of the mass spectrometer. Appendices C and D provides data used for hyperbranched polymer study in chapter 3 and gas separation SEM images for all tested membranes in chapter 4. Appendices E and F contain results from the pervaporation study and SEM images from pervaporation study in chapter 4 followed by the references.

CHAPTER II

BACKGROUND

Introduction

For many years, politicians and scientists have discussed whether humans and manmade processes have an effect on the earth's climate system, but the debate has nearly come to an end. The topic has left the category of debate and entered the realm of fact. The first eight months of 2012 have been the hottest of any year on record, with this summer being the 3rd hottest summer ever recorded in the history of the United States. Since July of 2011 temperatures have been above average which is something that has not happened in the last 117 years of U.S. record [3]. Other changes have also been witnessed including; bleaching of coral reefs [3,4], increased hurricane intensity [3,4], and many animal species facing extinction, all because of a specific change to the atmosphere. The primary cause of all of these drastic changes is the emission of greenhouse gases (GHG) primarily carbon dioxide into the atmosphere when fossil fuels are burned. However, the burning of fossil fuels has become the cornerstone of modern society. Almost every process, including food production, consumer goods production, transportation and water purification, relies, in some way, on the use of burning fossil fuels.

Though we depend heavily on fossil fuels, the consequences of using these fuel sources are becoming too difficult to ignore. This has led to many governments implementing programs to limit CO_2 emissions and internationally nations are working together to form agreements that would curtail emissions worldwide. There are multiple options being explored to reduce emissions and this paper will review new methods and test some of the methods which will have the largest impact.

Carbon Capture Methods

Since fossil fuel combustion from point sources such as power plants account for over 60% of greenhouse gas emissions, it is the ideal place to investigate methods to reduce CO_2 emissions. This problem has been divided into two major parts, CO_2 capture and CO_2 separation. Many different methods have been developed and continue to be studied for capture including pre-combustion, post combustion and oxy combustion methods. For post combustion methods, solvent absorptions, solid sorbent, membranes and cryogenic distillations have been the most heavily researched methods for reducing emissions. With regards to membranes technology, carbon capture could be the new frontier.

Before understanding the added benefits of membrane technology a review of current CO_2 capture and separation processes is required. Since coal-fired power plants emit over 2 billion tons of CO_2 each year they are the main sources scientists focus on for carbon capture according to the Department of Energy (DOE) [5, 6]. Current strategies being tested for use with these facilities include oxy-fuel combustion, pre-

combustion and post combustion capture. Oxy-fuel combustion takes place when coal is burned with pure oxygen instead of air. This combustion process produces a relatively pure stream of CO_2 and water with very low amounts of nitrogen [6]. This flue gas stream can be further cooled allowing for separation of CO_2 and water and also scrubbed to remove trace elements such as dust, sulfur oxides and nitrogen oxides leaving a relatively pure CO_2 stream [6, 7]. This method shows extreme promise due to the benefits of not requiring solvents, having small equipment size, and the fact that the process incorporates commonly used technologies and processes. Challenges still remain in the fact that separation of air into pure oxygen and CO_2 scrubbing raise plant energy costs immensely, high CO_2 purity also raise plant costs and the process has limited operational flexibility. A 1MW oxy-fuel test unit is already in place at the E.ON United Kingdom Ratcliffe power station in central England [6]. Test trials have shown that the unit can simulate the combustion process under real operating conditions. Next stages include installing the unit in larger pilot plants to refine the technology to make it more viable. Current methods to create pure oxygen are from cryogenic air separation. As stated before, this process requires lots of energy and will need to be replaced for commercial use, but research in membrane technology is currently being conducted and holds promise to become a more efficient way to produce pure oxygen [5].

Pre-combustion CO_2 separation takes place by converting fuel streams into a mixture of hydrogen and carbon monoxide using various methods which depend on the composition of the fuel stream and power plant setup. The method by which this conversion reaction takes place includes partial oxidation or steam reformation. Partial

oxidation is a sub-stoichiometric chemical reaction of a fuel-air mixture which is partially combusted in a reformer. Steam reforming takes place by a similar reaction where steam reacts with the fuel gas performing an endothermic reaction creating carbon monoxide and hydrogen which can then undergo another low temperature gas-shift reaction with the carbon monoxide produced from the first reaction creating carbon dioxide and more hydrogen which can then be separated [5, 7, 8]. The second reaction is mildly exothermic so this process is not ideal for power plants, but it is better suited for the production of hydrogen which can be used as a fuel source for fuel cells.

Of the three locations mentioned to implement CO_2 separation technology in a power plant, the last stop, post-combustion capture, has the most challenges associated with it. However, it is the most applicable to coal fire powered plants and is the focus of the study in this thesis due to its ease of being able to retrofit new technology onto existing plants. Again, this method separates CO_2 from the flue gas after the combustion process [7].

Separation is accomplished by absorption, adsorption or cryogenic separation in post-combustion capture. Adsorption takes place by using an amine based solution typically aqueous monethanolamine(MEA) to absorb CO_2 from flue gas into the solvent stream [9,10]. The stream is then moved to a desorber where the CO_2 is separated and the lean solvent is recycled back to the absorber. CO_2 adsorption is a process which is still being developed. Pressure swing adsorption is a process by which CO_2 is absorbed on a porous material at high pressure, and then the CO_2 is released from the material on

a lower pressure side with the porous material being recycled back for continued adsorption. Students at the University of Queensland in Queensland Australia have tested this process using calcium based sorbents which were carbonated then calcinated for the pressure swing absorption process [11]. Their results showed challenges with loss of capacity in the sorbents and unmatched reaction rates of chemical-controlled carbonation and calcination, but promising results were found for specific sorbents which proves this technology as a low cost strategy for CO_2 separation.

The Cryogenic CO_2 capture (CCC) process is a relatively new technology that has only recently been introduced as a source for carbon capture and storage. This process involves the drying and cooling of flue gas to temperatures slightly above the point where CO_2 solidifies, its then compressed and expanded to further cool it and precipitate out CO_2 as a solid [12, 13]. The CO_2 is then depressurized and reheated while the flue gas is cooled, thus leaving a CO_2 liquid phase and a gaseous nitrogen stream. The main benefits from this technology are that it operates relatively close to atmospheric pressure and there is no use of chemical solvents. Key challenges include specifying the requirement of feed streams, restricting water levels to prevent plugging by ice and large increases in pressure during operation. These challenges lead to increased costs for water removal and have so far left this technology only viable for the treatment of large flue gas streams.

More innovative attempts to perfect CO_2 capture have emerged through the use of hybrid technologies. Hybrid technologies merge two or more types of CO_2 capture

technologies to enhance the advantages of the combined technologies while reducing the challenges associated with each of the individual technologies. A prime example of this method includes research taking place at UND. Xuefei Zhang UND Ph.D. research student has combined absorption techniques using chemical solvents with the desorption method of a composite membrane. The purpose of his project is to evaluate the use of composite polymer membranes and porous membrane contactors for the recovery of CO_2 from CO_2-rich solvent streams. The bench scale system has been successfully created and calibrated followed by testing simple substrates. More tests have begun with composite polymer membranes and soon tests will begin with porous membrane contactors [10]. Another hybrid technology being tested at UND is headed by another PH.D student at UND Ali Alireza where he is attempting to combine the benefits of physical absorption with composite polymer membranes to reduce the heating cost associated with desorption of CO_2 [14]. Since physical solvents are predicted by solubility which is a function of Henry's Law, we know that the capacity of a physical solvent is the direct effect of the partial pressure (from Henry's law) which is a major advantage over chemical solvents. This process is still in its early phases, but the bench scale setup has already been created and calibrated and tests have begun with basic composite membranes with further studies planned.

Membranes for Carbon Capture

Due to the many challenges involved with the various possible technologies, CO_2 separation membranes have become a source of great interest for CO_2 separation. Membranes are viable for CO_2 separation because of their low cost for separation.

Like all technologies thus far, membranes still have challenges which need to be resolved before they can be implemented in post combustion capture. High temperatures of flue gases have the potential to destroy the membranes which means flue gas streams need to be cooled to temperatures below 100°C prior to separation. Also various compounds found in flue gases, such as nitrous oxide, sulfur dioxide and halogens, run the risk of destroying the membranes. These compounds either need to be removed from the flue gas or the membrane must be made chemically resistant to them. Lastly since membrane separation is driven by pressure changes, power will be required to maintain the pressure driven flow which will lower a plants overall energy efficiency. Furthermore, due to various coal and natural gas composition from different fuel sources around the world, specifications will need to be made depending on the fuel source, power plant, and prior flue gas treatment methods.

Though there are many factors affecting the design of a proper membrane, fundamental specifications have been defined for the development of useful membranes [15, 16]. For a membrane to be viable for CO_2 separation it should have high CO_2 permeability, high carbon dioxide/nitrogen selectivity, be chemically and thermally resistant, resistant to plasticization, resistant to aging, cost effective and

cheaply manufactured. Of the materials fitting this description polyimides are a class of polymer with the largest volume of research. Due to their thermal and chemical stability and ease of membrane formation they have become of extreme interest for CO_2 separation. Polyimides which show the highest CO_2 permeability and CO_2/N_2 selectivity are polyimides containing the 6FDA functional group [16, 17, 18]. The 6FDA functional group is shown in figure 1. The increases in permeability and selectivity are due to the CF_3 group increasing the stiffness of the chains which allow for better separation on the basis of steric bulk and reduced chain packing which lead to increased permeability. Other strong electronegative halogens have also shown similar effects on polyimides. Polyimides which have been functionalized by bromination have led to membranes with increased CO_2 permeability and CO_2/N_2 selectivity [35].

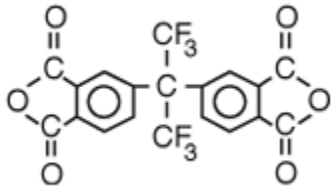

Figure 1: 6FDA Functional Group

Facilitated transport membranes are another type of membrane with potential for this application. They are composed of carrier's usually metal ions with an affinity to CO_2 which allows for control of CO_2 transport. Membranes of these types have been researched by Kovvali and Sirkar Ph.D. students at the New Jersey Institute of Technology discovered excellent CO_2/N_2 selectivity for immobilized liquid poly(amindoamine) (PAMAM) dendrimer membranes [19]. The membranes tested

showed good selectivity in the presence of water, but were unable to handle large pressure swings or very large gas fluxes. These challenges inspired them to create PAMAM composite membranes which continued to yield excellent selectivity and meet conditions required for IGCC application, but improvement on their mechanical properties and CO_2 separation capabilities are still required [20, 21].

Another type of membrane with practical application to CO_2 separation is mixed matrix membranes. These membranes are made from inorganic materials based on micro or nano-particles built into the polymer matrix [22, 23, 24]. This allows for the membrane to be formed from two different materials with different permeability and selectivity which lead to better design for CO_2 capture. The addition of inorganic materials allows for improved physical, thermal and mechanical properties ideal for dealing with aggressive chemicals. Challenges associated with these types of membranes include cost, commercial scale manufacturing and brittleness. Koros an engineering student at the University of Texas developed criteria for material selection and preparation of these types of membranes, but much more research is required [24].

Finally, poly(ethylene oxide) (PEO) membranes are of extreme interest for CO_2 separation due to the polymer chains' strong affinity to CO_2 molecules in the presence of polar ether oxygen[25, 26]. Many challenges still prevent this technology from being implemented into IGCC systems. Initial challenges begin with membrane formation, due to PEO's tendency to crystalize [26]. Proper membranes have been difficult and costly to fabricate. Techniques such as using low molecular weight PEOs, using block copolymers with ethylene oxide segments too short for crystallization or using highly branched PEOs

have helped reduce crystalinity, but testing still remains only at the lab scale. An example of these lab scale tests include studies done by Nijimeijer a research student at the Impact Institute of Energy and Resources investigated the behavior of hydrophilic, highly permeable PEO based block copolymer composite membranes for the removal of water vapor from nitrogen [27]. His results showed that the CO_2 interaction with the polar ether linkages in the PEO membranes led to these membranes having good potential for CO_2 capture.

Though many types of membranes are being developed for CO_2 capture, not many studies have looked at membranes that are commercially available for CO_2 separation. Favre and colleagues conducted a study comparing commercially available polymeric dense membranes against amine absorption in post combustion capture [28]. His studies show that the energy requirement for CO_2 separation in membrane systems was a function of the CO_2 concentration in the flue gas streams. Flue gases with 10% CO_2 concentration had an energy consumption rate larger than that for anime separation, but for the flue gas with 20% CO_2 concentration the energy consumption was much less than absorption. Other results concluded that the use of a vacuum on the permeate side reduced energy requirements considerably. Another study on making commercial membranes viable for gas separation was conducted by R.W. Baker where he proposed an integrated multistage (3) solution for the separation of a 13% CO_2 flue gas stream which performed very well [29]. The wealth of these studies show that either through creating membranes for CO_2 capture, or through using commercial grade

membranes, there remains a lot of potential for CO_2 capture using membrane processes.

Another comparison of membrane separation with amine separation was performed at Laboratoire des Sciences du Genie Chimique where energy consumption, among other factors, was compared to that of the most proven and used technology which is amine absorption. Their research showed that membrane systems use a lot less energy (3.5 – 5 GJ/ ton CO_2 recovered) than its proven counterpart [30]. With the use of membranes, energy cost would reduce a great deal, but there is no type of membrane which could get the separation, which is required by most government standards. A membrane with the potential to solve this problem is micro porous organic polymers (MOPS). Research conducted at the Institute of Chemical Process and Environmental Technology in Ottawa Ontario Canada has shown that MOPS membranes created from cycloaddition modification allowed for membranes with excellent CO_2 separation due to the introduction of tetrazole groups into the membrane's framework [31]. As you can see, there is a lot of work being done in this field which could become the industry standard for CO_2 separation. Students at the Laboratoire des Sciences du Genie Chimique performed a parameter study to compare the membrane process to the amine absorption process. Choosing the right membrane-solvent combination is very critical and a key first step in developing membrane gas absorption processes [32]. Now that a general explanation of different carbon captures technologies has been explained we will dive deeper into membrane technology and how it has evolved over the past century.

Membrane History

Originally developed as an analytical tool in chemical and biomedical laboratories, membranes and membrane technologies have quickly developed into products, which have had considerable commercial impact [33]. The earliest recorded study of membrane phenomenon was conducted by a French cleric named J. Abbe Nollet in 1748. Nollet discovered the process of osmosis by permeating water molecules though a diaphragm [34]. Nearly a century later, work continued on the study of osmosis using membranes made from animal and plant materials. It wasn't until 1855 when the next major breakthrough occurred. Thomas Graham isolated bacteria and colloids from crystalloids and became the first to use the term dialysis [35]. Working with Mr. Graham at the time was Aldof Fick who is credited for performing dialysis of solutions made from collodion during that same year. Fick was also credited for creating the first synthetic membrane in 1865 from nitrocellulose. A year later these men worked together to perform the first gas separation through a synthetic rubber membrane in 1867 [36]. The theory of osmosis wasn't explained until 1877 by Gibbs Ivan Hoff when he used osmotic pressure measurements to develop his "Limit Law" which eventually developed into Van't Hoff equations[1, 37]. Van't Hoff's equation relates the change in temperature (T) to the change in equilibrium constant (K) given the standard enthalpy (ΔH) and is shown below as equation 1.

$$\frac{dLnK}{dT} = \frac{\Delta H}{RT^2} \qquad 1)$$

The study of membrane technology became of high interest during this era as new findings on dialysis, reverse osmosis and electrodialysis were published frequently [38]. Even more notable were the advancements in the study of synthetic polymers. The first commercially available successful synthetic polymer was phenol-formaldehyde made by Arthur Smith in 1899 [39]. The first gas separation from silicon rubber was performed by Karl Kammermeyer in 1957 [40]. The first composite layer membrane was developed in 1960 by HK Lonsdale [41].

It wasn't until 1962 when Loeb I Surirayan prepared the first asymmetric membrane that the study of membranes took flight. This discovery was very significant because it was the first membrane that could properly be used in an industrial facility. In addition, these membranes were defect-free, they had a high flux and had stronger mechanical properties compared to commercially available membranes of the time. Another improvement he implemented with these membranes was membrane pore manipulation. It was the first generation of membranes where one could control the size of pores inside the membranes. Expansion of these methods would lead to the development of interfacial polymerization, multilayer composite casting and coated membranes [42]. Through these major developments and many others, membrane separation has been applied to microfiltration, ultrafiltration nanofiltration, reverse osmosis, gas separations and pervaporation, dialysis, osmosis electro dialysis and even membrane distillation. There are still many unexplored areas where membrane technology could someday be of great service.

Among the developing applications in which membrane technology can be applied is the replacement of a stripper in the CO_2 capture process, which would involve solvent regeneration by the use of an absorber and a stripper column. Stripper replacement has the potential to lead to lower capital costs, lower energy requirements and a wider operating range. Membranes even have practical applications in developing technologies such as the use of bio-ethanol as a fuel source. The use of an internal membrane separation unit in a pervaporation-bioreactor hybrid process could lead to higher efficiencies, easier operation and potential increases in microorganism productivity in a side stream membrane unit while submerged membrane units could benefit from no extra internal circulation in the reactor and simpler operating conditions [44]. With more research and understanding of membrane systems and applications these units could have applications in systems we never thought possible. To understand their behavior in various systems we must understand the driving forces which make this technology possible.

Gas Permeation

When performing a study on the behavior of membranes there are important factors to be considered. One of the most basic factors is gas permeation. Permeation in our case is defined as the penetration of a permeate stream (the gas CO_2) through a membrane and a measure of the rate of permeation is known as the permeability. Permeation through a polymeric film exhibits behavior which follows the solution-diffusion model [44]. The solution diffusion model can be used for reverse osmosis, gas separation and pervaporation systems.

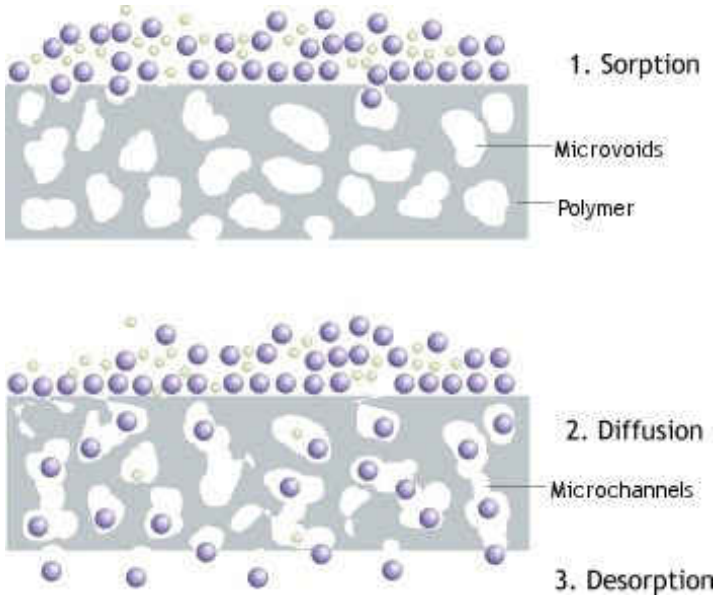

Figure 2: Solution Diffusion Mechanism [46]

Thomas Graham originally developed this method when he observed the inflation of a pig's bladder with CO_2 during the late 1870's [45]. In his study, he learned how the permeate moves through a membrane. First the permeate dissolves into the membrane material as shown in step 1 of figure 2. Then solution diffuses through micro channels in the membrane following a concentration gradient as shown in step 2. And lastly gas phase components are desorbed on the retenate side of the membrane (step 3) and leave the system. Graham concluded from his experiment that the transport of components through a membrane depend on the rate at which the permeate dissolves into the membrane material and the rate at which they diffuse through. He learned that the driving forces for flow are either a pressure or concentration gradient or some function of both. Other factors to consider include the solubility, chemical potential and or diffusivity of the membrane because changes in these factors can enhance or inhibit membrane permeability considerably.

The solution diffusion model described in step 2 of Figure 2, the diffusion of molecules, is a mechanism which drives permeability and is determined by an array of factors. Diffusion is a function of the diffusing component and the polymer. What affects the diffusing component is the size of the diffusing molecules polarity, temperature, state of diffusing molecule, and pore size of the polymer, type of polymer, its structure and its thickness [44]. Though all 4 components have effects on diffusion, some have more of an impact than others. Molecular size and temperature are relatively easy to control and typically remain constant, but the polymer pore size and thickness can vary greatly depending on if the polymer is above or below its glass transition temperature ($T_{g.}$). The glass transition temperature is the lowest temperature a polymer can withstand before the polymer transitions into a glass-like structure, becoming hard and brittle [47]. Different polymers are used above and below their T_g. A rubber like polyisoprene is used below its Tg. Rubber has many uses but mainly to form tires. Rubber polymers are usually irreversibly cured as thermosets before use in most applications. The PDMS used in my study went through this process so that it could be used for CO_2 separation

The overall equation to describe diffusion was derived by Adolf Fick in 1855. His first law creates a relation between the diffusion flux (J) and concentration(C) of substance in the system as it passes through the membrane assuming steady state. This law further stated that concentration follows by gradient through the membrane from a high side to a low side in each of the axial planes. Equation 2 is a one planar example of

Fick's equation. It assumes flow takes place in one direction and x is the total length of the membrane**.**

$$J = -D\frac{\partial C}{\partial x} \quad (2)$$

After integrating equation 2 it reduces to equation 3:

$$J = \frac{-D_x}{1-f}\left(\frac{c_2 - c_1}{x_2 - x_1}\right) \quad (3)$$

Where, J is the mass flux or movement of an object from one point to another in units of moles/(time*area) f is the mass fraction of gas in the polymer and D_x is the binary mutual diffusion coefficient describing the speed at which the object diffuses in units of area/time. Integrating across the membrane from 0 to the total length of the membrane yields equation 4:

$$J = \frac{1}{l}\int_{c_1}^{c_2} \frac{D_x}{1-f} * dC \quad (4)$$

Since the system is at a steady state then the external concentrations are at equilibrium with the external pressures yielding equation 5:

$$N = \frac{c_2 - c_1}{l} D \quad (5)$$

Where D is the average diffusion coefficient, which is defined in equation 6 as:

$$D = \frac{1}{c_2 - c_1} \int_{c_1}^{c_2} \frac{D_x}{1 - f} * dC \qquad 6)$$

This then allows for us to define a permeability equation as seen in equation 7:

$$P = \left(\frac{c_2 - c_1}{p_{2-}p_1}\right) D \qquad 7)$$

For our case of a binary mixture p_2 and p_1 are replaced with the partial pressure of the respected gases. Also the concentration of c_1 is practically zero thus reducing our equation to:

$$P = \frac{c_2}{p_2} D \qquad 8)$$

Since it has become a binary mixture the behavior inside the membrane has changed and a solubility coefficient must be added. This coefficient is the ratio of gas dissolved at equilibrium to partial pressure on the low-pressure side in equation 4:

$$S = \frac{C}{P} \qquad 9)$$

When we assume that concentration has no effect of diffusivity and solubility and it is also at a steady state one ends up with the equations defined by Wroblewski as:

$$J = D * S * \Delta P \qquad 10)$$

Where ΔP is the pressure gradient across the membrane. Through some simple changes for the setup design we have in the lab this equation is converted to equation 11:

$$J_A = \frac{F_t y_{t,A}}{\rho_A A} = P_A \frac{\Delta p_A}{t_{ms}} \qquad 11)$$

Where J_A is the volumetric flux of A, F_t is the molar transfer rate of gas, y_{ta} is the mole fraction of A in the permeate, ρ_A is the molar density of solute, A represents the membrane area available for transfer, P_A is the permeability of species A, Δp_A is the pressure change across the membrane chamber and t_{ms} is the membrane thickness. Rearranging and solving for permeability yields equation 12:

$$\mathrm{P_A} = \frac{t_{ms} * \left(\frac{V * \%C_F * A}{\%N_{2\,F}} - \frac{V * \%C_I * A}{\%N_{2\,I}}\right)}{\Delta p_A} \qquad 12)$$

Where V is the volumetric flow rate of carrier gas, $\%C_I$, $\%C_F$ represents initial and final concentration of CO_2 in the permeate while $\%N_{2I}$, $\%N_{2F}$ represent initial and final percentages of Nitrogen in the permeate. A direct sample calculation for equation 12 is available in the appendices. With a basic understanding of how membrane systems work, we will now look at one of the major factors that influence permeation.

Hyperbranched Polymers

In order to create membranes with high permeability to CO_2, different polymer architectures and morphologies had to be considered. Maintaining proper balances between flux and selectivity in final membrane forms can be challenging when creating membranes. When considering membrane materials thermosets are a better option than thermoplastics because thermoplastics are soft and bendable above the glass

transition temperature and glassy and brittle below. Thermosets, in comparison, harden into a final shape once they are heated or cured to the proper temperature.

Leo Baekeland was the first to create a fully synthetic thermoset in the early 1900's called Bakelite, but it wasn't until after World War I that this technology advanced. The advantage of thermosets is the fact that they can melt and take shape in an irreversible chemical reaction and once that occurs they remain a solid indefinitely. In addition to achieving a solid state, chemists have been able to control the chemical reactions that take place to improve the physical properties of any polymer they choose to form. A method which has proven to improve membrane permeance behavior has been the cross-linking of a thermosets with an HBP. These beneficial effects can only be described through the properties of the HBPs. Hyperbranched polymers are defined as highly branched three-dimensional dendritic structures [48]. An example of a dendrimers is shown below in figure 3.

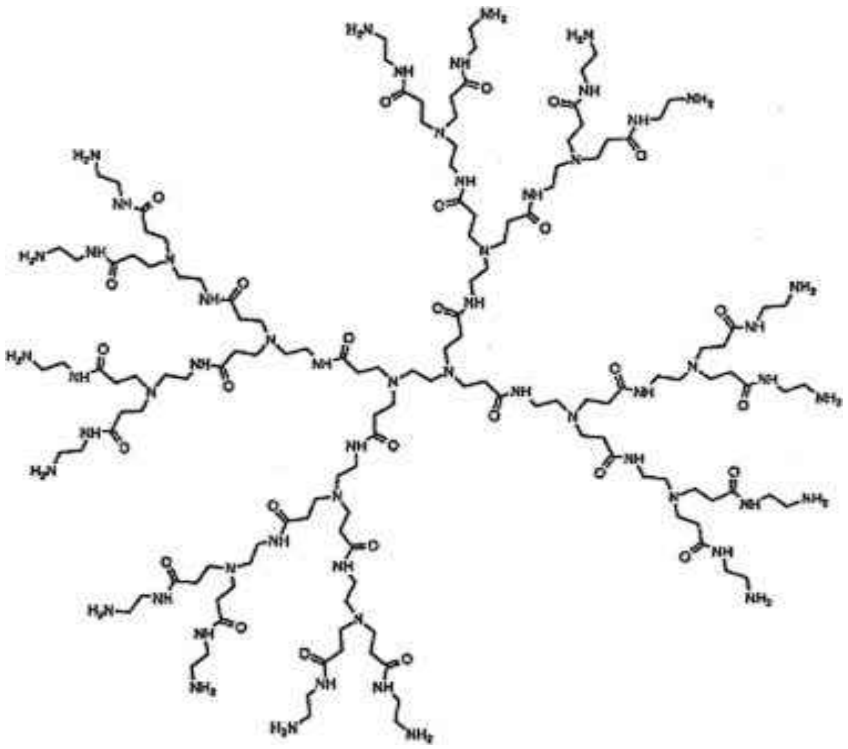

Figure 3: Example of a Dendrimer Poly(amido amine) PAMAM [49]

As in all polymers one can see typical dendrimers are made of many monomer units linked together. Dendrimers' main components are the core groups, the branch groups, and the end groups. What this image cannot show is that this structure is 3-d in nature, spanning out in the z plane as well. Though HBPs and dendrimers are in the same group, there is a fundamental difference which lies in the way each are made. Dendrimers are formed in one of two ways, which can be seen in Figure 4.

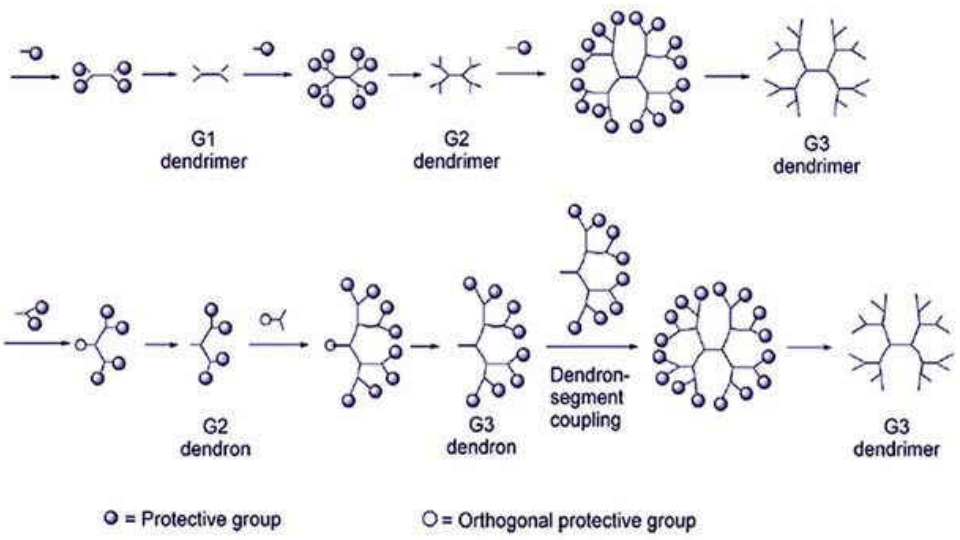

Figure 4: Methods for Dendrimer Formation [50]

The method displayed at the top of Figure 4 is known as the divergent method. Monomers react with a core molecule to start large monomer chains. These monomer chains then diverge from a core molecule in every direction sterically possible to form a treelike material as the one shown above. The convergence model is where you have built several monomer chains first and then they converge on the core molecule. The common occurrence of all dendrimers though, is that they have uniform monomers and spacing throughout the molecule. HBPs on the other hand are quite the opposite, having irregular lengths and structures in one or more directions. This added variability in the monomer chain contributes more void spaces in the polymer chain form. These void spaces should prove to allow more permeate to penetrate through a membrane surface, which should allow for higher permeability and was investigated in this study.

Pervaporation

Membranes of polymeric origin not only have use in gas separation but are also viable in pervaporation processes. Pervaporation is a technique used to separate compounds in a mixture by taking a liquid feed, partially vaporizing a component, and allowing the vaporized component to permeate through the membrane and enter a gaseous state on the permeate side. Regarded as one of the most important processes in membrane separation [51], it has applications in many different industries including purification, separation and compound analysis. Pervaporation gets its name from the two-membrane processes, which takes place during pervaporation: First is the feed permeating through the membrane and then partially vaporizing into a vapor phase. During this process the membrane behaves as the selective barrier only allowing desired components to permeate through. Typical pervaporation processes take place with one chamber containing a liquid at atmospheric pressure and another chamber under a vacuum, which allows for a partial pressure gradient, thus allowing for permeation. A schematic of a typical pervaporation can be seen in Figure 5:

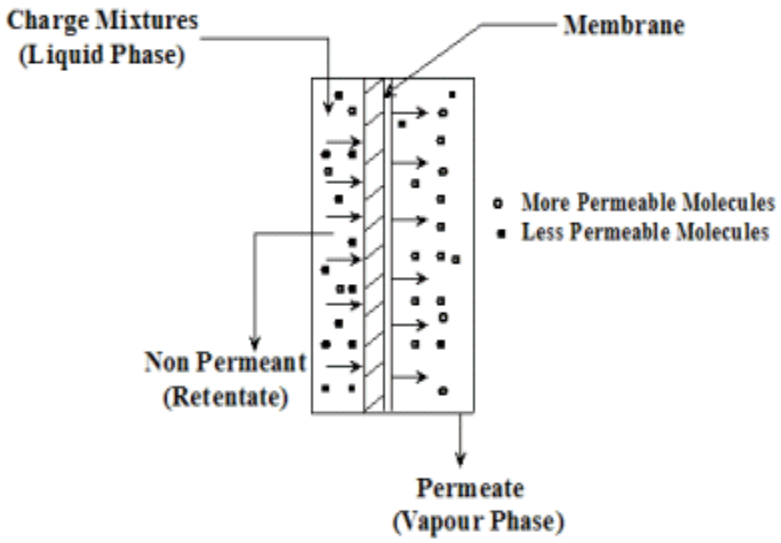

Figure 5: Overview of the Pervaporation Process [52]

The driving force which allows for permeation to take place is the chemical potential gradient between the liquid phase and the vapor phase. The transport properties for this process are expressed through the chemical potential difference between the charged mixture and the retentate. This chemical potential difference is mathematically expressed through the fugacity in Raoult's Law, which states that the vapor pressure of an ideal solution is a function of each chemical component and the mole fraction of that component in the solution. Raoults law is derived from the chemical potential equation for an ideal solution shown in equation 13:

$$\mu_i = \mu_i^* + RT\ lnx_i \qquad 13)$$

μ_i^* is the chemical potential for pure component, R is the gas constant T is temperature and x_i is the mole fraction of i in the solution. When this system is at equilibrium then the chemical potential of both phases is at equilibrium, thus equation 14:

$$\mu_i = \mu_i^* + RT\ lnx_i \quad (14)$$

Since we are assuming that the solution is ideal we can combine equations 13 and 14 to get equation 15:

$$\mu_{i,vapor}^{ref} + RT\ ln\frac{f_i}{p^{ref}} = \mu_{i,liquid}^* + RT\ lnx_i \quad (15)$$

Where f_i is the fugacity of species i. Fugacity is essentially the pressure of ideal gas which contains the same chemical potential of a real gas. This term is defined experimentally and is dimensionless as defined by the fugacity coefficient shown in equation 16:

$$\emptyset = f/P \quad (16)$$

For pure component i in equilibrium with its vapor, the equation can be expressed as:

$$\mu_{i,vapor}^{ref} + RT\ ln\frac{f_i}{p^{ref}} = \mu_{i,liquid}^* \quad (17)$$

Combining equation 17 with equation 15 and subtracting yields equation 18:

$$RT\ lnx_i = RT\ ln\frac{f_i}{f_i^{iP}} \quad (18)$$

This can be simplified to equation 19:

$$f_i = x_i f_i^{iP} \quad (19)$$

This can then be converted to the Raoults Law:

$$p_i = x_i p_i^{ip} \quad 20)$$

This is the basic form of Raoults law. This can be combined with Dalton's Law, which assumes that the sum of partial pressures is equal to the total pressure expressed by equation 21:

$$P_{total} = p_1 + p_2 + p_{3+\cdots\ldots+p_n} \quad 21)$$

Transport in pervaporation also behaves according to the solution-diffusion model since permeation is taking place. Between those equations we can express permeability through a pervaporation system. One of the other major basic factors for understanding pervaporation processes is the use of a solvent in this process.

Solvents

A vast number of different technologies are currently being studied for use in carbon capture, but by far the most developed of these technologies is the use of solvents for CO_2 capture. Developed over 60 years ago solvent scrubbing has been used to remove hydrogen sulfide and carbon dioxide from gas streams. The use of solvents can be divided into two categories: chemical solvents and physical solvents. Physical solvents as implied in the name mean the physical solubility of gas has the main effect on separation. Molecules with high solubility is one of the most important requirements for the process to work successfully and also high partial pressures are necessary for the constituents this being the main elements of the driving force for absorption. First used

in the 1980's for the Texaco/cool water gasification system, Selexol is a proven physical solvent that has been tested to work well for this application.

In chemical solvents the driving force for mass transfer is the partial pressure. Unlike physical solvents, chemical solvents have a non-linear dependence on partial pressure, which leads to large increases in the partial pressure having very small increases in the solvent loading. This means the absorption of a chemical solvent is higher at lower partial pressure which is the opposite of physical solvents. The most popular of solvents used and characterized for this process is mono-ethanolamine (MEA). It has been known to achieve CO_2 recovery rates of 98% with over 99% purity [53]. Many coal fired power plants and various chemical processes have already begun using this technology to remove CO_2 including the warrior run coal fired power plant where 150 t/d of CO_2 is captured and the Fluor (Econamine FG Plus) process where 30 weight% aqueous MEA solution is used to remove up to 330 t/d of CO_2 from natural gas for food applications. Challenges still exist in the fact that most practical applications involve gas streams, which are chemical reducing and the opposite of the oxidizing environment of flue gas streams. Investigation into improved solvents could lead to a reduction of over 40% in energy requirements compared to the use of MEA in amine scrubbing processes.

CHAPTER III

POLYDIMETHYLSILOXANE (PDMS) COMPOSITE MEMBRANES

INTRODUCTION

Membrane techniques implemented into coal fire power plants has great potential to reduce CO_2 emissions, but combining it with other technologies has even greater potential to improve overall efficiency of the plant. The regeneration of chemical and physical solvents for CO_2 capture has the potential to make use of composite membranes due to the larger interfacial contact area between flue gas streams with the membrane surfaces compared to desorbers. This larger area allows for a larger volume of CO_2 rich solvent to be in contact with the membrane, allowing for increased CO_2 separation from the solvent stream while using less space. Chemical solvents use the acid-base reaction between CO_2 and the solvent to remove CO_2 while physical solvents rely on non-covalent attractions between solvent molecules and CO_2 for CO_2 removal. Both of these processes have severe energy penalties, which result from re-compressing the gas or heating the solvent. The use of thin-film composite based polymer membranes has the potential to reduce the energy penalties in these processes. Thin-film composite membranes are semi permeable membranes which usually consist of one or more layers designed to be durable yet permeable for desired

gases. Composite membranes are typically used to combine the benefits of two or more materials for a desired operation. A potential reduction in energy cost comes from the replacement of the desorber with these membranes. The desorber requires heat to remove CO_2 from the CO_2 rich solvent stream, while membranes use the partial pressure difference between the CO_2 rich solvent stream and the permeate for separation. The larger contact area is a tremendous advantage membranes have over packed columns. A packed column's area can vary between 30-3000 m^2/m^3 of interfacial area while composite membranes have over 6000 m^2/m^3 of area while using a fraction of the space of packed columns [54]. A research study is being conducted at UND to use physical and chemical solvents to recover CO_2 from flue gas streams in gasification systems using composite polymer membranes and porous membrane contactors**.** This study aims to contribute to that work.

When deciding on which polymer to use in the study for the thin film layer of a composite layer membrane, the major factors considered were: the cost effectiveness, temperature range, hydrophobicity and permeability to CO_2. Hydrophobicity was a major factor because I wanted to reduce the amount of water leaving the system so that the MEA loading was consistent. Table 1 lists the other polymers that were considered for membrane testing with a more detailed list available in appendix G. Commercial availability and ease of use in the end became the final deciding factors so more focus could be spent on curing the selective layer. Some experiments were conducted with cis-polyisoprene, but due to large variability in the cured layer formed,

polydimethylsiloxane (PDMS) was ultimately selected. PDMS is an excellent starting point for creating composite membranes for use in an absorption system because it is optically transparent, flexible, gas-permeable and cheap enough to use in large amounts. A porous support layer is necessary because of the rubbery characteristics of PDMS in addition the added support layer increases the overall structure and durability of the membrane and provides support for the thin film [54, 55, 56]. An investigation into the effects of polymers substrates effecting overall permeability needed to be done to determine which substrate would be the most effective for CO_2 removal in a composite layer membrane. In this study PDMS was cast upon polyethersulfone (PES), polyamide, Teflon, polycarbonate, polyester, and polyvinylidene fluoride (PVDF) and evaluated for CO_2 permeability in a gas separation system and a liquid pervaporation system. The substrates were selected for their high chemical resistance, thermal stability and durability. The membranes created were characterized using a scanning electron microscope (SEM) and permeability values were calculated.

Table 1 Potential Polymers with good CO2 Separation

Polymer	***Name***	***P(CO_2)(barrer)***	***Tg (C)***	***Tm(C)***
poly(1-trimethylsilyl-1-propyne)	*PTMSP*	*3520[2]*	*262[2]*	*323[2]*
polydimethylsiloxane	*PDMS*	*3100[5],4553[7]*	*-128[4]*	*-40[3]*
6FDA-based polyimides	*6FDA–durene*	*456[1], 24.2[5]*	*300-350[9]*	*N/A*
Poly(phenylene oxide)	*PDMPO (60.0% brominated)*	*159.9[1]*	*184[2]*	*279-285[2]*
cis-polyisoprene	*cis-PIP*	*134[5],191[7]*	*99[2]*	*156[2]*
Polycarbonates	*TMHFPC*	*111[1]*	*217[2]*	*270[2]*
Polysulfones	*PSF*	*110[1], 5.6[5]4.6[7]*	*237[2]186-190[9]*	*N/A*
Poly(ether-b-amide)	*PEBAX[6]*	*30-104[15]*	*-60 to -70[2] -30to 160[9]*	*120-210[2]*

MATERIALS

Composite polymeric membranes were made using the following materials. Polydimethylsiloxane (PDMS) hydroxyl terminated (Sigma-Aldrich Inc.), tetraethyl orthosilicate (TEOS) (Sigma-Aldrich Inc.) was used as a cross-linker with dibutyltin dilaurate (DBTD) (Sigma-Aldrich Inc.) used as the catalyst to begin the cross-linking reaction. These chemicals were combined with either reagent grade anhydrous toluene (Sigma-Aldrich Inc.) or anhydrous chloroform (Sigma-Aldrich Inc.) to create a polymer solution which was cast on the various substrates using a spin coater. All substrates were commercial grade and purchased from the suppliers shown in table 2.

Table 2 Substrates used in study of membranes

Substrates used in study of membranes			
Name	Pore Size (µm)	Supplier	Diameter(mm)
Polyethersulfone (PES)	0.22	Millipore	47
Polyamide	0.45	Sartorius Stedim	47
Laminated Teflon	0.45	GE Water & Process Technologies	47
Polyvinylidene fluoride (PVDF)	0.45	Millipore	47
Polyester	0.4	GE Water & Process Technologies	47
Polypropylene	0.4	GE Water & Process Technologies	47

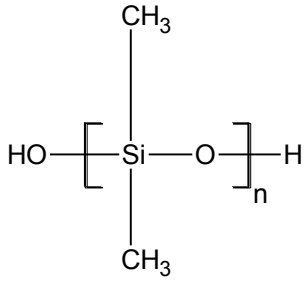

Figure 6: Structure of Hydroxyl Terminated Polydimethylsiloxane

PDMS is a polymeric organosilicone compound, also known as a silicone. Its chemical formula is $CH_3[Si(CH_3)_2O]_nSi(CH_3)_3$ and its chemical structure is shown in figure 6. This polymer was used as the selective layer after going through the step growth polymerization reaction shown in reaction 1 in the presence of DBTD and solvent.

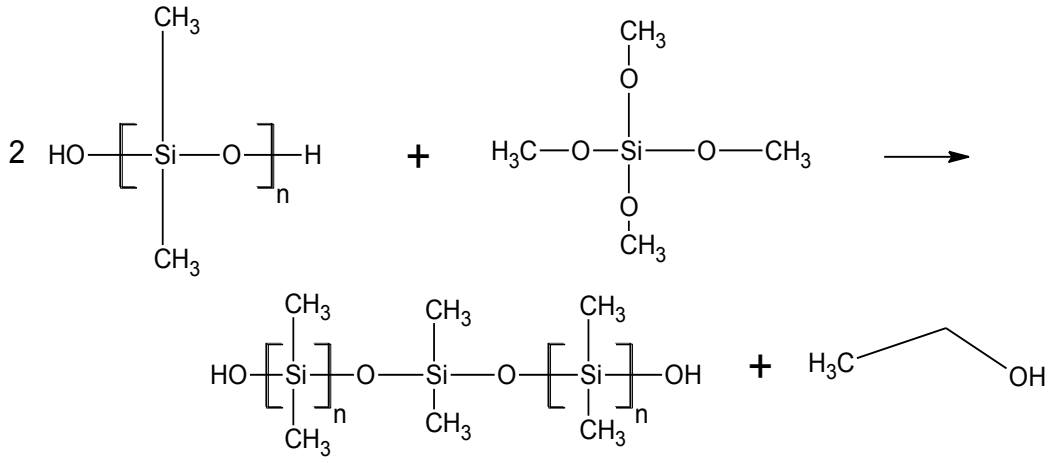

Reaction 1: Formation of PDMS layer

The addition of cross-linkers served as a way of connecting the PDMS polymer chains together to form a flexible rubbery surface. TEOS acts like a bridge connecting the PDMS chains together. The catalyst DBTD was added to provide reaction sites when the polymer begins mixing in excess amounts of solvent. This reaction, which took place in either chloroform or toluene (the solvent) was spin coated onto the substrate. After the solvent vaporized at room temperature leaving the desired polymer layer, the composite membranes were cured at 120°C to complete the reaction and vaporize any excess ethanol from Reaction 1.

The substrates were composed of various polymers and tested as is from the manufacturer or had a PDMS layer of varying thickness cast upon it. The substrates used

included polyethersulfone which is a hydrophilic material with a pore size of .22µm and thickness of 160 to 185 microns. Polyamide from Sartorius Stedim is also a hydrophilic material with a pore size of .2µm and a thickness of about 115µm. Polyvinylidene fluoride (PVDF) is again hydrophilic with a pore size of .45µm and thickness of 125µm.

The composite membranes were formed by taking a 10:1 ratio of PDMS and TEOS/DBTD and mixing it in the presence of a solvent. The cross-linker to catalyst ratio was 4:1 as recommended by the literature [57, 58, 59]. The solution was continuously stirred for 10 minutes in excess of solvent. The solution was then spin coated onto the substrate and excess solvent was allowed to evaporate at room temperature for 24 hours. The substrate was taped to the metal plate of the spin coater during the spin coating process. The spin coater was a MTI corp. VTC-50 spin coater, which allowed for spin speeds up to 5000 rpm and is displayed in figure 7. As recommended by the literature an initial coating of the surface with our target solution occurred at ¼ and ½ the final spin time to ensure a uniform coat of the solution. The remainder of the solution was poured on during the first 2 to 4 minutes of spinning at its final spin speed. After the solution was deposited onto the top of the substrate the membrane was allowed to continue spinning to remove excess solution from the substrate. From this point the membranes were allowed to dry for 24 hours at room temperature to remove any excess solvent that remained after spinning. After the solvent evaporated from the substrate the membranes were placed in an oven for 12 hours and heated up to 130°C to ensure that a complete cure occurred.

Figure 7: VTC-50 Spin Coater

Permeation testing Methods

To test the composite membranes two different systems were used. A schematic of the first system used is shown below in figure 8.

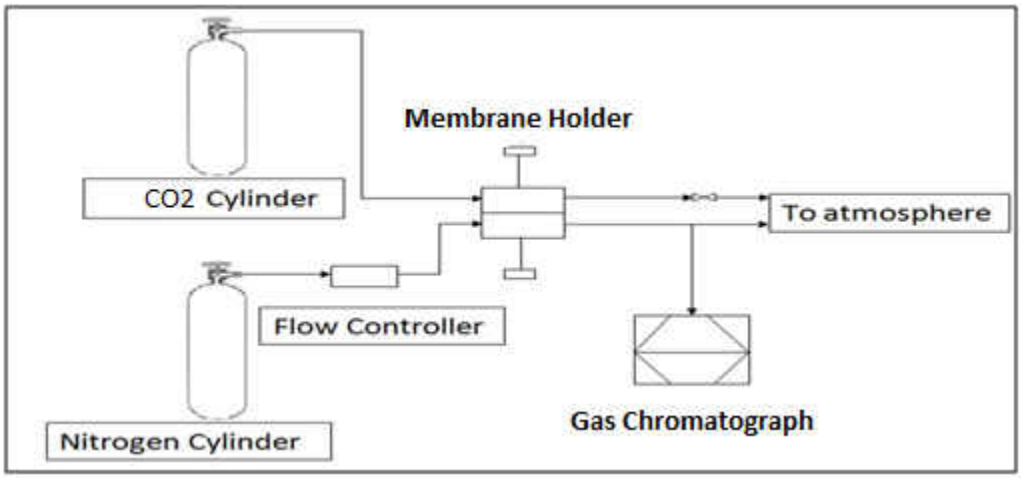

Figure 8: Apparatus used for Gas Separation Analysis

Figure 8 above shows the system used to test the membranes permeability in a gas separation system. In this setup all lines for the setup were made from ¼ inch plastic

piping and diffusion cell was manufactured by the Millipore Corporation. The cell included an in-line filter holder designed to filter gases and liquids. Maximum pressure for this device was 275 psi. The material used in the design of the chamber was 316-stainless steel, which was chosen for its degree of withstanding aggressive fluids and gases.

The gas chromatograph used in the analysis was an Agilent 7890A series GC which included a packed column equipped with two detectors, a thermal conductivity detector (TCD) and a flame ionization detector (FID). The packed column was chosen for this type of separation because of its ability to separate nitrogen and carbon dioxide fairly quickly. Two detectors were used in this design to ensure high sensitivity while providing the flexibility to monitor trace elements which may have remained in the system. The TCD detects the difference between the carrier gas with sample components thermal conductivity and the carrier gas without sample components thermal conductivity. Detection limits for this detector are around 100ppm. Since an FID can only detect hydrocarbons the G.C. came equipped with a methanizer to convert CO_2 into methane gas. The detector was primarily used because of its high sensitivity which is able to detect concentration levels as low as .1ppm. The G.C. also included a split-splitless injection system, which enhanced accuracy and allowed for better analysis of a sample. The G.C. received continuous streams of permeate from the diffusion cell and took 1µL sample of permeate every 30 minutes and recorded the data until steady state was reached. The system was monitored and controlled by Chemstation software,

which came standard with the G.C. system. Operational procedures are provided in full detail in Appendix A.

The second system was a pervaporation unit built and designed for laboratory testing at UND. Figure 9 is a schematic of the permeation system.

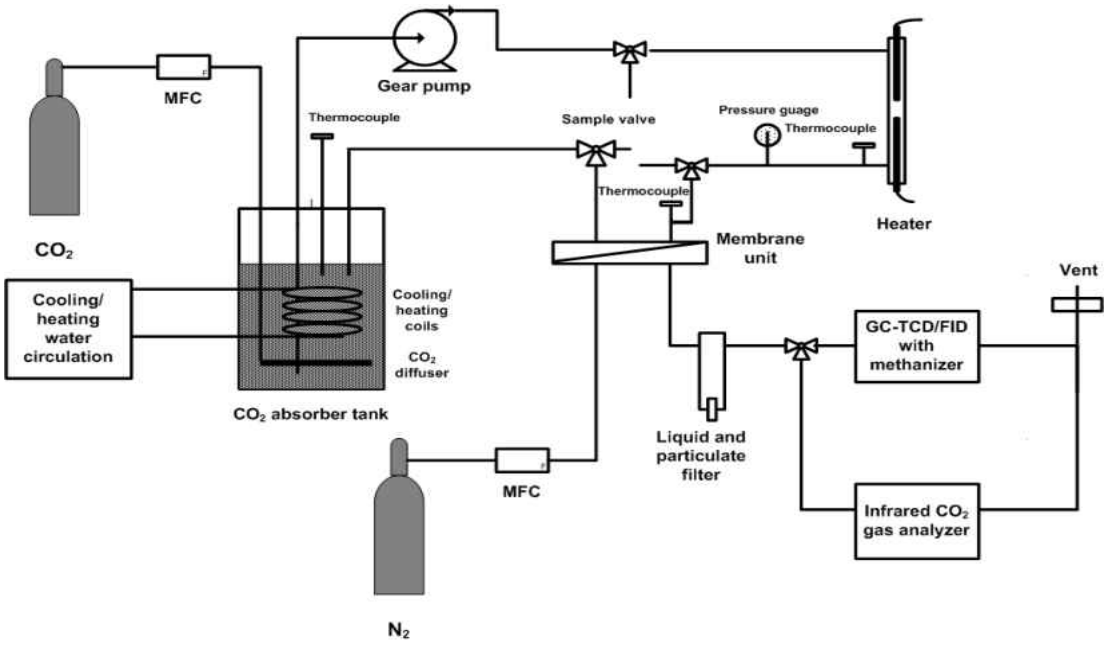

Figure 9: Schematic of Permeation System

The system from figure 9 was built using Swagelok fittings and valves for each line in the system. The membrane unit was a Millipore 47mm stainless steel membrane holder the same type used in the gas separation system. The pump responsible for pumping the MEA solution from the absorber to the heater was a Cole-Parmer digital gear pump with pumping speeds of up to 330 ml/min. The absorption tank was custom built at UND for this specific purpose. It was a 6-liter tank made from 6" PVC pipe. The tank was equipped with homemade heating exchange coils to ensure constant absorption solution temperature and also included was a gas sparger to diffuse and

saturate CO_2 in the absorption solution. A pressure release valve and an Omega thermocouple K type were installed in the lid for monitoring conditions inside the absorber.

The temperature of the solvent was also monitored and controlled. The temperature was changed by heating a low flow air system and liquid circulation heater from Omega Engineering Inc. The heating system was a 1200W stainless steel enclosure with an outlet temperature of up to 430°C, flow rates of up to 15cfm and maximum pressure of 100psi. It consisted of full PID auto tuning temperature controller, alarms with 5 options and IP66 protection from the front panel. Pressure transducers with a range up to 500psi were used to convert system pressures to a signal, which was detected by pressure gauges all of which were purchased from Omega.

CO_2 and N_2 which flowed in the system were purchased from Praxair and their flow rates were monitored and controlled. Flows for both gases were controlled by Brooks 4800 series mass flow controllers, which had a maximum flow of 10 SLPM. The liquid and particulate filter which prevented liquid permeates from entering the CO_2 analyzer or the G.C. was a coalescing filter from Cole Parmer. CO_2 concentrations in the permeate stream were analyzed by either a Li-Cor 820 non-dispersive infrared CO_2 analyzer or the Agilent 7850A G.C. The deciding factor for which analyzing method was used for examining permeate gases was the total concentration of CO_2. If the concentration was above below 20000ppm the Li-Cor analyzer was used for higher

concentration the G.C. was used. Data acquisition was done by the Labview software from National Instruments for all other controlled parameters.

All substrates used were ready made to fit in the Milipore diffusion chamber. PDMS was casted on the top of the surface and controlled to keep the same surface area as the substrate. Three bolts are removed from the cell and the sample is placed into the apparatus. The membrane is then placed in the bottom chamber of the cell with an under-drain screen beneath it. A silicone O-ring is positioned on the membrane to prevent gas leaks around the sides of the membrane. A support screen is placed over the membrane to prevent back surges. Both chambers are properly aligned, sealed and tightened with the three bolts. To ensure an even seal all screws are twisted an equal amount of times for a tight firm seal.

Air and other contaminants enter the membrane holder at the moment the membrane is inserted. To ensure these contaminants are not read in the results, pure nitrogen is flushed through the system to push out all the contaminants. Once the chamber is flushed with carrier gas, samples are recorded to confirm that only nitrogen is in the bottom chamber before proper analysis can begin. Once purity is confirmed by G.C., bottled CO_2 gas is slowly turned on and allowed to fill up the top chamber and permeate through into the bottom chamber. The permeated gas is then allowed to flow from the bottom chamber and through to the G.C. for proper analysis. Measurements are taken every 15 minutes to test for steady state permeation. Steady state

permeation is confirmed when CO_2 flux is constant in the permeate stream. After confirmation, three replicate readings are taken of each sample.

Pervaporation System Preparation

Use of the pervaporation system required preparation of an amine solution; 2500ml of deionized (DI) water was poured into the absorption tank followed by 890 ml of monoethanolamine (MEA). After adding the MEA the absorption tank was filled with another 2600ml of DI water, the lid was sealed and the CO_2 was turned on and allowed to absorb into the solution for 12 hours. This was done to ensure that an aqueous solution of 15wt**%** was used for the experiments. This concentration was chosen because it can absorb sufficient CO_2 that can be quickly analyzed and is not too corrosive. Also this concentration is equal to the concentration of CO_2 from a flue gas stream in a coal fired power plant. Once the solution was properly prepared, the test membrane was inserted into the membrane holder and sweep gas lines were connected along with inlet and outlet lines for the feed and permeate sides of the chambers. After the solvent solution began to flow from the top chamber, the heater was set to 70°C, valves were checked to ensure flow and sweep gas and CO_2 set points were inserted. Next the pump was set to the desired flow rate and the analytical devices were activated. The settings used for pervaporation analysis included a pump flow rate of 180 ml/min, N_2 flow rate of 500 sccm, and a CO_2 flow of 400 sccm. These settings were chosen based off of sample runs provided by Xuefei Zhang and literature values for similar testing [10,60]. The temperature varied from 70-90°C because temperature was

expected to have a major effect on CO_2 flux due to a decrease of CO_2 loading in MEA with increase in temperature.

Scanning Electron Microscopy

The membranes investigated in this study were examined using a scanning electron microscope (SEM) at NDSU Electron Microscopy Center in Fargo, North Dakota. Cross sections of the samples were obtained by cutting with a new double-edge razor blade. Images of the surface of the substrate in which the polymer was applied were also taken and will be referred to as surface images. Separate samples oriented for surface and edge views were then mounted on aluminum mounts with carbon adhesive tape and coated with gold palladium using a Blazers SCD 030 sputter coater, an example of one of the mounted samples is shown in figure 10a. Once mounted the images were obtained using a JEOLJSM-6490 scanning electron microscope at an accelerating voltage of 15 keV. An image of this device is shown in figure 10b.

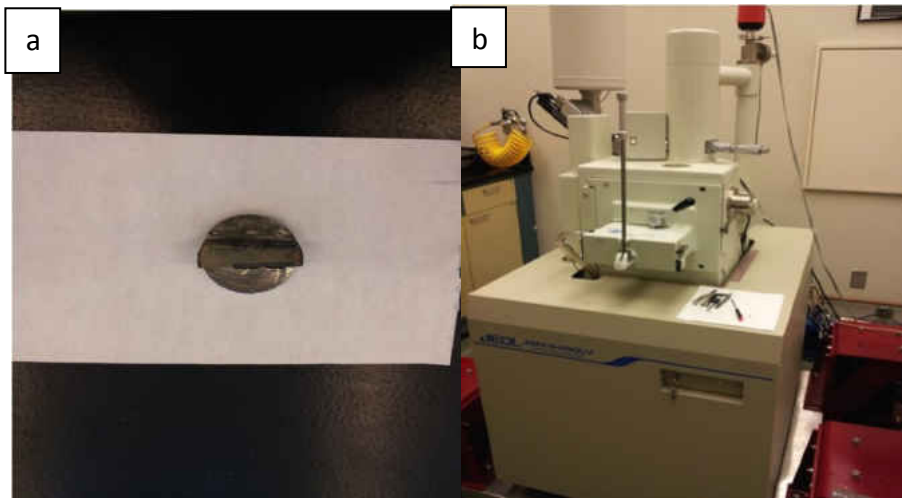

Figure 10: a) Mounted sample ready for SEM Imaging, b) JEOLISM-6490 Scanning Electron Microscope

RESULTS & DISCUSSION

Characterization of Membranes

The spin coater method was used to create all of the composite membranes. Those samples along with substrates containing no PDMS were analyzed using the microscope shown in figure 10b. Figure 11a displays the substrate polyamide before adding PDMS, b is the substrate with the 10µm PDMS layer and c is the substrate with the 20µm PDMS layer.

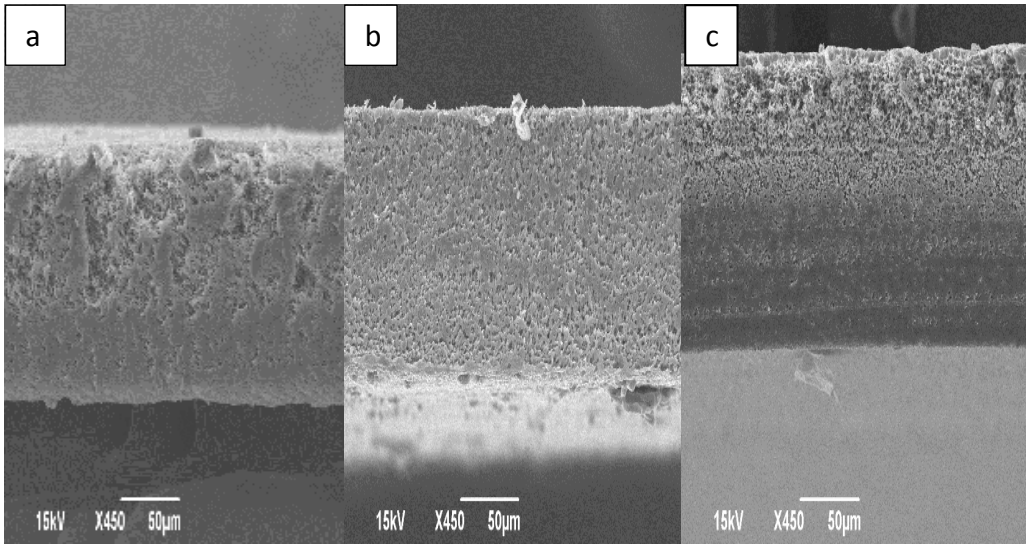

Figure 11: a) Polyamide No PDMS b) Polyamide 10µm PDMS c) Polyamide 20µm PDMS

The image of polyamide containing no PDMS (figure 11a) displayed a solid structure with a very small pore size. Figure 11b, which is an image of a membrane where we attempted to add the 10µm layers shows a membrane which appears to have no layering but a complete penetration of PDMS through the substrate. The purpose of the images in figure 11a is to show the effects of adding the PDMS layer to the substrate. Figure 11a of polyamide with no PDMS show a surface with little to no pores which are not uniformly distributed. Figure b is of the same substrate, but with PDMS cast upon it. Comparing a and b shows that the PDMS went through the entire substrate but figure 12 suggest that under higher magnification of this sample the layer of PDMS can be seen and is shown in figure 12. A major concern with this composite membrane is the interfacial layer is much too large as it can be seen covering the entire substrate.

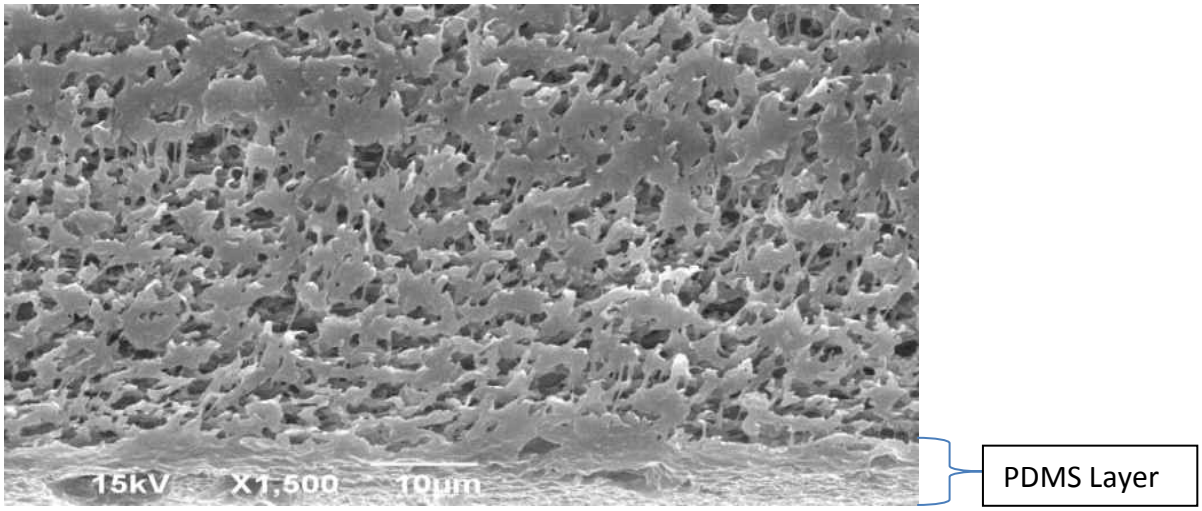

Figure 12: 10µm PDMS/Polyamide Composite Membrane at 1500 Magnification Cross-section View

The 20µm image showed a definite layering of the PDMS. The layer appears to be larger than our target thickness, but it's difficult to tell due to the interfacial layer as shown in figure 13.

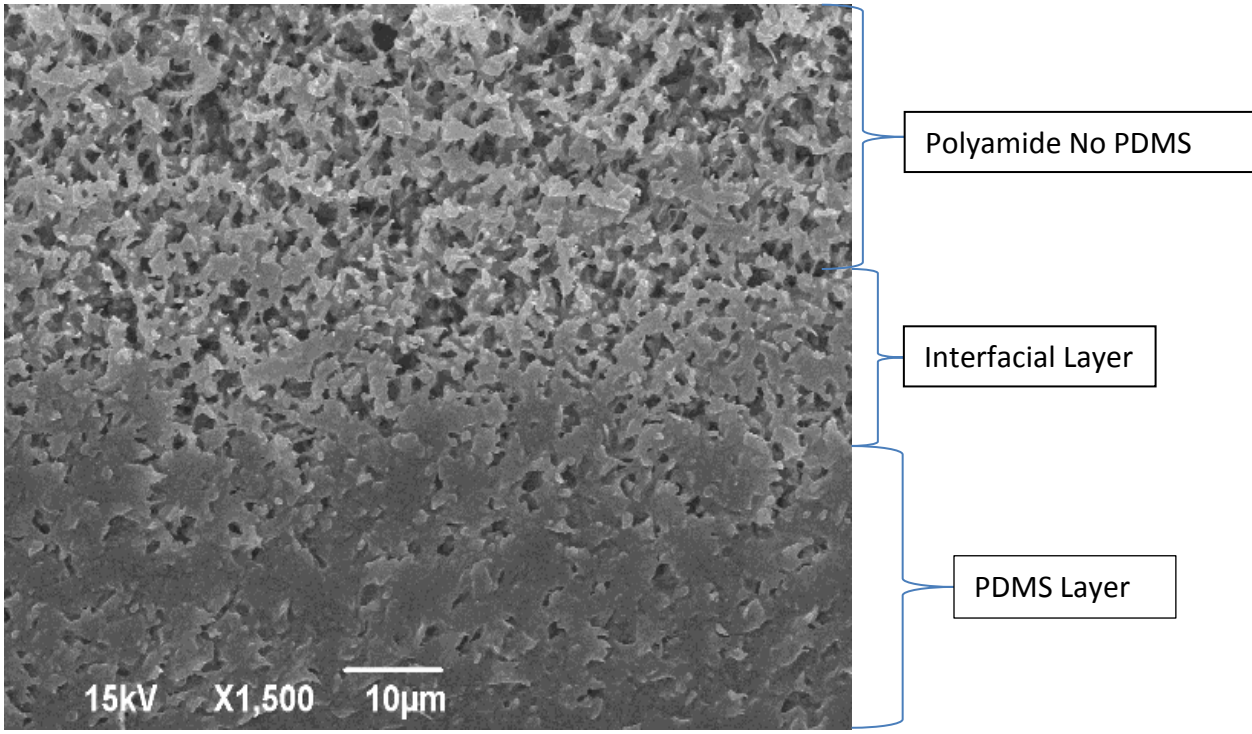

Figure 13: 20µm PDMS/Polyamide Composite Membrane at 1500 Magnification Cross-section View

Surface images of these membranes were also taken and are displayed below in figure 14. The polyamide with no PDMS, figure 14a, has string like chains all woven together in a structure. The 10µm image displays much smaller pore sizes and more of a coated thicker structure which is the polymer layer that was added. The 20µm images show that same layer coating from figure 14b, but with smaller pore sizes which result from the increased amount of PDMS on the surface. These images were to verify the differences which result from adding the PDMS layer as can be seen from comparing figures 14 a and b or a and c.

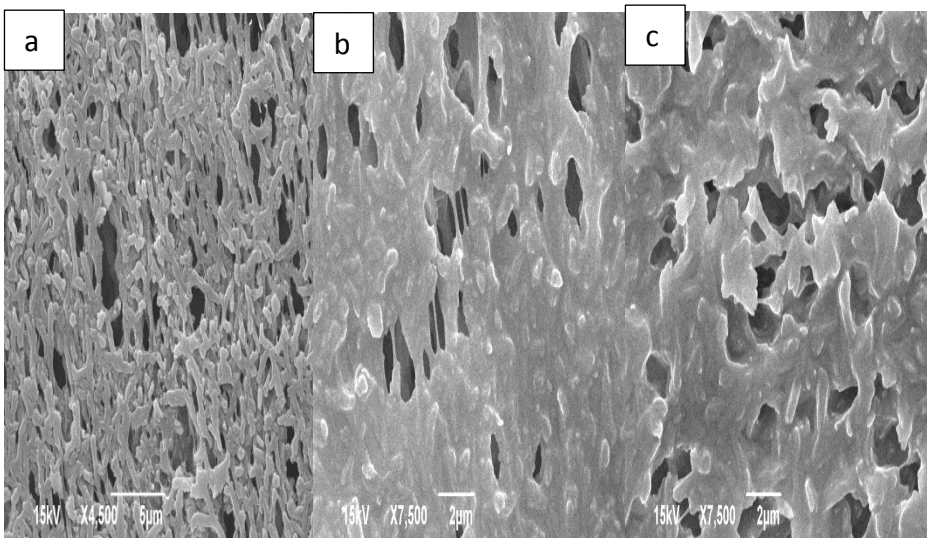

Figure 14: a) Polyamide No PDMS b) Polyamide 10µm PDMS c) Polyamide 20µm PDMS

Below is an example for polyethersulfone (PES) where SEM images suggest a proper composite was formed. Figure 15a is an image of an uncoated PES substrate. The pores in the image appear to get smaller across the cross section of the substrate. The layering in figures 15a and b are a direct result of the addition of PDMS. As seen from the images the PDMS penetrated the top layer, but it did not completely cover the substrate creating a composite layer membrane. The changing pore structure of the PES substrate is the reason the layers formed so well. Though PES formed an excellent composite it did not perform well. Shrinking from the curing process led to leaks around the edges as show in figure 16. Figure 16 shows before and after curing images of PES. Just from looking at the images it is clear the substrate shrunk during curing. The shrinking is a direct result of heating PES [61]. Since the curing temperatures approach the T_g for PES which is 185°C, deformations were observed in the support layer. Also the composite membrane was not run in the pervaporation system due to excess fouling when the substrate was run without the PDMS composite layer [61].

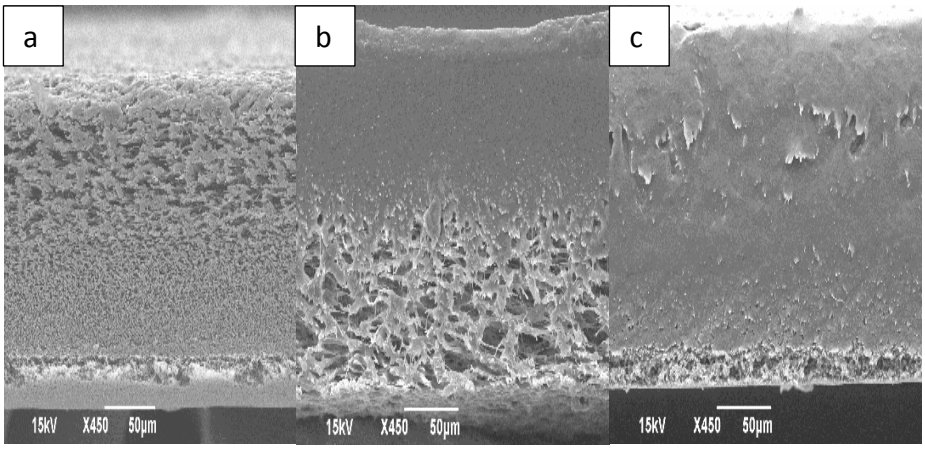

Figure 15: a) Polyethersulfone No PDMS, b) Polyethersulfone with 10µm PDMS layer c) Polyethersulfone with 20µm PDMS layer

Figure 16: Bottom Image PES Composite Membrane before Curing, Top image PES after Curing

Figure 17a is an image of polycarbonate before the addition of PDMS, 17b is with the 10µm layer of PDMS and 17c is with the 20µm of PDMS. The before images reveal a substrate with linear pores throughout the substrate. The after image displays a substrate totally penetrated and covered throughout with PDMS. The cause of this

behavior is the linearity of the pores. As seen from figure 17a, which is the image of a polycarbonate containing no PDMS, the pores were microscopic holes in the membrane which easily allowed for PDMS to totally penetrate the substrate under our spin coater. This effect was not our desired goal for these composite membranes because of the inconsistencies it created in the permeation. When the substrate became totally covered with PDMS, the risk of CO_2 molecules only penetrating the PDMS was very likely which was not our desired effect. If this is the case then it is highly probable that other CO_2 molecules may go through the PDMS layer and the substrate. Since the substrate is totally submersed inside the PDMS there is no way of defining the path, which the CO_2 will take though the membrane, making a proper analysis impossible.

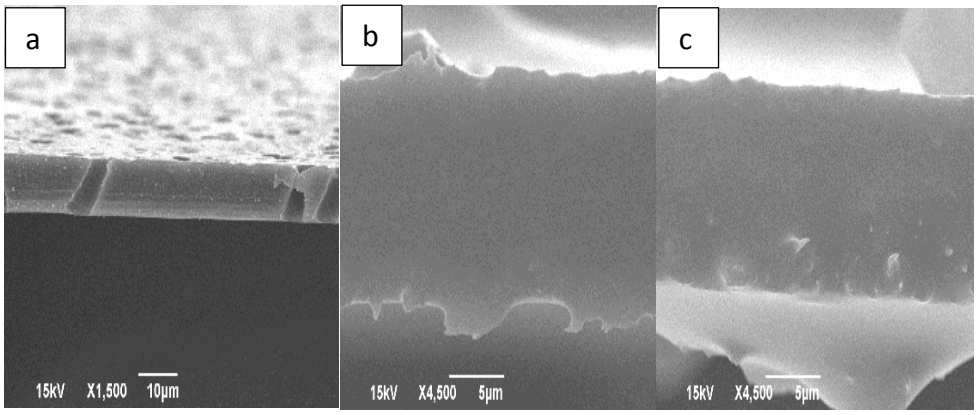

Figure 17: a) Polycarbonate No PDMS, b) Polycarbonate 10µm PDMS, c) Polycarbonate 20µm PDMS

The characterization of polyester was quite interesting. As seen in the image without PDMS the membrane appears to be a solid structure with small randomly distributed pores, which suggest that it would be a good candidate for forming a proper composite membrane. The 10µm image appears to show some promising layering but the 20µm image suggests no layering at all and that total PDMS penetration occurred. In addition to total penetration, excess PDMS was layered on top of the substrate. This could be because of the higher spin speeds associated with the 10µm PDMS layering compared to the 20µm layering. However, no conclusion could be made at this time. Since enough information could not be determined from the SEM images alone this membrane was tested in the pervaporation system for further analysis.

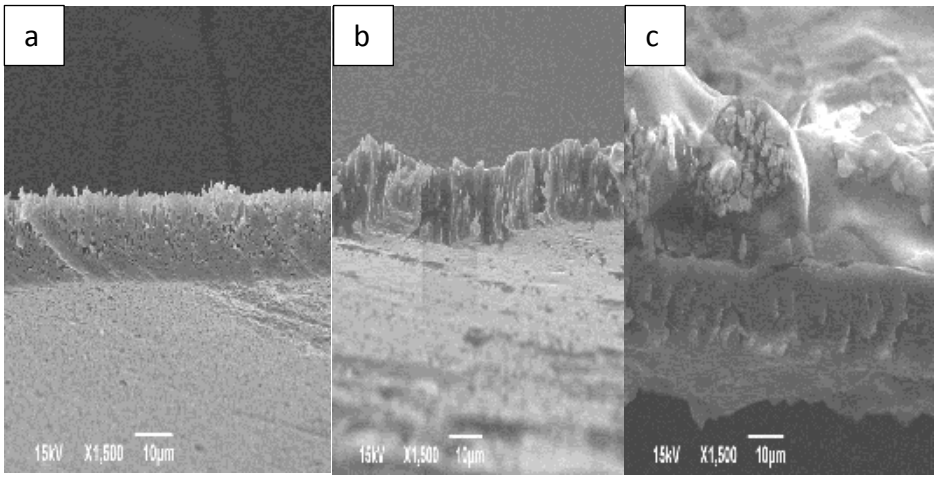

Figure 18: a) Polyester No PDMS, b) Polyester 10µm PDMS, c) 20µm Polyester PDMS

Polyvinylidene fluoride (PVDF) was one of the few composite membranes which showed some degree of forming a proper composite membrane. As shown in figure 19a, the substrate with no PDMS has a beehive-like structure. The 10µm layer displays a very large interfacial layer and a very small PDMS layer on top of the membrane. A larger view of this layer can be seen in the appendix D figure 52. The 20µm sample had the PDMS layering much larger than expected and with smaller pore sizes, seen in figure 19b. The composite membrane was also tested in the pervaporation system due to its potential layering.

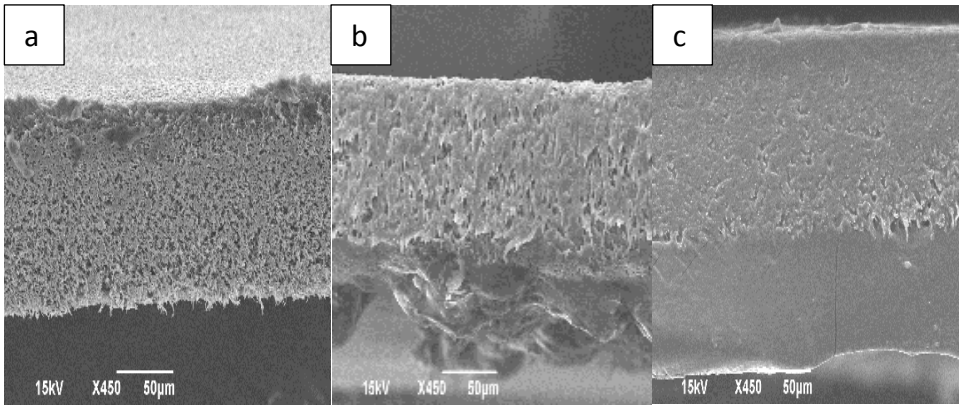

Figure 19: a) PVDF No PDMS, b) PVDF 10µm PDMS, c) PVDF 20µm PDMS

The last substrate tested was laminated Teflon. As seen from the images of the top down and cross sectional views this substrate had a spider web like formation initially. This substrate had one of the largest pore sizes and the structure made it easy for PDMS to penetrate it thus yielding the images of totally penetrated PDMS.

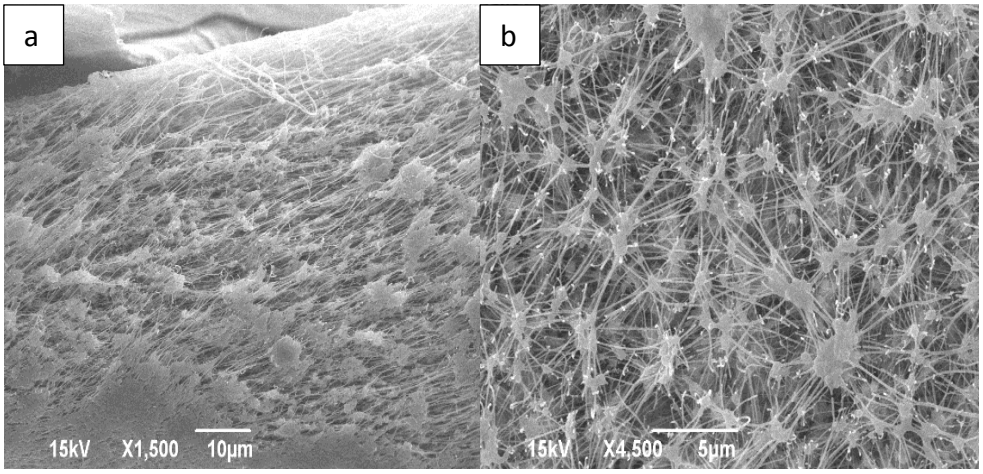

Figure 20: a) Cross Section view Teflon, b) Top down view Teflon No PDMS

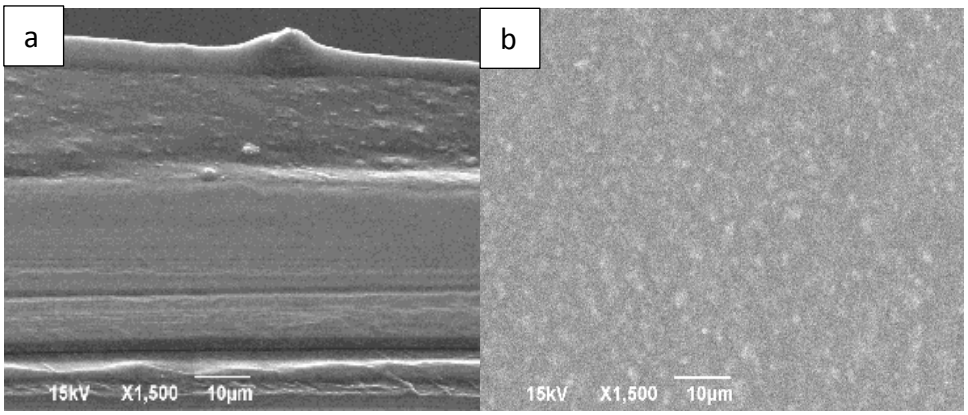

Figure 21: a) Cross-Section Laminated Teflon, b) Top down view of the same Membrane

Gas Permeability Results

The results of the gas separation runs was one of the first criteria used to decide which membranes would be best for pervaporation analysis along with SEM characterization. All the substrates from table 2 were ran with no PDMS, then 10µm concentration of PDMS and finally 20µm concentrations of PDMS. The gas separation results are shown in figure 22.

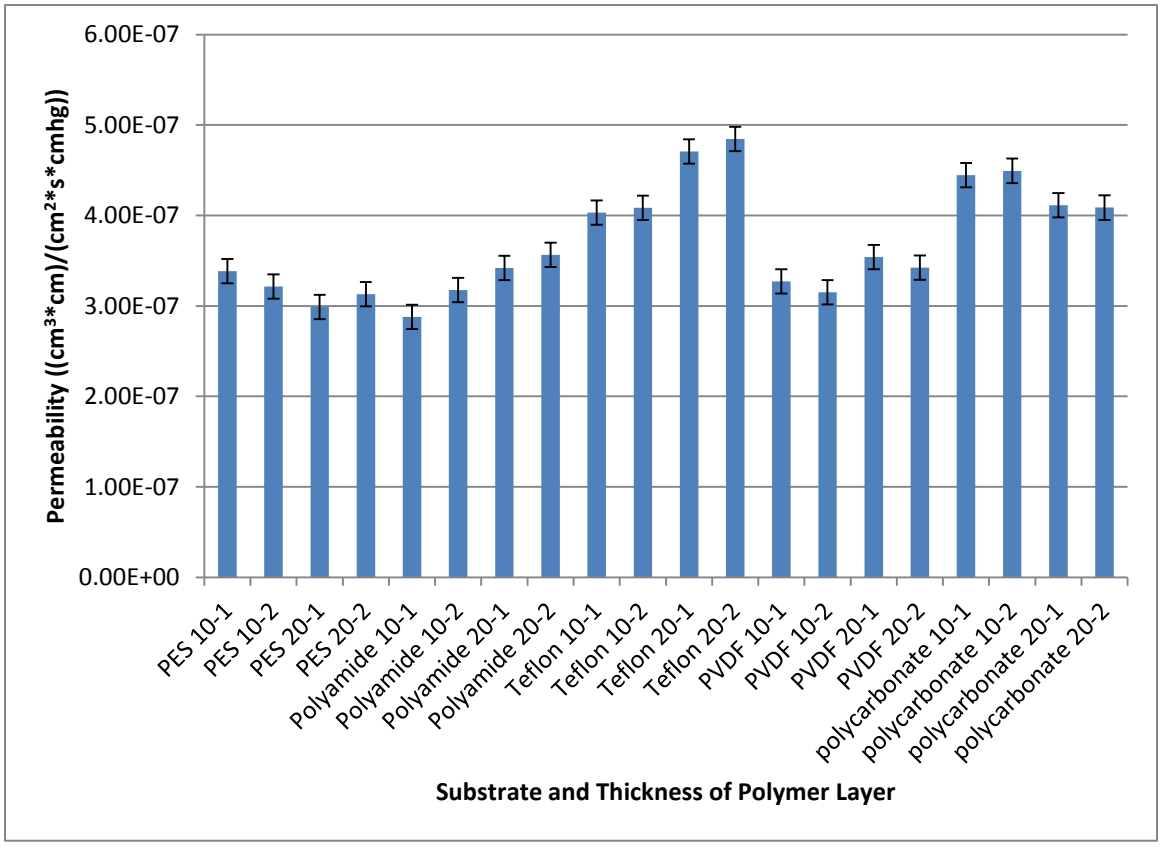

Figure 22: Permeability vs. Sample run for PDMS sample

Figure 22 shows the permeability coefficient values of the composite membranes in the units of $((cm^3*cm)/(cm^2*s*cmhg))$. From this data one can conclude

that the permeability coefficients are unaffected by changes in the membrane thickness. Literature on the subject confirms that permeability coefficients are invariant with respect to membrane thickness and the membrane area [54, 56].The composite membranes with highest permeability values were the membranes where the composite layer was not properly formed. The samples of substrates without PDMS were omitted from this graph due to the extremely high flux. The error bars are standard deviations based on the number of runs performed by the G.C. Because the CO_2 flux for all of the substrates without PDMS were significantly higher than the substrates containing PDMS, they were omitted from this graph but can be seen below in Figure 23.

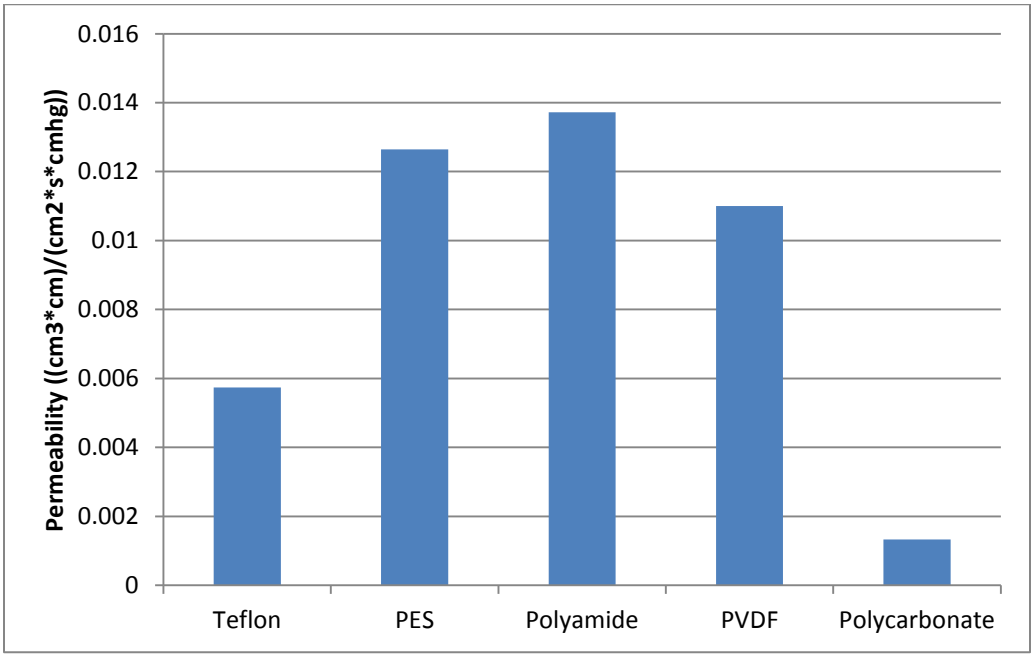

Figure 23: Substrates Permeability's with No PDMS

The reduction in the permeability value shown in figure 22 is because the PDMS layering was the predominant selective layer for CO_2 permeation. The permeability

values shown in figure 23 are extremely high because the substrate was behaving as the selective layer. Since substrates are highly porous almost all chemical compounds will have high permeability's through substrates because they are not very selective. Polycarbonate is quite lower than the others because the overall pore size and thickness of the substrate was significantly smaller than the other substrates. One can also note that the values in figure 22 are within the range of the permeability value of PDMS published from other studies, which is $3.23*10^{-7}$ $((cm^3*cm)/(cm^2*s*cmhg))$ [39]. This is also the same range for permeability as the values shown in table 1. Since the values displayed are in literature value range, it also confirms that PDMS has become the predominant selective layer for the membranes.

However, the desired effect of attempting to create composite membranes was achieved in this study. The PDMS layer became the selective layer for permeation. On analysis of the membrane by SEM imaging, a clearer understanding of why the membranes behave this way is understood. The idea was to use the spin coating technique to create composite layer membranes, but that did not work for all the membranes. SEM imaging revealed that for some of the substrates the PDMS totally penetrated the substrate leaving a substrate suspended in polymer and yet for others it did not. The main cause of this is the capillary forces during and after the spin coating process. An attempt to create composite membranes from a dip-coating method was tried before using the spin coating method, but this led to PDMS layers on both sides of the substrate which was not the desired outcome for these membranes. Dip coating is

the method recommended by the literature [47] as the ideal method for creating composite membranes but actions must be taken to prevent double PDMS layers from forming on each side of the substrate if this method is used in the future.

For future membrane production, new techniques must be tested to prevent pore penetration. Some possible solutions are pre-filling the pores with solution before spin coating or using a solvent with higher surface energies than the substrate to create the solvent solution. Another technique would be to select substrates with a narrower pore size distribution but this would require working with the manufacturer to develop the substrates or creating the substrates from raw compounds. Also, higher molecular weight PDMS would increase the viscosity of the polymer solvent solution which could lead to less pore penetration but the concentration of the solvent solution would need to change so the solution would behave more like the polymer instead of the solvent.

Chloroform and toluene were used as solvents for the spin coating process, but a better solvent could have been Benzene since the substrates which were chosen for their low wettability. Table 3 below show the surface energies of all the substrates used in the composite membranes and there respected contact angles.

Table 3: Surface energy of Substrates used for composite membranes

Substrate	Pore diameter (nm)	Energy (mJ/m^2)	Solvent	Contact Angle
PVDF	450	30.3	Toluene	84.2
Teflon	450	20	Toluene	105.8
Polyester	400	28.9	Chloroform	89.0
Polyamide	450	40.7	Chloroform	64.3
PP	400	30.1	Toluene	84.6
PES	220	32.09	Chloroform	82.5
Polycarbonate	500	34.2	Chloroform	78.2

If the contact angle is below 90 degrees then wetting occurs. It is shown that the majority of the membranes were wetted due to the contact angle of the solvent solution used. Laminated Teflon was used and by looking at its contact angle it should not have wetted but the lamination process altered its properties considerably and, according to the company which produced the substrate, testing had to be done to understand its behavior [62]. From the SEM images produced for the Teflon composite membranes, full penetration occurred which was due to the lamination process that the manufacturers performed before distributing the substrate; it changed the surface energy of Teflon. Non laminated Teflon should produce a better composite membrane without having to change the solvent. One of the main drawbacks of these experiments was that we had to wait a few weeks to send the samples to NDSU to characterize the membranes after the membranes were formed. If the membranes could have been created and characterized before testing, it would have led to much better composite membranes.

Though many of the composite membranes we created did not yield the desired results, a minority did form into a proper composite membrane. The success in the polyamide and PVDF composite membranes was mainly a factor of the pore size distribution in the substrates. Since the pores in the membranes changed across the thickness of the membrane it prevented polymer solution from fully penetrating the substrate. Though we had success in creating a couple composite membranes the process failed to give us much control over the thickness of the polymer layer or the

interfacial layer. To control the polymer membrane thickness, a lower concentration PDMS solution would allow for a thinner membrane layer or using a solvent with higher surface energy could also be the solution. Applying these methods to the PVDF and polyamide membranes would yield smaller PDMS layers as well as more effective layers when attempting to recreate some of the other unsuccessful composite membranes from this study.

Proof of Concept

To prove the suggested methods were viable to create improved membranes over the originals, a new series of membranes were made using the suggestions from the results of the previous membranes. In this new series the solvent was changed to acetone in one group and the other group of membranes had the substrate presoaked in solvent before the polymer solution was cast onto the membranes. All other parameters remained the same. Figure 24 is of the composite membrane presoaked in the solvent acetone. The immediate difference one observed is the distinct layer of PDMS displayed on top of the substrate. This is a direct result, as the literature states, of the pores being completely filled before adding the polymer layer. Since the pores are filled, little to no polymer solution was able to penetrate the substrate, allowing for a proper PDMS layer to form on the substrate. The small amount of polymer penetrating the substrate cannot be avoided due to some solvent vaporizing before the polymer was added, but the distinction between the two layers is a result not seen in the other samples.

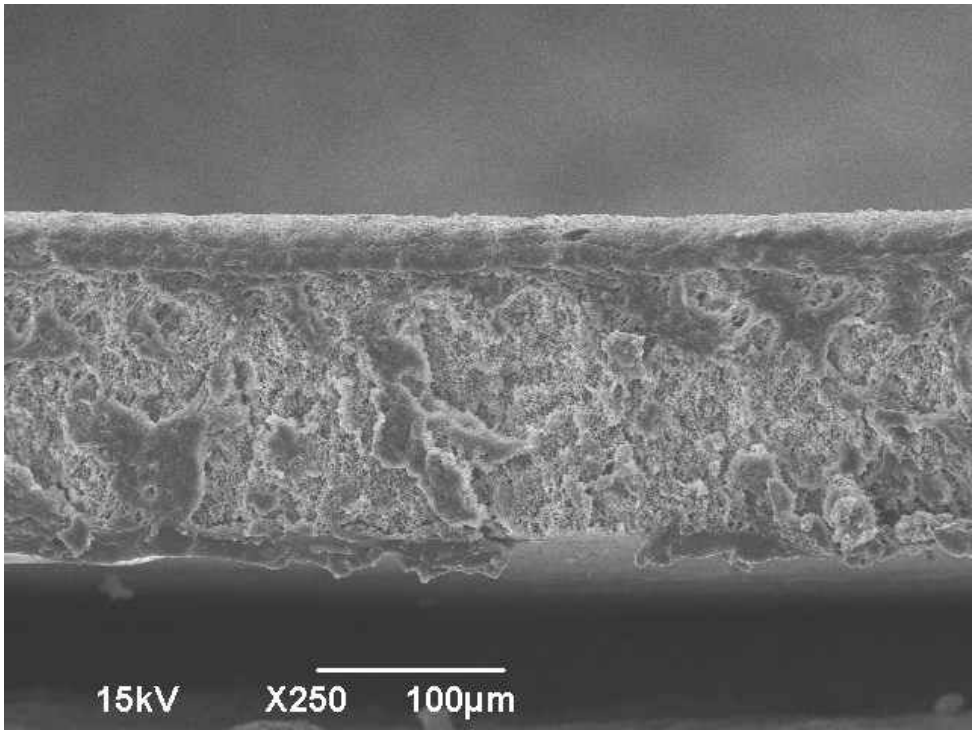

Figure 24: Polyamide Composite Presoaked with Acetone

Similar results were observed when a different solvent was used with a contact angle above 90°, as shown in figure 25. In this image, the definitive layers are like figure 24 but the layers are not as uniform as in figure 25. Also the interfacial layer is a lot larger than in figure 25. Another observation is that the layer is not as uniform as figure 25 leading us to conclude that the presoaked method should get better results for composite layer membranes using the spin coater method. The variation in these membranes are most likely because of the larger amount of solution which penetration the pores. Though the contact angle has improved over the previous samples, the pores are empty allowing for excess solution to penetrate the substrate. These membranes

were also tested for CO_2 permeability which, as expected, resulted in higher permeability than the previous membranes due to the thinner layer present on the membranes surface.

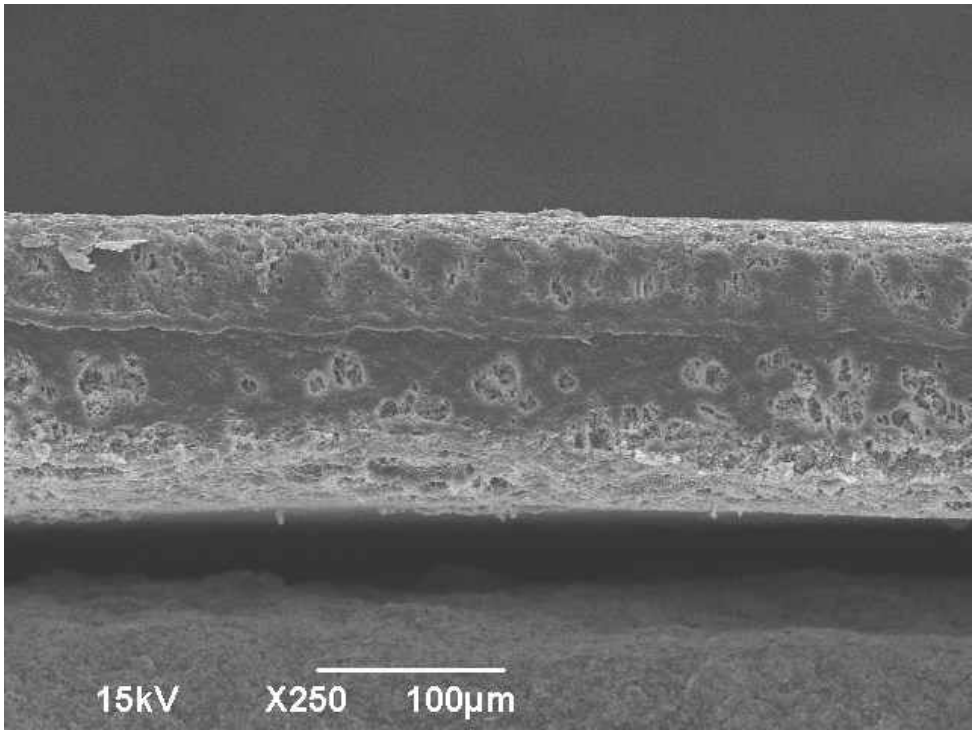

Figure 25: Polyamide cured with the Solvent Acetone

A comparison of gas separation permeability coefficients for the three series of polyamide membranes is shown in figure 26. Series 1 is the original permeability coefficient from the membranes tested in figure 13B. Series 2 is the coefficient from testing the membrane in figure 24 which was presoaked in solvent and lastly series 3 is the coefficient from the membranes made with a different solvent figure 25. The increases in series 2 are a direct result of the removal of defects in the composite membrane, visible through comparison of the two images. The third series was an

improvement on the 1st but because of the variability in the PDMS layer permeability, they were not as high as the values in series 2.

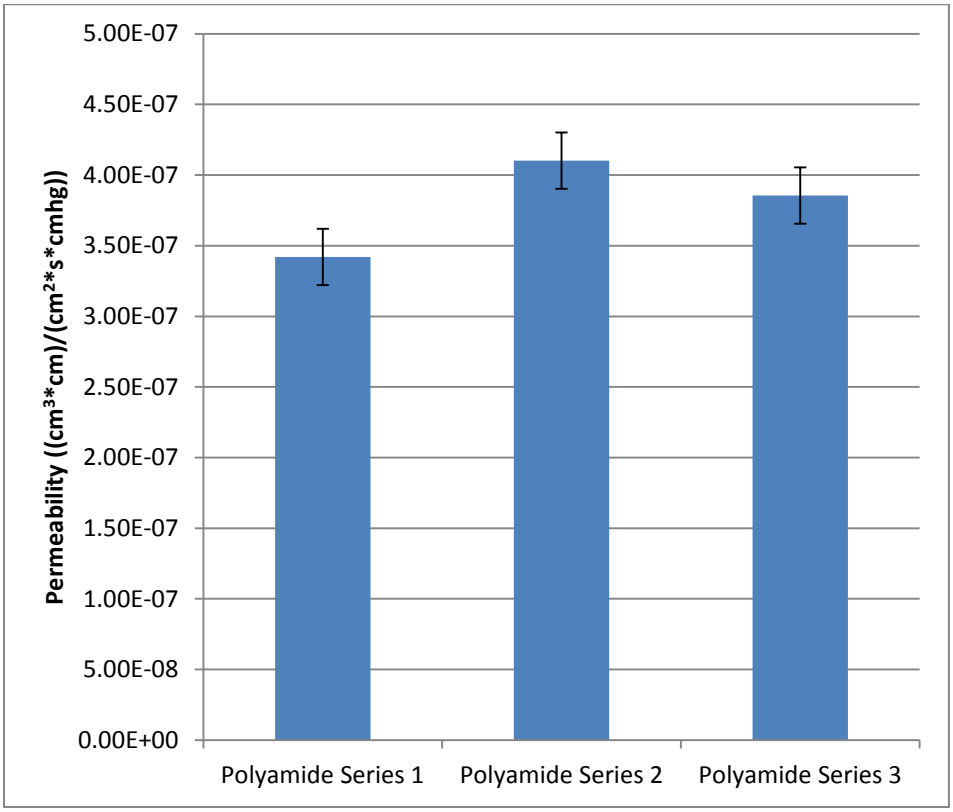

Figure 26: Comparison of All Polyamide Composite Membranes Permeability

Based on the information gathered from the SEM images for all the membranes tested, it was decided that the membranes to be tested in the pervaporation system would include PVDF, polyamide, PES and polyester. Though the polyamide runs will provide the most useful information, the other membranes were tested for better understanding of the composite membrane behavior for future purposes. Full size SEM images of all these membranes and all others tested in the gas separation process are available in appendix D.

Pervaporation Results

Since temperature is known to have a large effect on flux due to a decrease in CO_2 loading in the MEA solution with increasing temperature, runs were conducted with varying temperature to observe it's behavior on the flux as well as verifying its effects on selectivity. The composite membranes selected from the gas separation screening were created and tested in the pervaporation system from figure 10. An aqueous 15wt% solution was pre-absorbed and saturated with CO_2. The solution was at a pumping speed of 330ml/min and was verified for no leaks at room temperature before increasing the temperature and changing the system to an operating pump speed of 180ml/min. The CO_2 flow rate was held steady at 400 standard cubic centimeters (sccm) to feed CO_2 to the absorption tank and keep the solution saturated with CO_2. Nitrogen sweep gas flowed steadily from the bottled cylinder at a rate of 500 sccm. The Li-Cor 820 CO_2 analyzer recorded CO_2 concentrations every 5 seconds. Selectivity was also calculated during each of the temperature set points. Water flux was calculated by collecting water samples from the retenate for fixed periods of time and dividing by the membrane area. Selectivity was then able to be determined by the ratio of the CO_2 flux and the liquid flux. Values for flux and selectivity at 80°C are displayed in table 5 with all values over the entire temperature range available in appendix E.

Table 4: Composite membranes flux and selectivity

Material	Thickness (mm)	CO_2 flux ($cm^3/(cm^2 s)$)	Liquid flux ($cm^3/(cm^2 s)$)	Selectivity
Polyamide	0.114	3.23±0.2	0.063	51.2
10um PDMS/Polyamide	0.114	0.474±0.06	0.057	8.31
20um PDMS/Polyamide	0.119	0.450±0.04	0.072	6.22
Acetone /Polyamide	0.117	0.522±0.05	0.035	11.2
Presoaked Acetone/Polyamide	0.119	0.549±0.05	0.049	9.24
Polyester	0.013	2.89±0.12	0.003	1120
10um PDMS/Polyester	0.025	0.560±0.03	0.004	160
20um PDMS/Polyester	0.038	0.450±0.08	0.004	114
PVPF	0.102	3.26±0.18	0.052	62.5
10um PDMS/PVPF	0.107	0.490±0.05	0.048	10.2
20um PDMS/PVPF	0.114	0.450±0.03	0.046	9.77

Table 3 shows that all the composite membranes had reduced CO_2 flux with relatively no change to water selectivity. The PDMS layer becomes the selective layer significantly reducing the CO_2 and liquid flux [63]. Deposits can still be seen on these membranes from comparison of before and after images of the pervaporation process as seen in figure 27.

Figure 27: Before (left) and after (right) pervaporation image of polyamide composite membrane

Variations in the Polyester results were probably the result of the PDMS layer not forming properly. Some CO_2 may have passed on through PDMS while other molecules went through PDMS and polyester substrate which could have varied the reading to a great degree as previously explained for gas separation, since both processes have similar driving forces. The polyamide and PVDF composite membranes both warrant further study for use in solvent regeneration processes, based on their flux behavior. New casting methods and refining the membrane formation process based on the results of this study can yield better membranes with more conclusive results.

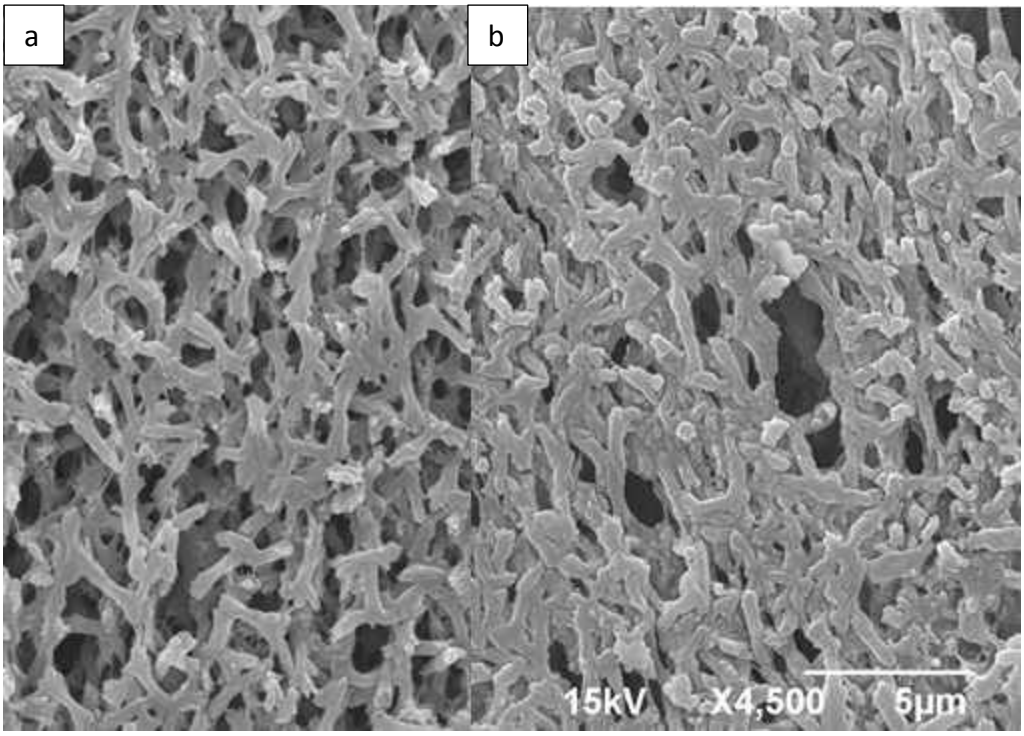

Figure 28: Surface view 10 a) Polyamide before pervaporation b) polyamide after pervaporation

Figure 28 is a comparison of polyamide substrate before and after the pervaporation process, they are both surface images of the 10µm polyamide samples. Both images were taken at the same magnification to compare differences, no major deposits or fouling was displayed through SEM imaging. Figure 29 is a comparison of the 20µm composite membranes before and after pervaporation. This figure confirmed what was displayed through figure 28: little to no major deposits where observed through the process.

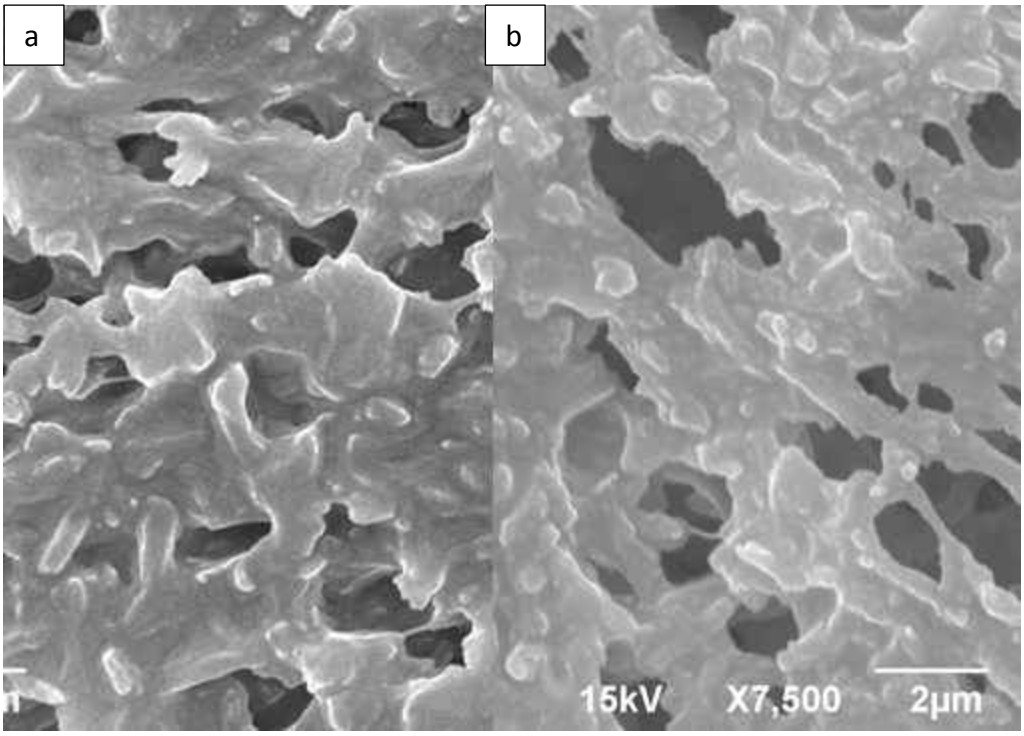

Figure 29: a) before pervaporation 20µm composite polyamide membrane b) after pervaporation same membrane same magnification

The polyamide composite membranes have potential in the solvent regeneration process. Polyamide has good mechanical and thermal properties and has the potential to be a great support for the extremely flexible PDMS. The benefit of its low surface energy allowed for the composite layer to form but thanks to its hydrophobicity it prevents excess water from leaking during the pervaporation process, as shown in table 3. The presoaked PDMS showed improved behavior over the previous results along with the composite created from a different solvent. The data proves that these membranes should be investigated with simulation flue gas from a power plant to understand how these membranes behave in non-ideal circumstances.

Conclusion

In conclusion, composite membranes were tested for CO_2 separation using a pervaporation process and gas separation. The gas phase sampling along with SEM imaging of those membranes gave us our final candidates. New methods were developed to create the desired membranes after learning from the challenges from previous membranes. Some of the suggested new methods were tested and yielded membranes with improved films and better gas separation results. After pervaporation runs of polyamide, polyester and PVDF composite layer membranes, results showed that Polyamide and PDVF has promising results that deserve further study. Further analysis into casting method, solvent choice and substrate surface energy and porosity can potentially yield more effective membranes for CO_2 separation.

CHAPTER IV

MEMBRANES BASED ON HYPERBRANCHED POLYMERS

Introduction

Hyperbranched polymers and dendrimers are of interest in regards to CO_2 permeability for many reasons. Jianhua Fang proved in his study of polyimide membranes that hyperbranched polymers increased the permeability of CO_2 to nitrogen. These membranes were created by polyimide HBP's which was cross-linked into tris(4-aminotphenyl)amine (TAPA), 2,2-bis(3,4-dicarboxypheny)hexafluoropropane dianhydride (6FDA), 3,3',4,4'-diphenylsulfonetetracarboxlic dianhydride (DSDA) and pyromellitic anhydride (PMDA)[64, 65]. In liquid membranes A. Sarma Kovvali and K.K. Sirkar found that dendrimer liquid membranes caused an increase in CO_2 separation from gas mixtures [66]. Though studies have been done to examine the effects of dendrimers and HBPs separately on permeability not many have been done on the effects of being incorporated into the membrane formation. The theory behind why these hybrid membranes should have increased permeability is because of the symmetric and non-symmetric properties of the branching groups. These membranes should contain random branching's and those branches should contain numerous end

groups. Membranes containing large non-symmetric end groups tend to have large internal voids within the structure, low viscosities and exhibit polymeric and colloidal behavior. The large internal voids which result from non-symmetry have the effect of increased permeability due to the fact that the targeted molecules are able to slip between the large void spaces. Separation is still achieved because of the polymer matrix which is responsible for separation. This study looked at incorporating HBPs into thermosetting polymers and observing their behavior. This study will examine the HBPs membranes made of Boltorn H2004. The structure of Boltorn H2004 is shown below in the figure 30.

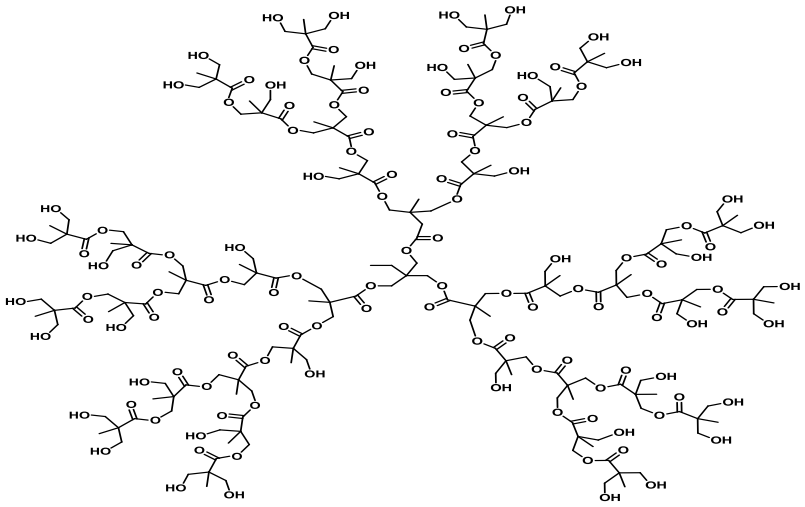

Figure 30 Chemical Structure of Boltorn

Boltorn was optimal for this experiment because of its high hydroxyl functionality. It is a polymer with a highly branched flexible backbone and has high solubility in glycols, ethers, alcohols, ketones, and aromatic solvents. Desmodur was used more for its hardening capabilities and its high resistance to chemicals. Various

ratios of these two polymers were added into polyurethane to evaluate the effects it has on permeability of CO_2.

Materials

The materials and preparation of these membranes began by first creating the dendrimer crosslinker. Boltorn H2004 (Perstorp Chemicals AB, Sweden), a dendritic polymer with high hydroxyl functionality, was mixed with Ethyl 3-ethoxy propionate(EEP) (Dow Chemical), a reactive ester, in the presence of BYK(Sino-composites INC), an air release additive, to remove excess air from the solution. The solution after mixing was then added in different concentrations to a polyurethane membrane solution. The polyurethane based membrane solution consisted of Joncryl 906 (72% solids) (BASF corporation) as the base polymer with p-toluenesulfonic acid (Sigma-Aldrich Inc.) as the initiator and resimene 755 (INEOS Melamine's) as an assist curing agent to the membrane in a ratio of 1:05:25 and a varying degree of crosslinker agent. After the membranes cured they were removed from the cover and left to dry at room temperature. The membranes were then cut to the design area for proper analysis and mailed to the UND for testing.

The membranes were formed by our partners at NDSU using the materials provided. Membranes in the first section varied in Boltorn composition by 5, 10 20 and 25 wt.% and specific ratios and weights of all materials used are available in table 3. The second series of membranes varying Boltorn between 0, 10 20 30 40 50 wt.% Boltorn were made using the compositions indicated in Table 2 shown in the appendix C.

Method

To determine flux and eventually calculate the permeability of the membranes provided by NDSU, a system was created consisting of a mass spectrometer, two pressure gauges a mass flow control and a membrane holder made of 316 stainless steel from Millipore Corp. The apparatus used to determine membrane permeability is shown in figure 31. The membrane holder was designed for gas inlet and outlet ports to allow for the proper transport of feed, permeate and retentate streams. These membrane holders were designed ideally for filtering off gasses and liquids and are capable of handling inlet pressure of up to 275 PSI. Stainless steel was used to create the holder. This metal allowed for the filtration of highly reactive and corrosive gases. The holder also contains a back pressure support screen which prevents back pressure surges. To ensure no leaks occurred around the edges of the membrane holder and the membrane interface, a Neoprene rubber “o” ring greased with Dow Corning high vacuum grease was used for a leak tight seal. All piping used to enter and exit the membrane holder was 1/16 inch polyethylene tubing. CO_2 flowing into the top chamber was pure highly pressurized CO_2 provided by Praxair, Praxair also provided the nitrogen carrier gas (N_2). Purity of the carrier gas was verified by the mass spectrometer before actual runs. The carrier gas was connected to a mass flow controller provided by Alborg Inc. to ensure constant flow of carrier gas during experimental runs. Pressure gauges where installed on the membrane holder to verify bottom pressure while the top

chamber was ventilated to atmospheric pressure. Permeate gas from the lower chamber flowed directly to the mass spectrometer where analysis of its composition took place. After analysis all gases were ventilated to atmospheric pressure.

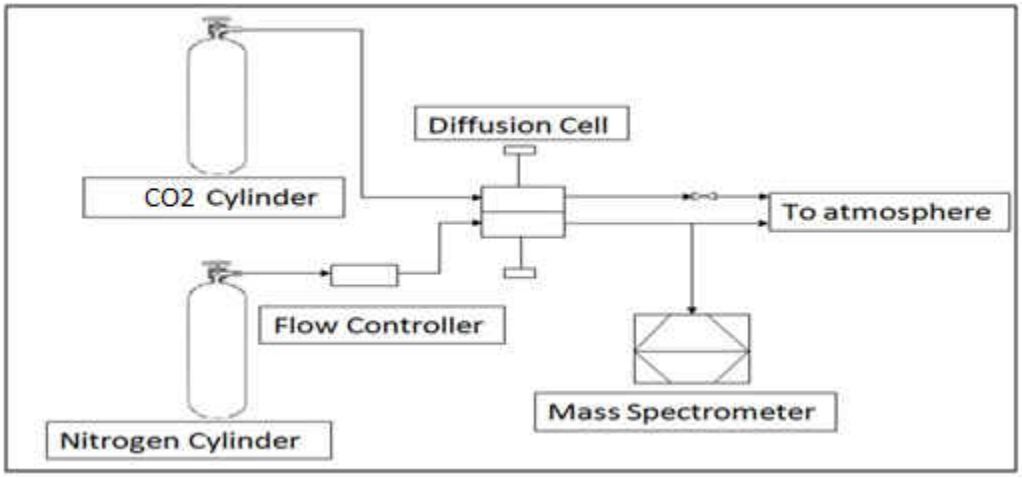

Figure 31: Experimental apparatus used to determine the properties of HBP's

.

Mass Spectrometer

The mass spectrometer was made by Pfeiffer and came equipped with residual gas analysis (RGA) software for proper analysis of the permeate stream.

Experimental runs took place to keep a constant flow of 10ml/min of carrier gas flowing through the bottom chamber of the membrane holder. After several hours a constant flow of N_2 gas was established by the mass spectrometer. This step was necessary to ensure no other gasses were present in the top chamber and a proper analysis of the carrier gas was conducted. After a steady state was achieved, CO_2 was slowly allowed to flow in the top chamber and after several more hours a new steady state was achieved for the permeate from the bottom chamber due to the amount of

CO_2 that was allowed to permeate through the given membrane. The change in CO_2 was recorded between the two steady states and was used for permeability calculations. A typical example of the results for the mass spectrometer is shown below in figure 32.

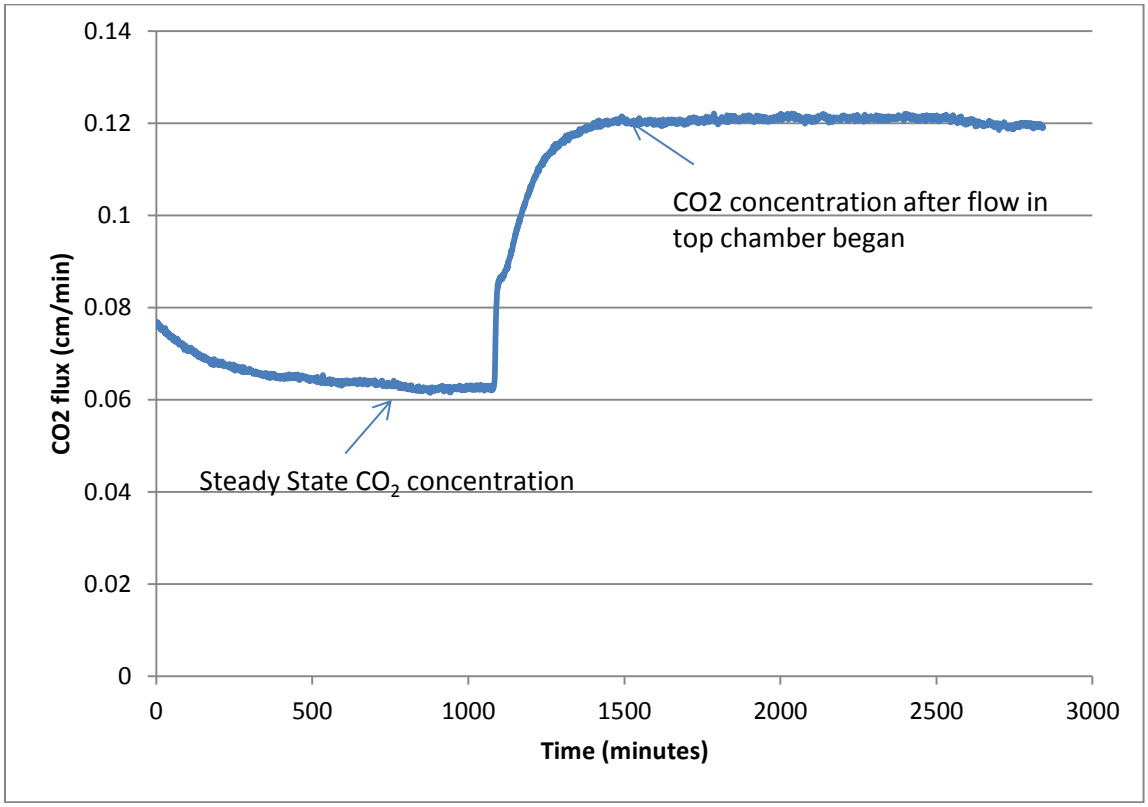

Figure 32 Sample example of Mass Spectrometer results for CO_2 Permeability measurements

Results and Discussion

Figure 33 shows the permeability as a function of HBPs in the first series of membranes. The x-axis represents the weight composition of Boltorn in the membrane and the y-axis shows the corresponding permeability for the given membrane composition of Boltorn.

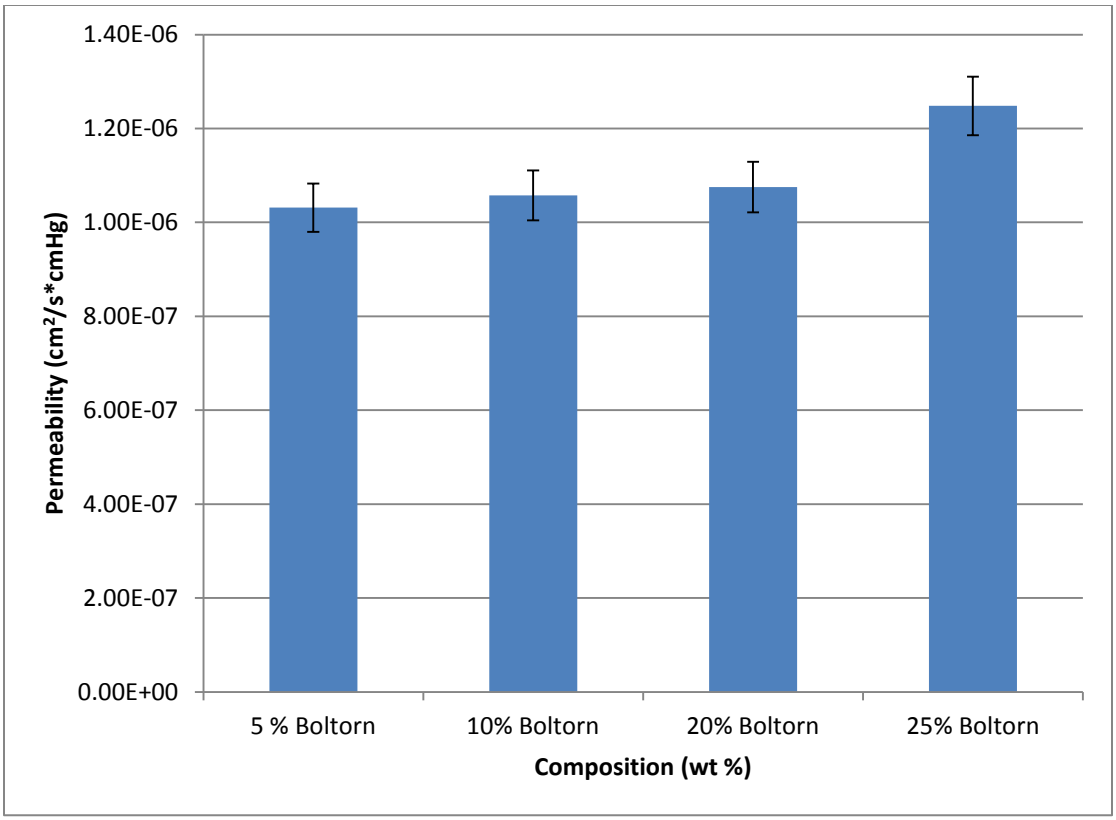

Figure 33: Permeability vs. Composition graph for HBP's

The data above suggests that permeability of CO_2 increased with increasing amounts of Boltorn and a much larger increase is displayed between 20 and 25% Boltorn. The error bars represent the standard deviation for each of the various samples. The increased permeability is an effect of the added void spaces created in the membrane matrix by the addition of the HBP group. The increasing compositions on the x-axis represent a weight percent increase in the amount of HBP added. Figure 30 shows Boltorn which was added to polyurethane, as the concentration increases within polyurethane there is an increase in free volume in the polymer. This can be seen from figure 30, when trying to imagine moving one of those molecules anywhere inside

another polymer's structure. This improved free volume which is the result of this addition allows for improved permeability which is shown in figure 8 while separation is completed inside the PDMS layer. The voids appear to allow for slightly increased amounts of CO_2 to permeate through. Similar results were found in a study where Junichiro Hayashi attempted to improve permeance and per selectivity of 3,3,4,4,-biphenyltetracarboxylic dianhydride-44-oxydianiline [67]. In his study they found that increases in permeance of CO_2 were mainly dependent on pore-size distribution of the polymer within the membrane. The sample here mirrors the trend found in Hayashi's data. The membranes containing the lower concentrations of HBP have a structure similar to pure polyurethane due to the network formation linking of HBPs to polyurethane thus leaving the lower concentration with values for permeability equal to that of polyurethane CO_2 permeability value. As the amount of CO_2 increases so do the void spaces, which leads the material to have behavior that varies from the polyurethane value. This behavior would be expected to increase until reaching a maximum value. That maximum is hypothesized to be around the 25% mark but without data for membranes with higher concentration than that, it cannot be confirmed.

As the concentration of HBPs increase the void spaces within the polymer matrix increase which leads to larger amounts of CO_2 to permeate. Hydroxyl terminated polyurethane has bonded with the HBPs forming a hydrogen bond thus retaining the HBPs into the polymer matrix and creating an extra interstitial chain space. These bonus chain spaces lead to increased free volume which allows for permeability to increase.

Further study must be conducted to see if and when the membranes would reach a maximum permeability as compared to other data [67]. Polyurethane could potentially have a maximum CO_2 permeance at a higher concentration of Boltorn but more data is required to confirm this. These findings suggest similar trends to data found in other studies, but future studies would be needed to confirm this. Further study into how HBPs affect the selectivity could help gain an understanding of which types of applications these membranes could be applied to but unfortunately the gas separation system at UND is not designed for selectivity analysis.

Polyurethane HBP membranes were fabricated at NDSU. These membranes were created with varying concentrations of Boltorn and tested in a gas separation system. The addition of HBPs into the polyurethane membrane matrix has led to higher permeability values. The data shown in figure 9 suggests an underlying pattern of increasing CO_2 permeability with increased amounts of HBP. Looking at figure 27 one notices that the increased permeance is very small, almost insignificant, until the 20-25% range. This observation can be attributed to the amount of void space added by each percentage increase. Though Boltorn is a very large monomer group the amount of space added into the polymer matrix may not be significant enough to increase the permeability of the membrane significantly. Only through higher percentages of Boltorn does the effect become significant enough to notice. The results from this study suggest that higher concentrations of Boltorn should be added to polyurethane to see if the suggested trend continues or if other trends are observed. Different HBPs can also be

crossed linked to polyurethane and observed for CO_2 behavior. By adding larger monomer groups or groups with larger branches to the base polymer, one might observe larger permeability changes for small concentrations of HBP. Future work could also investigate the strength of these types of membranes. It was observed during testing that these membranes were very brittle and often broke during experimental testing. A look into how HBPs affect strength and durability could help lead to finding a better relationship between crosslink HBPs and durability to create a longer lasting membrane.

Conclusion

In conclusion the results of this test proved successful. There was a trend of increasing permeability for the range of Boltorn added to the membranes tested. Future study into adding increased amounts of HBPs and strength tests for these membranes are needed.

CHAPTER V

SOL-GEL COATING EFFECTS ON PERMEABILITY

Introduction

Several industrial applications require the removal of carbon dioxide (CO_2) from flue gas streams. This process is of extreme importance to coal fired power plant processes. Different studies have been performed on various types of membranes and some which show promise have included membranes that have primary, secondary and tertiary amine moiety. Liguang Wu [68] performed a study on the CO_2 permeability of membranes containing tertiary amine groups. These membranes were made by copolymerizing 2-(dimethylamino)ethyl methacrylate (DMAEMA) and acrylonitrile (AN). These membranes showed CO_2 selective sorption behavior. In this study we investigated CO_2 permeability of 3-methacryloxypropyltrimethoxysilane (3-MPS) copolymers made with the addition of DMAEMA and or methyl methacrylate (MMA). The membranes were made by using a grafting technique in which pre-synthesized polymers (DMAEMA and MMA) are attached to a polymer backbone (3-MPS) which is originally grafted to organomodified clay. After this reaction had taken place the new groups were cross-linked and casted on PTFE substrates. Previous studies on 3-MPS have shown that simple organomodified clay compounds in varying ratios of 3-MPS

have led to increased permeability of CO_2 [69]. This study aims to take that research a step

further by adding polymer chains to the backbone of room 3-MPS monomer to better understand its effect of CO_2 permeability. The addition of these functional groups to the various methacrylate groups should add void spaces to the polymer matrix which increases the permeability due to the larger area in the polymer which CO_2 molecules are allowed to permeate through. The objective of this study is to understand the effect of backbone functionality (addition of DMAEMA and MMA) on the CO_2 permeability of 3-MPS coatings on PTFE.

Materials

Organomodified Clay (Sigma Aldrich Inc.) and 3-MPS (Polyscience Inc.) where mixed in the presence of acetone and side chance of either DMAEMA (Sigma Aldrich Inc.)or MMA(Sigma Aldrich Inc.) in 0,1,2,5,10% of clay loading with (4-Methoxyphenyl)phenyl Iodonium Triflate (MPIT) (Polyscience Inc.) used as an initiator. The solution was mixed 2 hours then tetraethyl orthosilicate (TEOS) (Sigma Aldrich Inc.)was used as a cross-linker for the DMAEMA solution and 3-aminopropyltrimethoxysilane(APTMS) (Sigma Aldrich Inc.) was used for cross linker in the MMA solutions. The membranes were then cured in the oven at 80^{o}C for 24 hours.

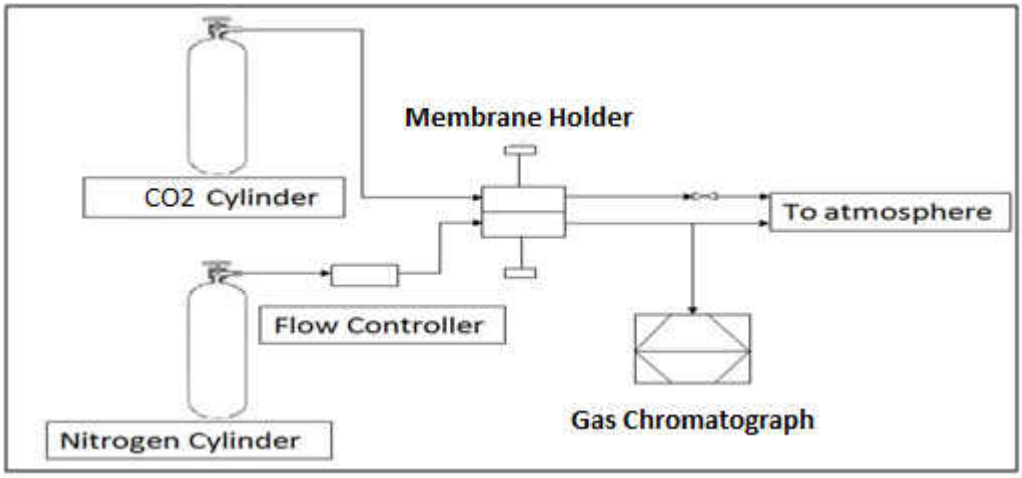

Figure 34 Apparatus used for gas separation analysis

Figure 33 above shows the system used in this analysis. In this setup all lines for the setup were made from ¼ inch plastic piping and diffusion cells created by Millipore Corporation. The cell included an in-line filter holder design to filter gases and liquids. Maximum pressure for this device was at 275 psi. The material used in the design of the chamber was 316-stainless steel which was chosen for its degree of withstanding aggressive fluids and gases.

The gas chromatograph used in the analysis was an Agilent 7890 series GC designed to include a packed column, equipped with two detector and thermal conductivity detector (TCD), and a flamed ionization detector (FID). The packed column was chosen for this type of separation because of its ability to separate nitrogen and carbon dioxide fairly quickly in a small amount of time. The use of two detectors ensures high sensitivity while providing the flexibility to monitor various gas membrane systems. The TCD was a standard type which detected the difference in thermal conductivity

between carrier gas with sample components and carrier gas alone and a detection limit of 100ppm. The FID came equipped with a methanizer to convert CO_2 into methane. This was necessary so the FID could detect hydrocarbon bonds at levels as low as .1ppm. The G.C. was also designed to include a split-splitless injection system which enhanced and allowed for more accuracy in analysis of a sample. The G.C. received continuous stream of permeate from the diffusion cell and took 1µL sample of permeate every 30 minutes until a steady state was reached. The system was monitored and controlled by chemstation software which came standard with the G.C. system. Operation procedures are provided in details in Appendix A.

Results and Discussion

Permeability values for DMAEMA membranes are shown in Figure 2. The x-axis represents the amount of clay loading in the sample and the y-axis shows the permeability values. After reaching the steady state condition, the permeability for each of the membranes was measured three times and averaged. The same method was applied for the coatings containing MMA and the results are summarized in Figure 35 and 36 respectively.

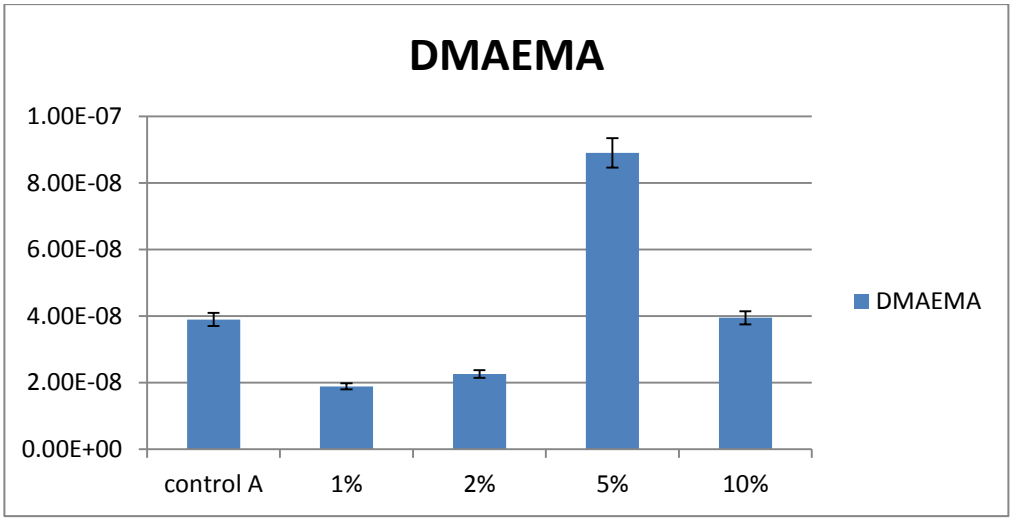

Figure 35 Permeability values for the DMAEMA membranes

The controls in each experiment represent pure polymer with no backbone functionality added. From comparison of the control the 1% value a slight increase in the permeability is shown for DMAEMA. As the amount of MPS begins to increase the permeability also increases. There is a very large jump between the 2% and 5% range but the values continue to level off at the 10% range. The data tends to suggest a slight trend of increased permeability with increasing amounts of DMAEMA. The trends in the DMAEMA values are not comparable to trends in the MMA experimental runs.

The 3-MPS coatings with the MMA added show a somewhat odd behavior. Between the initial control and the addition of MMA there was a slight drop in permeability. As the amount of MMA increases the same trend from the DMAEMA runs is witnesses where there is an increase in permeability then the permeability

again decreases before increasing again. The 10% percentage suggested the largest increase in permeability which could be due to the even larger amounts of voids in the coatings. Overall the data is inconclusive and more studies need to be understood to fully characterize the membranes before testing them in different systems. If defects or voids where present in the membrane's structure during creation the membrane's behavior could be affected. Miscibility of clay particles could also have an effect. Lastly inconsistent reparation techniques may have contributed to this phenomenon.

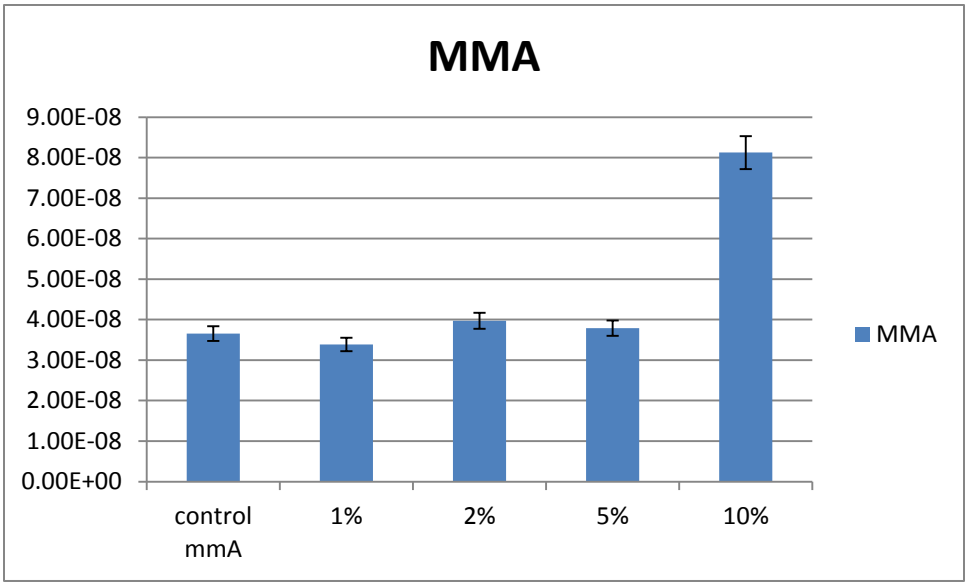

Figure 36 Permeability values for the MMA membranes

The aim of this study was to understand the behavior of adding monomer backbone chains to two different types of polymers. It was witnessed in both polymers that the additions of this chain in increased concentrations has led to increased permeability or suggest increasing trends toward CO_2 permeability. The general trend between these two polymers is different and must be observed with more details before solid

conclusions can be made. DMAEMA had a larger increase in permeability and this behavior can be explained through the addition of MPS. As the amount of MPS increased the polymer began to act more like a brand new polymer with properties more similar to MPS than the original polymer. Future studies should be performed with different host polymers to confirm with behavior with the MPS added. Also other curing techniques should be performed on the formation of these membranes to confirm behavior. By using different techniques the resultant polymer matrix formed from curing can be quite different thus affecting permeability but the hypothesis can't be confirmed without more tests.

CONCLUSIONS & RECOMMENDATIONS

The objective of the first series of samples was to observe the behavior of membrane performance with the addition of HBPs added to the backbone chain of polyurethane. It was expected that a trend of increasing permeability would be witnessed with an increased concentration of HBPs inside the polymer matrix. The data agrees with our hypothesis to a lesser extent. A small increase is witnessed through 20%, then the value jumps considerably. Figure 33 suggests that increased amounts of HBPs would continue to increase the CO_2. Further study is needed to confirm the continuing trend through larger concentration of HBPs and determine if a maximum point is reached when larger concentrations of HBPs will no longer have an effect on the permeance**.** Also a second look in HBP concentration effects on strength and durability of these membranes can yield more results.

Ideal gas separation methods where used to investigate the behavior of various composite polymer membranes. The results from these studies including the scanning electron microscope images from those runs showed that only three membranes had the potential to be applied to chemical solvent regeneration processes and those were composite PVPF, polyester and polyamide. The results of this study, including basic

operations from experimental runs, resulted in PVPF and polyamide having the potential to continued being studied for future applications.

The effects of adding 3-MPS into DMAEMA and MMA at different concentrations was monitored and observed. From this study are assumptions on the effects 3-MPS would have on DMAEMA were confirmed through the data. The results from the MMA runs were unclear. The uncertainty in those values could be the result of defects and voids in clay particles at the formation of the membranes in question, immiscible particles in the polymer phase or inconsistent preparation techniques. Transmission electron microscopy (TEM) analysis performed on the membranes yielding troubled data would help understand the process data from this work and give a clearer future on where this work should be headed.

This thesis has yet to prove that all highly branched polymers can increase CO_2 permeability, but data does suggest that incorporating highly branched polymers into the base polymers can have major influences on the permeability and selectivity of gas molecules. Due to availability and price advantages of hyperbranched polymers they have the potential to become a major controlling factor for perm-selective applications of polymeric membranes.

APPENDCIES

Appendix A
Sample Permeability Calculation

$$\frac{t_{ms} * \left(\frac{V * \%O_{2\,F} * A}{\%N_{2\,F}} - \frac{V * \%O_{2\,I} * A}{\%N_{2\,I}}\right)}{\Delta p} = P$$

$$\frac{0.0069\ cm * \left(\frac{0.5\ ml/_{sec} * 0.0303}{0.966 * 9.62\ cm^2} - \frac{0.5\ ml/_{sec} * 0.000703}{0.996 * 9.62\ cm^2}\right)}{50\ cm\ hg} = 2.08 * 10^{-7}$$

t_{ms}	Thickness of the membrane
$\%O_{2\,F}$	Percent of oxygen in the carrier gas, nitrogen, stream when steady state is reached before oxygen pressure increase
$\%O_{2\,I}$	Percent of oxygen in the carrier gas, nitrogen, stream when steady state is reached after oxygen pressure increase
$\%N_{2\,F}$	Percent of nitrogen in the carrier gas stream when steady state is reached before oxygen pressure increase
$\%N_{2\,I}$	Percent of nitrogen in the carrier gas stream when steady state is reached after oxygen pressure increase
A	Area of the membrane exposed to the permeating gas, 9.67 cm
V	Volumetric flow rate of the carrier gas, nitrogen, 10 ml/sec
Δp	Pressure difference of the top chamber and bottom chamber
P	Permeability of the membrane

Appendix B
Mass Spectrometer Procedure

1. Cut the membrane into a circle of diameter using an X-acto craft knife. The diameter of the membrane depends on the size on the size of the membrane holder. .
2. Place the membrane or the test specimen in the bottom chamber of the membrane holder.
3. Apply a thin layer of vacuum grease around the O-ring that goes around the membrane. This will help in ensure a good seal and prevent leakage.
4. Place the top chamber on the bottom chamber and screw in the three helix screws. The screws should be tight enough to make sure there are no leaks, but not tight enough to strip the threads of the bolts.
5. Check the pressure gauge on the mass spectrometer. If the pressure is below $1*10^{-4}$ mbar plug in the power card into the mass spectrometer to turn on the ion emission source. If the pressure is above $1*10^{-4}$ mbar the mass spectrometer needs maintenance.
6. Open the *RGA program* under the *QUADSTAR 32-Bit* folder in the computer attached in the mass spectrometer. The RGA stands for residual gas analysis and is the software used to run the mass spectrometer. The software will ask a few questions on startup about the mass spectrometer. Then proceed to selection boxes and to do so just click on the Proceed to Selection Boxes.

7. Click on the calibration sensitivity (Cal. Sens.) Button. This will determine the sensitivity of the mass spectrometer. Before the calibration you will need to enter the pressure of the mass spectrometer which is shown on the mass spectrometer LCD display screen.
8. Next, click on calibration offset (Cal. Offset*)* button. This will calibrate the amplifier offset. This will automatically determine by all necessary correction values to compensate offsets of the measure amplifier under different conditions.
9. Next, click on Mass Scale button. This will calibrate the mass scale. For accurate measure of the concentration of the gas mixture it is necessary to always measure at the peak maximum. Calibrating the mass scale will correct these deviations
10. Open the valves on the carrier gas cylinder and increase the pressure to 10 psi. The Pressure can be read on the pressure gauge attached to the gas cylinder.
11. Plug in the mass flow controller and increase the mass flow rate to approximately 90 ml/min. The bottom chamber must be completely filled with the carrier gas and must have reached a steady state before the top chamber can be pressurized with the permeate gas. This system can take several hours to reach steady state. Use the gas analysis, done by the RGA software, on the computer screen to ensure that the steady state has been reached in the bottom

chamber. If the permeate gas composition has reached zero or the composition is not decreasing anymore, the system is at steady state

Appendix C
Data from Hyperbranched Polymer Study

Table 5 Composition of HBP polymers

	Ratio	Amount Used
pg64a,64b		
Joncryl 507 (80 % solids)	1	5 g
pTSA (10 % sol. in MAK)	0.5 wt. % total solids	0.3 g
Resimene 755	25 wt. % of Joncryl/Boltorn	1.0 g
Boltorn H2004	None	0
pg93-1b, 93-1c		
Joncryl 507 (80 % solids)	1	5 g
pTSA (5 % sol. in EEP)	0.5 wt. % total solids	0.52 g
Resimene 755	25 wt. % of Joncryl/Boltorn	1.0 g
Boltorn H2004	5 wt. % based on Joncryl	0.25 g
EEP		0.52 g
BYK (50% in EEP)		0.025 g
pg93-2a, 93-2b, 93-2c		
Joncryl 507 (80 % solids)	1	5 g
pTSA (5 % sol. in EEP)	0.5 wt. % total solids	0.56 g
Resimene 755	25 wt. % of Joncryl/Boltorn	1.125 g
Boltorn H2004	10 wt. % based on Joncryl	0.5 g
EEP		0.56 g
BYK (50% in EEP)		0.025 g
pg93-3a, 93-3b, 93-3b		
Joncryl 507 (80 % solids)	1	5 g
pTSA (5 % sol. in EEP)	0.5 wt. % total solids	0.62 g
Resimene 755	25 wt. % of Joncryl/Boltorn	1.25 g
Boltorn H2004	20 wt. % based on Joncryl	1.0 g
EEP		0.62 g
BYK (50% in EEP)		0.025 g
pg93-4b, 93-4c		
Joncryl 507 (80 % solids)	1	5 g
pTSA (5 % sol. in EEP)	0.5 wt. % total solids	0.5 g
Resimene 755	25 wt. % of Joncryl/Boltorn	1.0 g
Boltorn H2004	None	
EEP		0.5 g
BYK (50% in EEP)		0.025 g

Table 6 Composition of Dendrimer Polymer

49a,49b,49c	Ratio	Amount Used
Joncryl 906	1	6.0 g
DBTD (1% in TBA)	0.01 wt. % solids	0.08 g
TBA (t-butylacetate)	25 wt. %	2.8 g
Desmodur N 3200	1.1	2.0 g
49d, 49e, 49f		
Joncryl 906	0.8	4.805 g
Boltorn H2004	0.2	0.967 g
DBTD (1% in TBA)	0.01 wt. % solids	0.078 g
TBA (*t*-butylacetate)	25 wt. %	2.6 g
Desmodur N 3200	1.1	2.0 g
49g, 49h, 49i		
Joncryl 906	0.7	4.22 g
Boltorn H2004	0.3	1.451 g
DBTD (1% in TBA)	0.01 wt. % solids	0.077 g
TBA (*t*-butylacetate)	25 wt. %	2.6 g
Desmodur N 3200	1.1	2.0 g
49j, 49k, 49l		
Joncryl 906	0.6	3.62 g
Boltorn H2004	0.4	1.934 g
DBTD (1% in TBA)	0.01 wt. % solids	0.075 g
TBA (*t*-butylacetate)	25 wt. %	2.5 g
Desmodur N 3200	1.1	2.0 g
49m, 49n, 49o		
Joncryl 906	0.5	3.02 g
Boltorn H2004	0.5	2.418 g
DBTD (1% in TBA)	0.01 wt. % solids	0.074 g
TBA (*t*-butylacetate)	25 wt. %	2.5 g
Desmodur N 3200	1.1	2.0 g
48a, 48b, 48c		
Joncryl 906	0.9	5.43 g
Boltorn H2004	0.1	0.48 g
DBTD (1% in TBA)	0.01 wt. % solids	0.08 g
TBA (*t*-butylacetate)	25 wt. %	2.7 g
Desmodur N 3200	1.1	2.0 g
48d,48e,48f		
Joncryl 906	1	4.84 g
DBTD (1% in TBA)	0.01 wt. % solids	0.068 g
TBA (t-butylacetate)	25 wt. %	2.3 g
Desmodur N 3200	1.1	2.0 g

Appendix D
SEM Images from Gas Separation Test

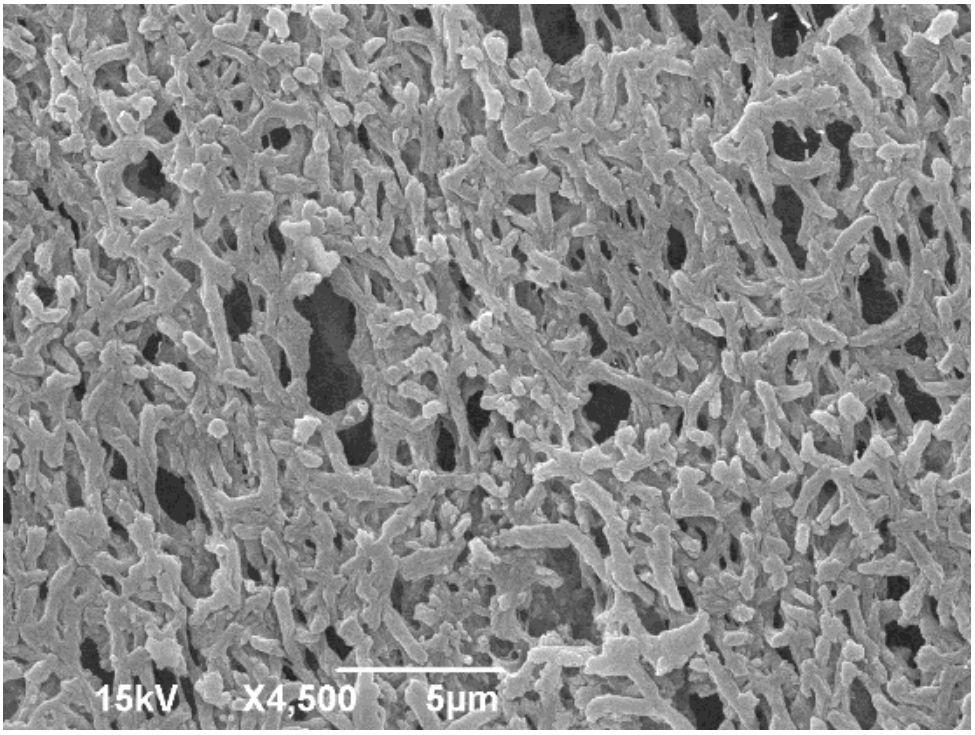

Figure 37: Polyamide No PDMS Surface view

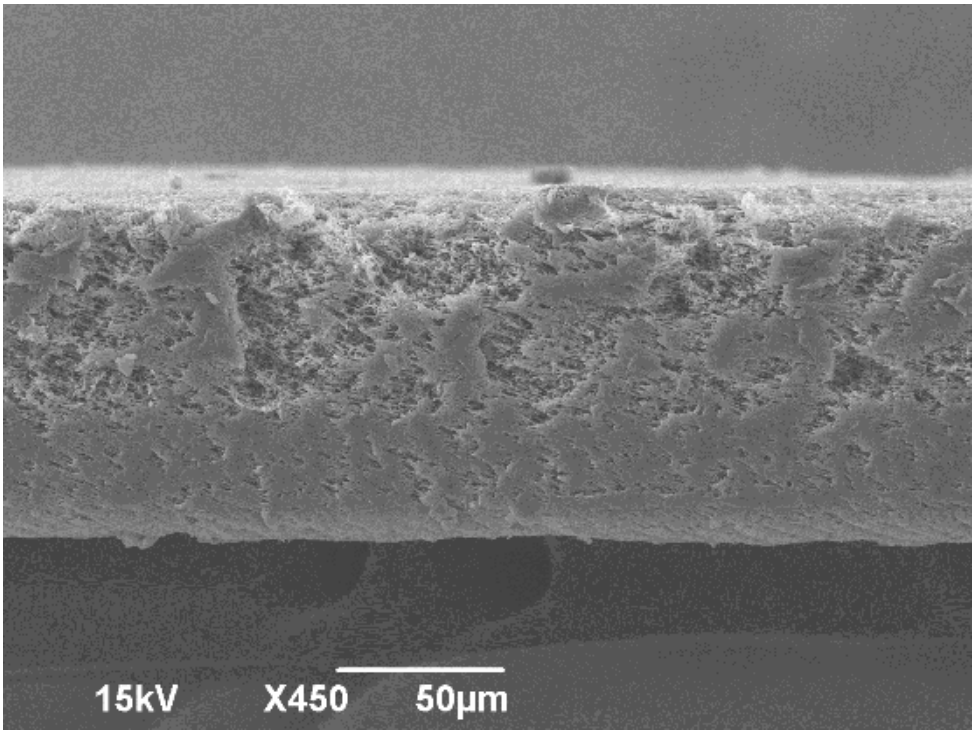

Figure 38: Polyamide No PDMS cross section view

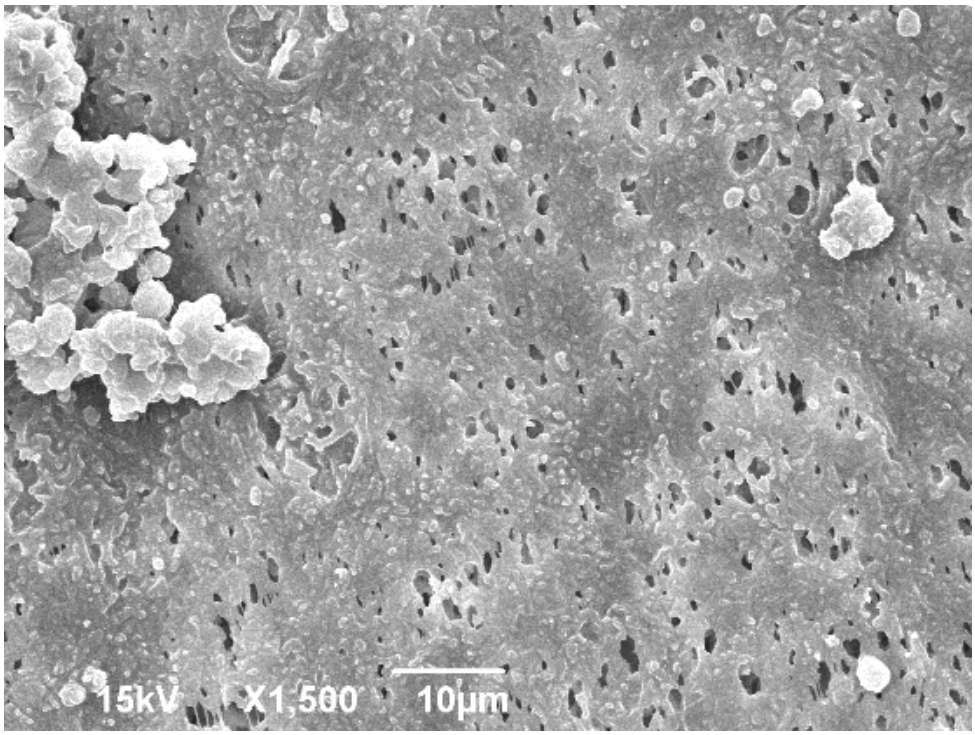

Figure 38: 10µm PDMS/Polyamide composite membrane at 1500 magnification top down view

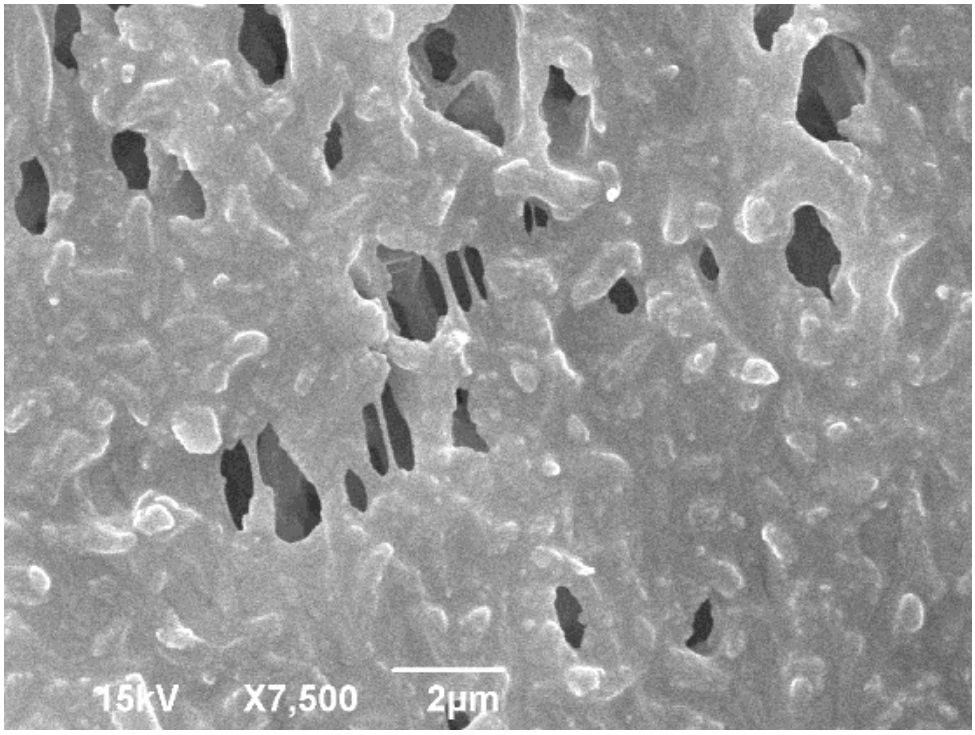

Figure 39: 10µm PDMS/Polyamide composite membrane at 7500 magnification top down view

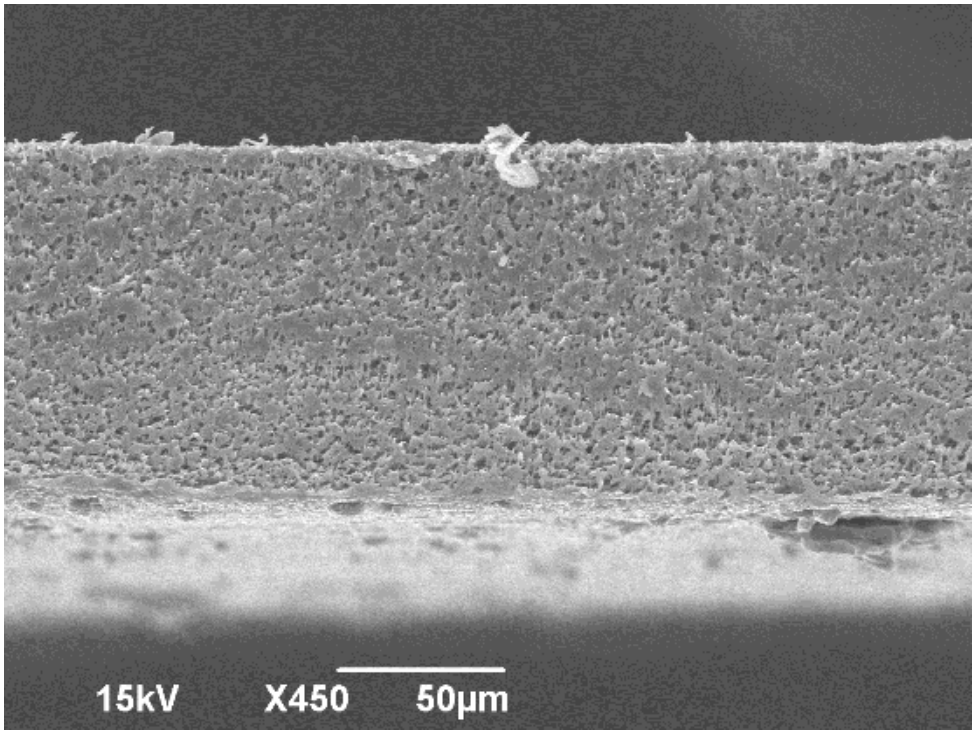

Figure 40: 10µm PDMS/Polyamide composite membrane at 450 magnification cross section view

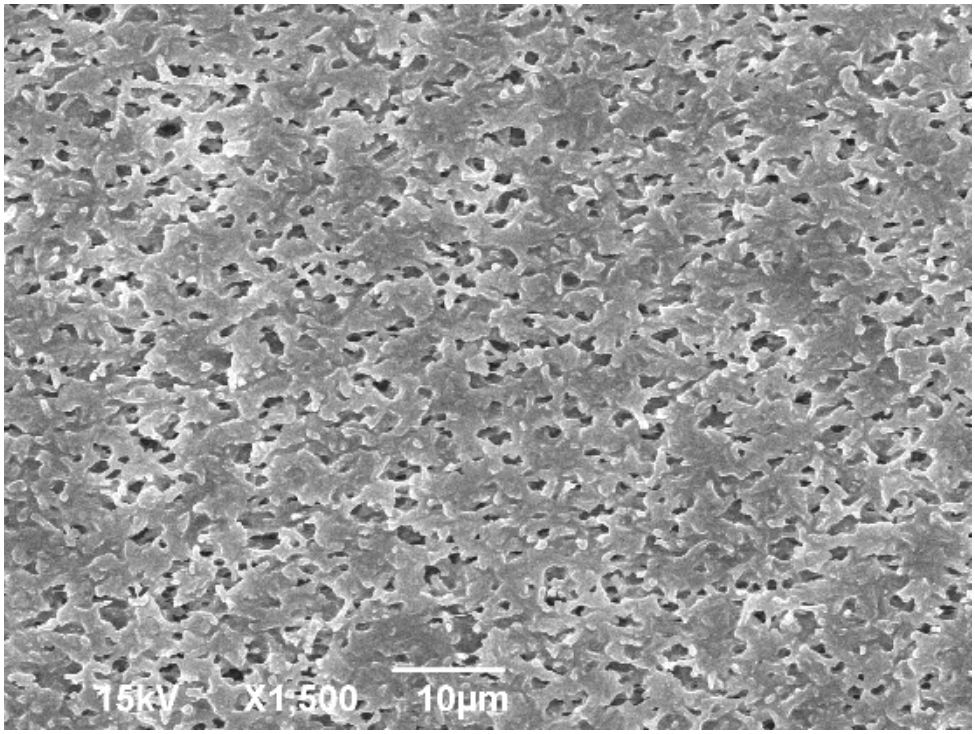

Figure 41: 20µm PDMS/Polyamide composite membrane at 1500 magnification top down view

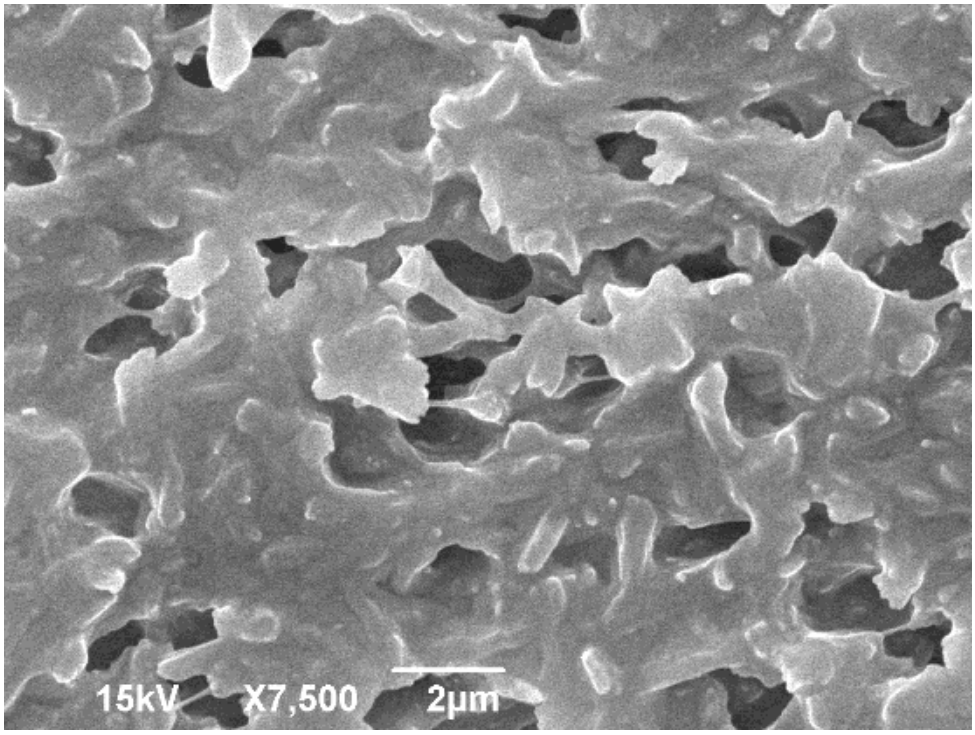

Figure 42: 20µm PDMS/Polyamide composite membrane at 7500 magnification top down view

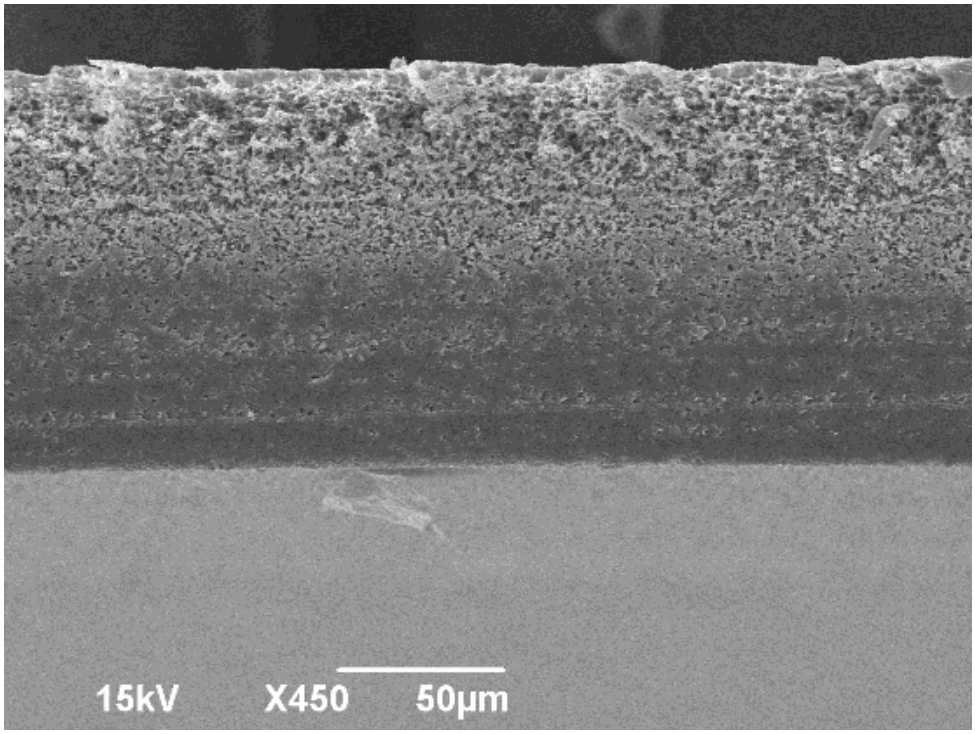

Figure 42: 20µm PDMS/Polyamide composite membrane at 450 magnification cross section view

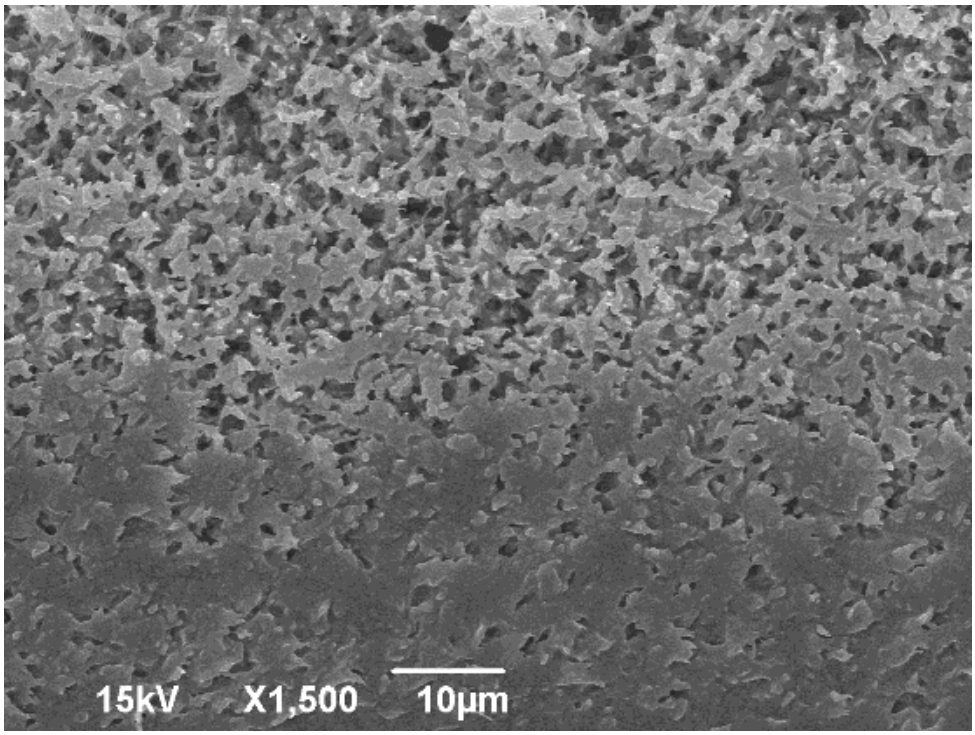

Figure 43: 20µm PDMS/Polyamide composite membrane at 1500 magnification cross section view

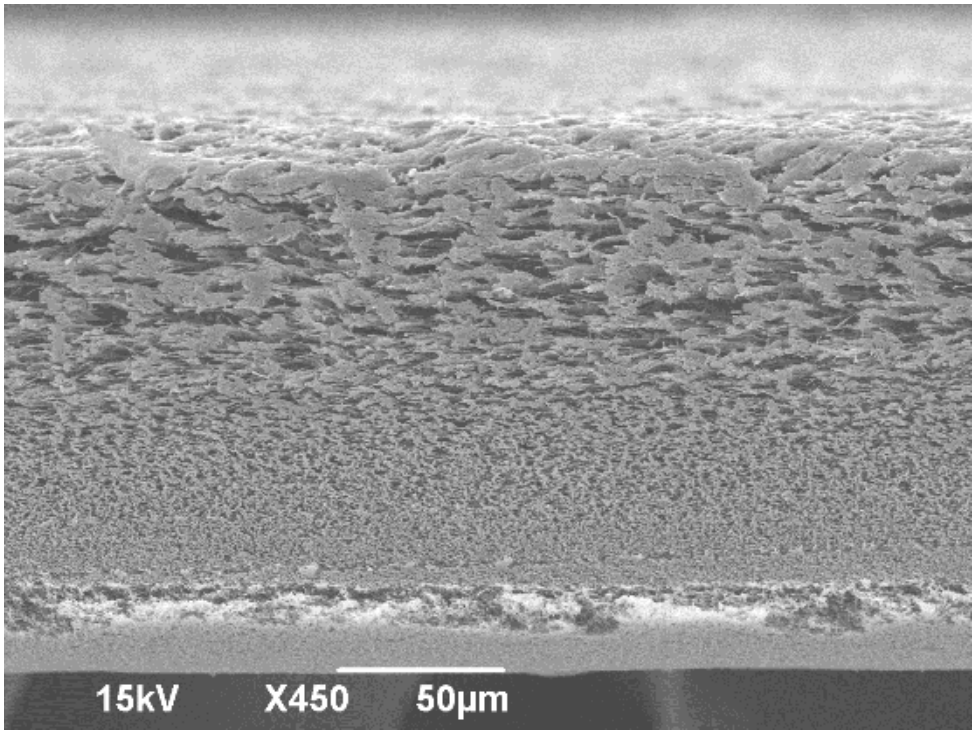

Figure 44: Uncoated PES at 450 magnifications

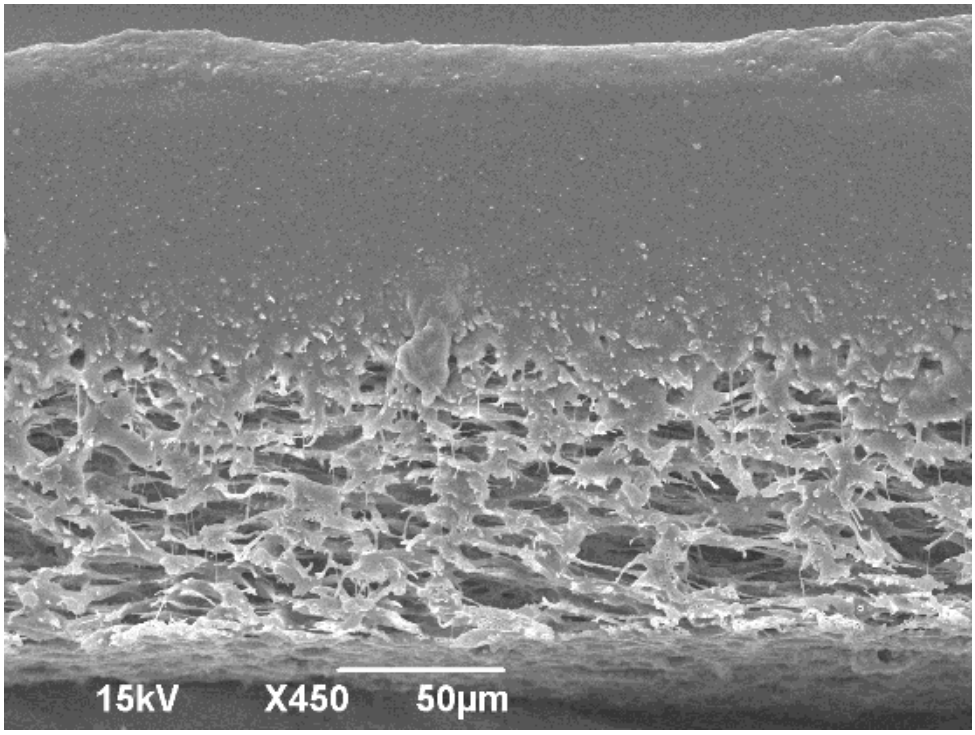

Figure 45: 10µm PDMS/PES 450 magnification

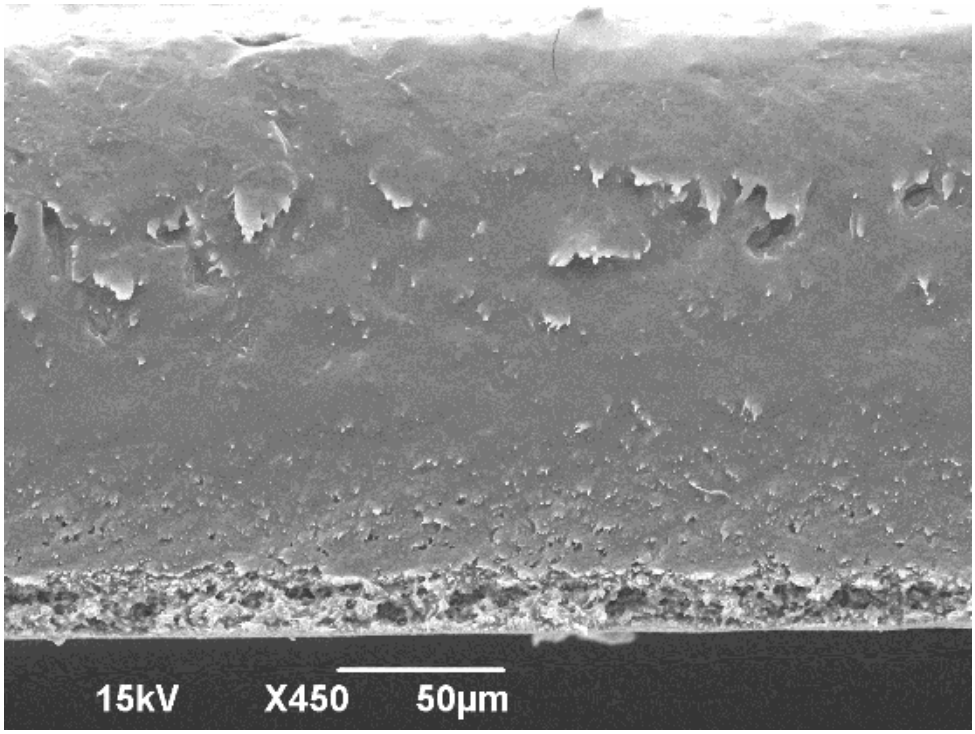

Figure 46: 20µm PDMS/PES 450 magnification

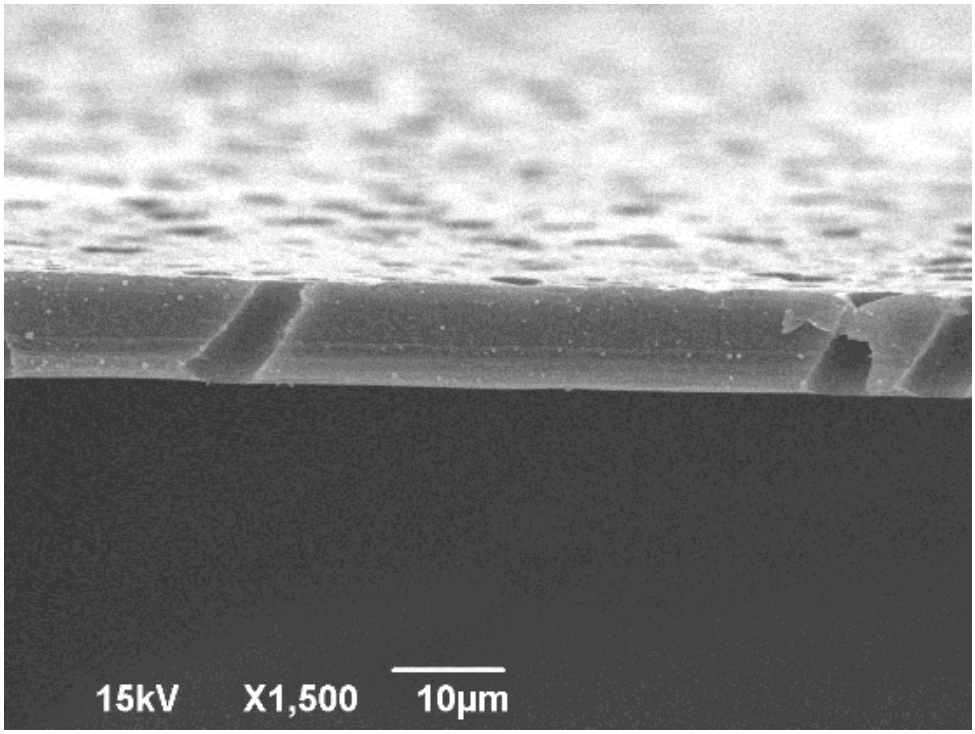

Figure 47: Polycarbonate substrate no PDMS 1500 magnification

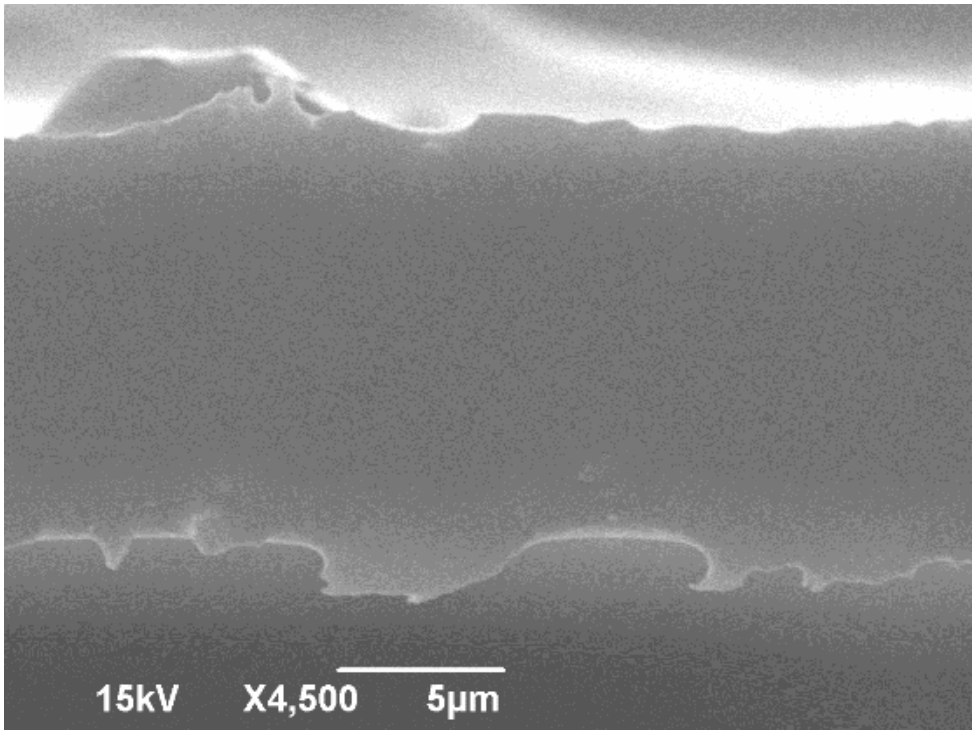

Figure 48: polycarbonate/PDMS composite membrane 10µm cross section view

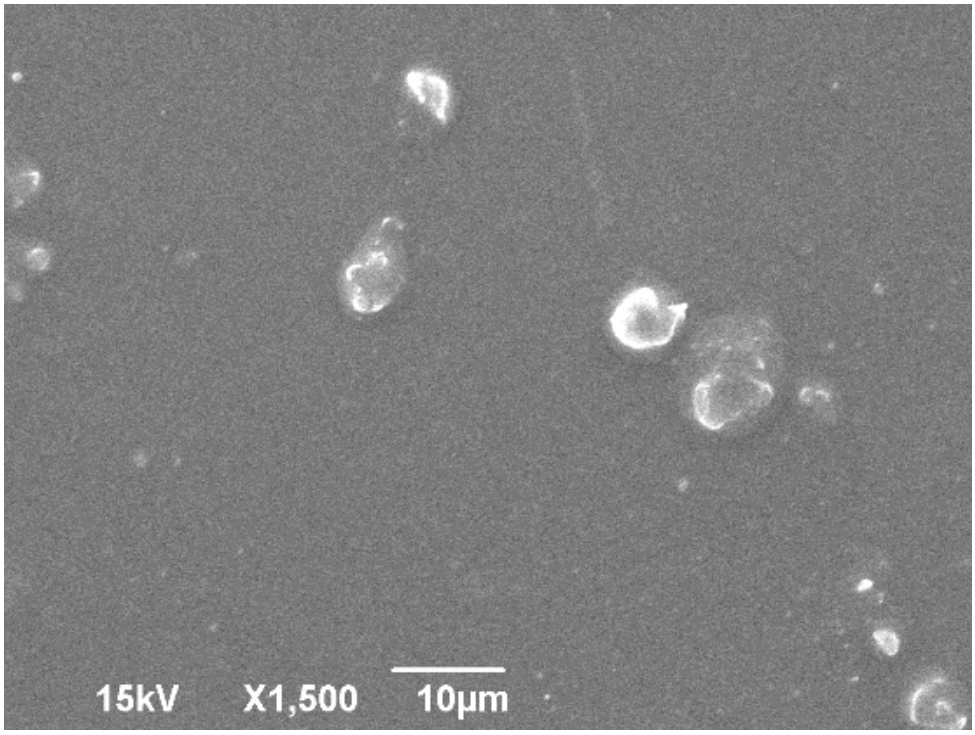

Figure 49: Polycarbonate/PDMS composite membrane 10µm Top down view

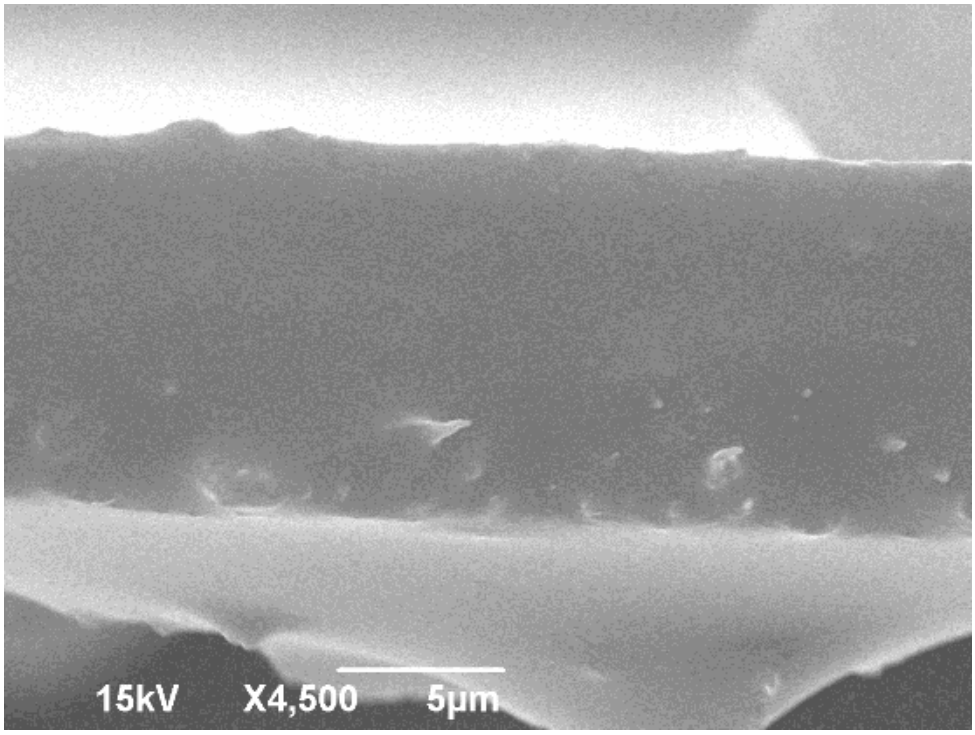

Figure 50: Polycarbonate/PDMS composite membrane 20µm cross section view

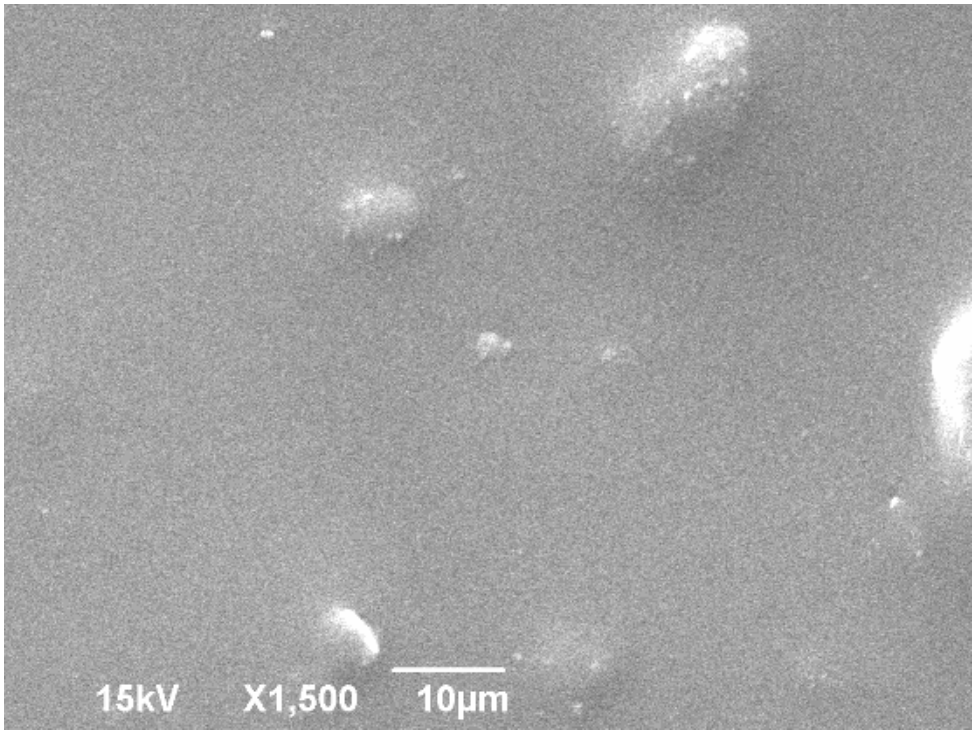

Figure 51: Polycarbonate/PDMS composite membrane 20µm top down view

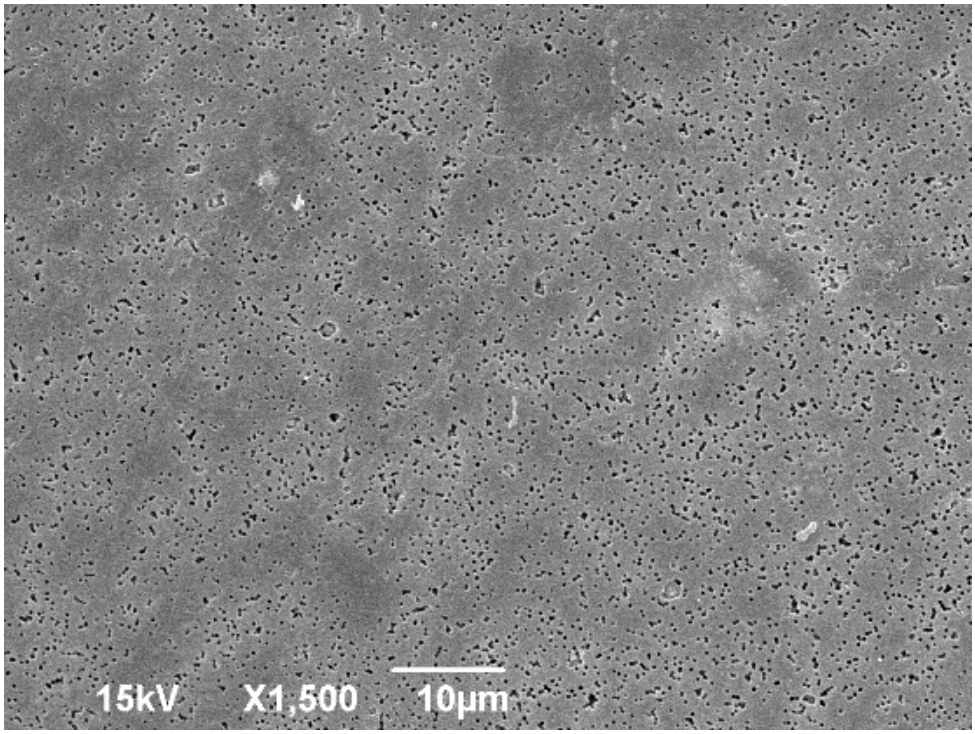

Figure 52: Top down view Polyester No PDMS 1,500 Magnification

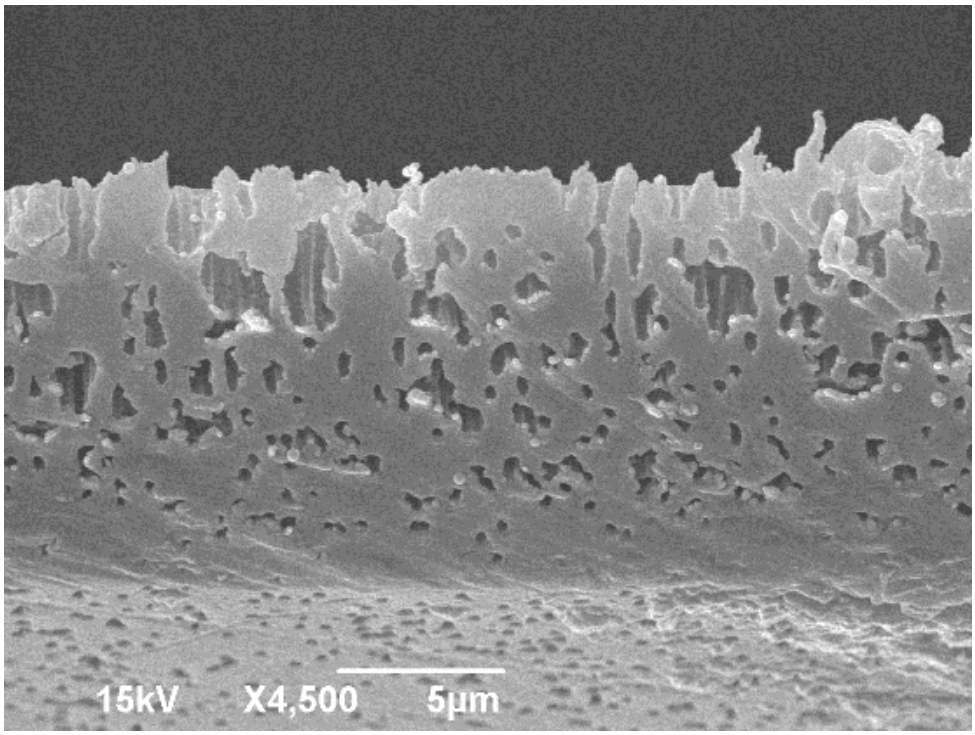

Figure 53: Cross-section view Polyester No PDMS 4,500 Magnification

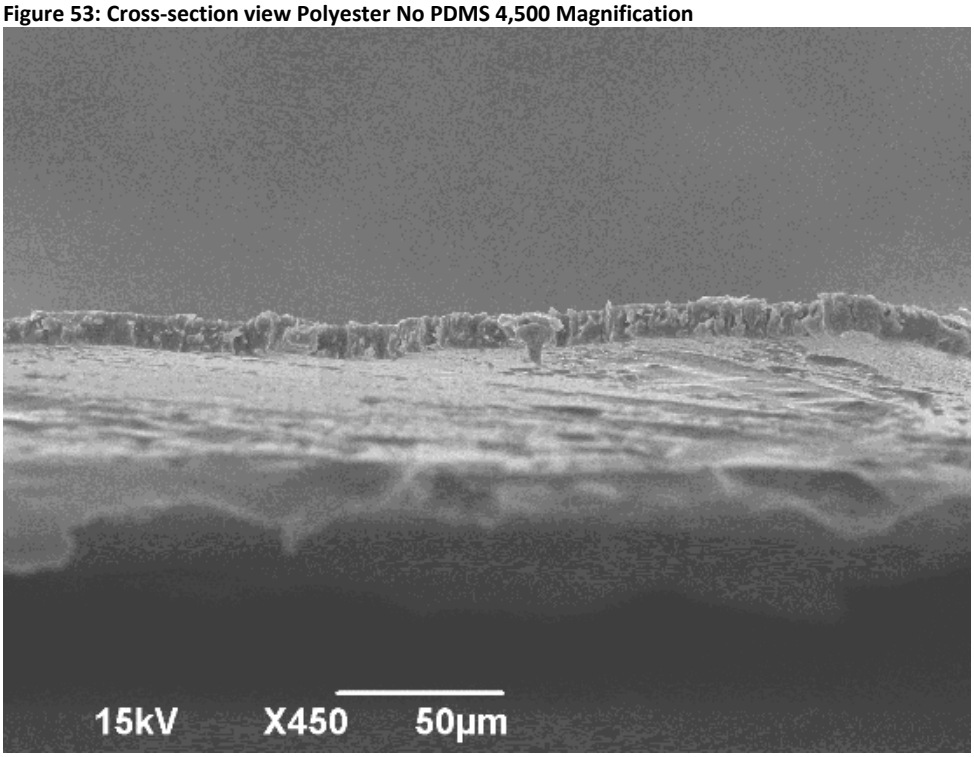

Figure 54: Cross-section view Polyester No PDMS 450 magnification

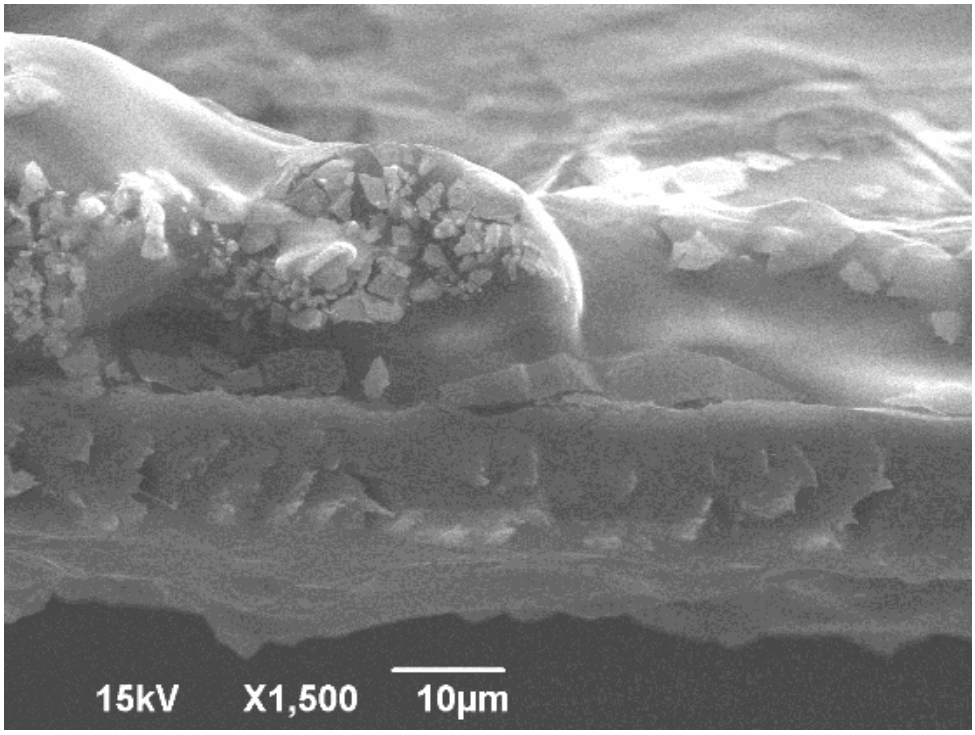

Figure 55: 20µm Polyester/PDMS 1,500 Magnification Cross section view

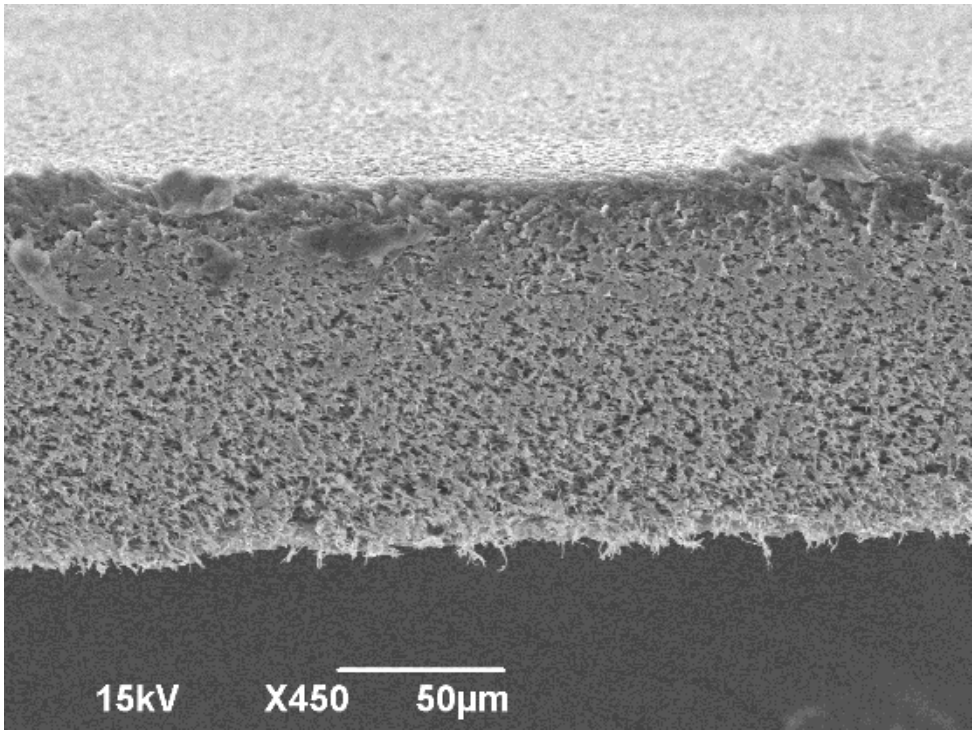

Figure 56: PVDF substrate No PDMS at 450 magnification cross-sectional view

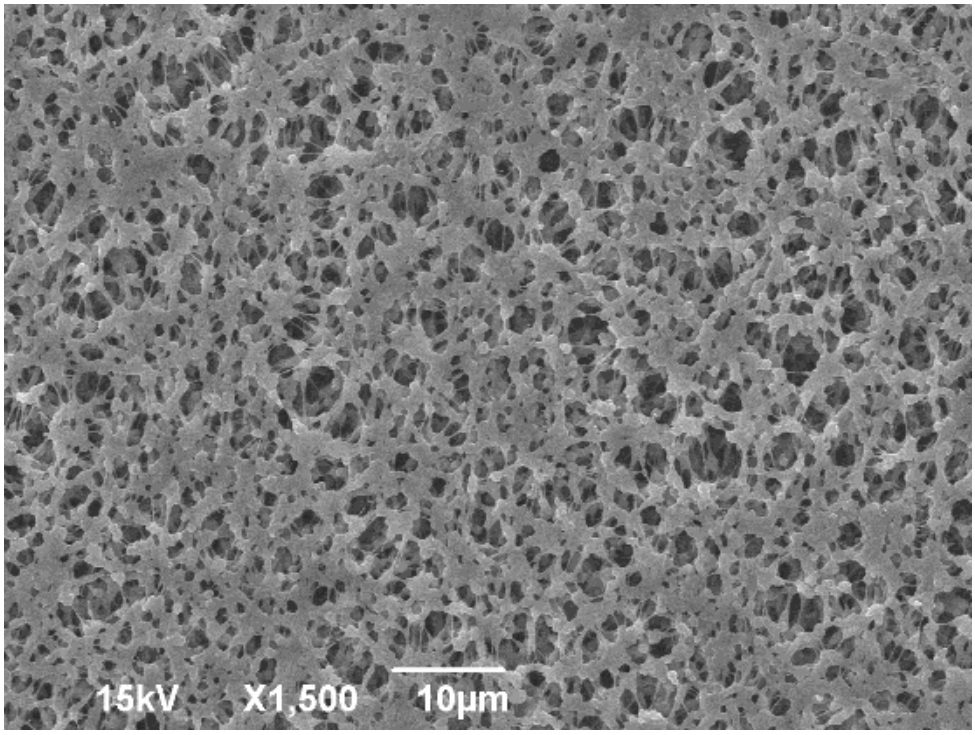

Figure 57: PVDF substrate No PDMS at 450 magnifications Top down view

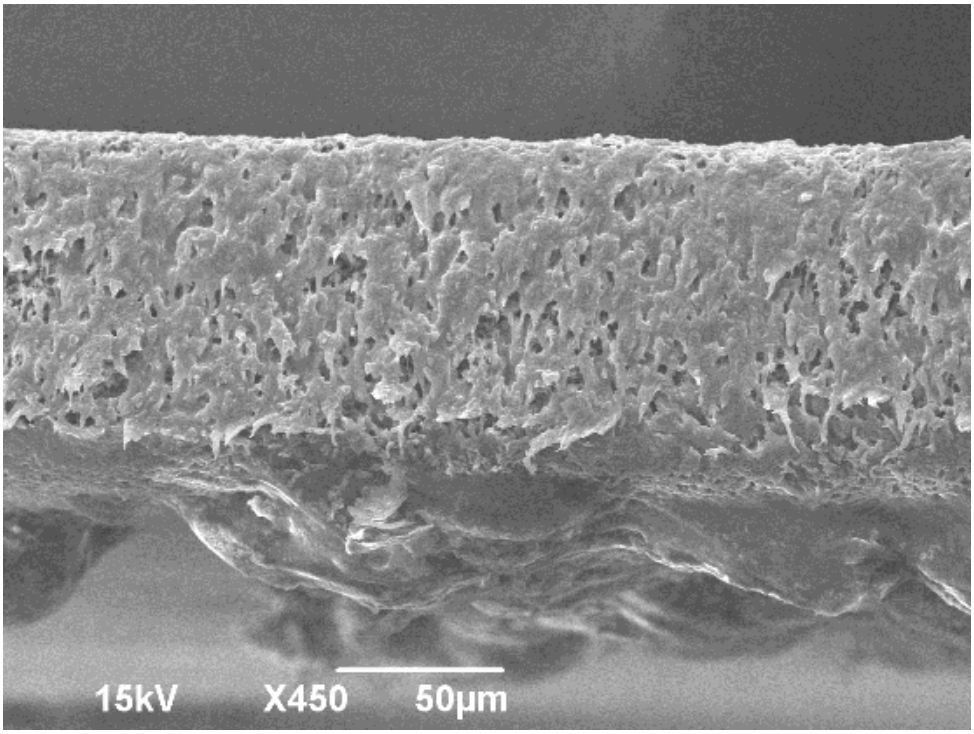

Figure 58: Cross sectional view PVDF 10µm PDMS 150 magnification

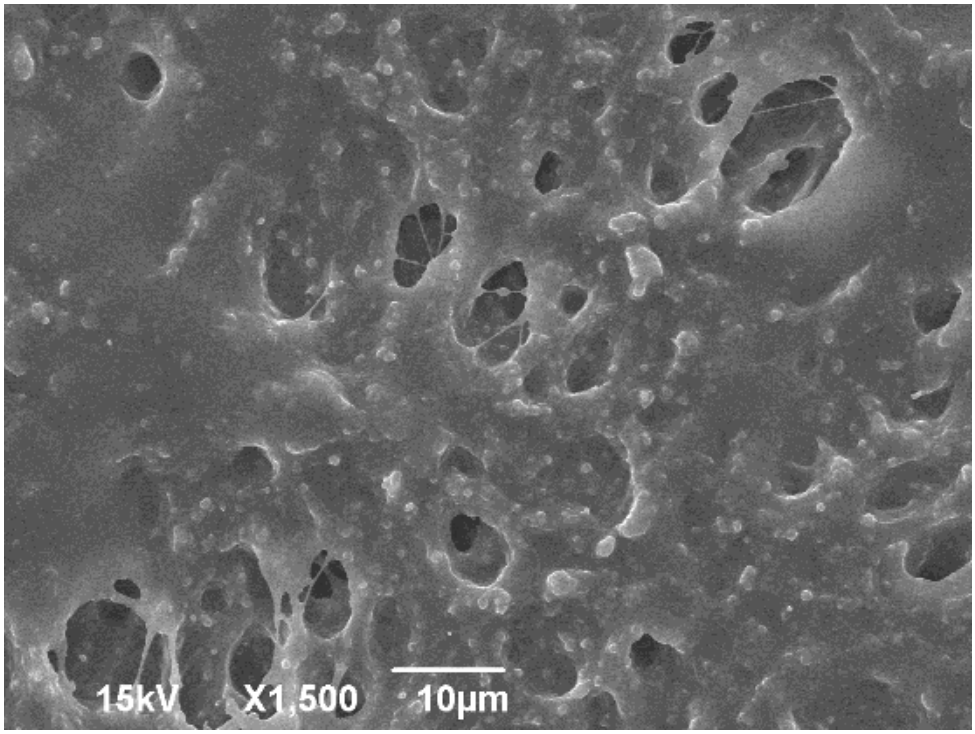

Figure 59: Top down view PVDF 10µm PDMS 150 magnification

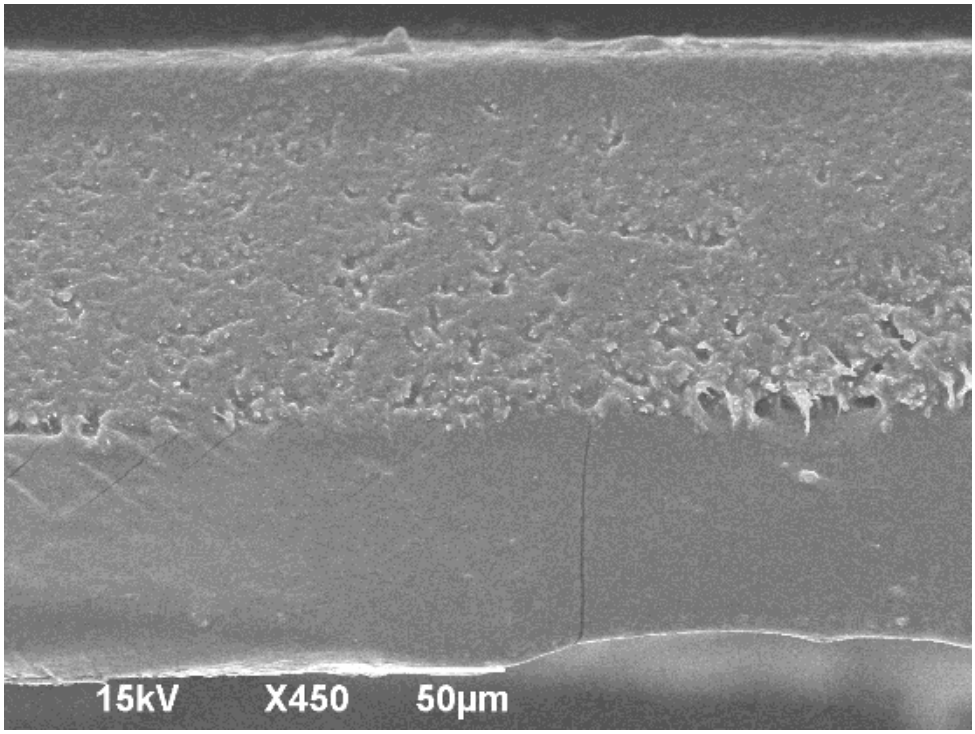

Figure 60: Cross sectional view PVDF 20µm PDMS 450 magnification

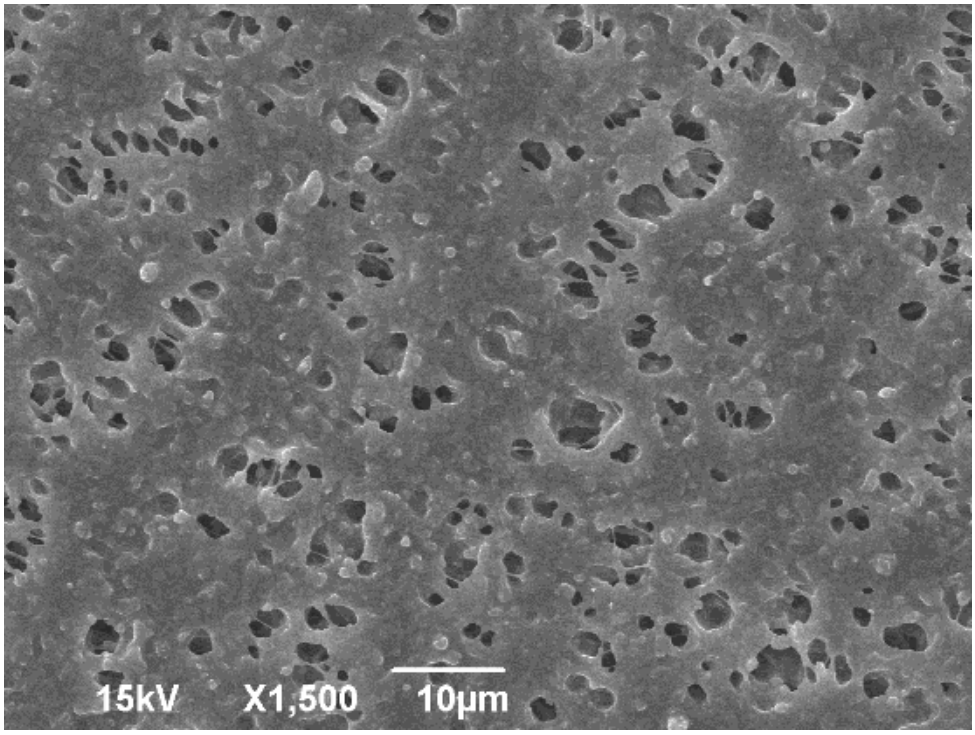

Figure 61: Top down view PVDF 20µm PDMS 1500 magnification

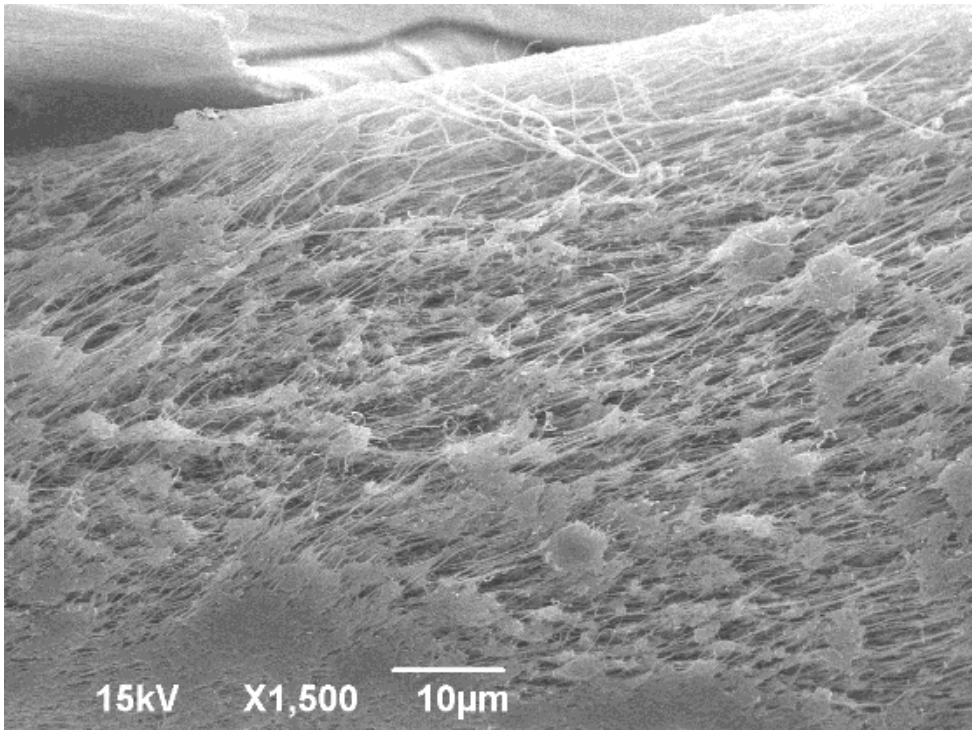

Figure 62: Teflon No PDMS cross sectional view 1500 magnification

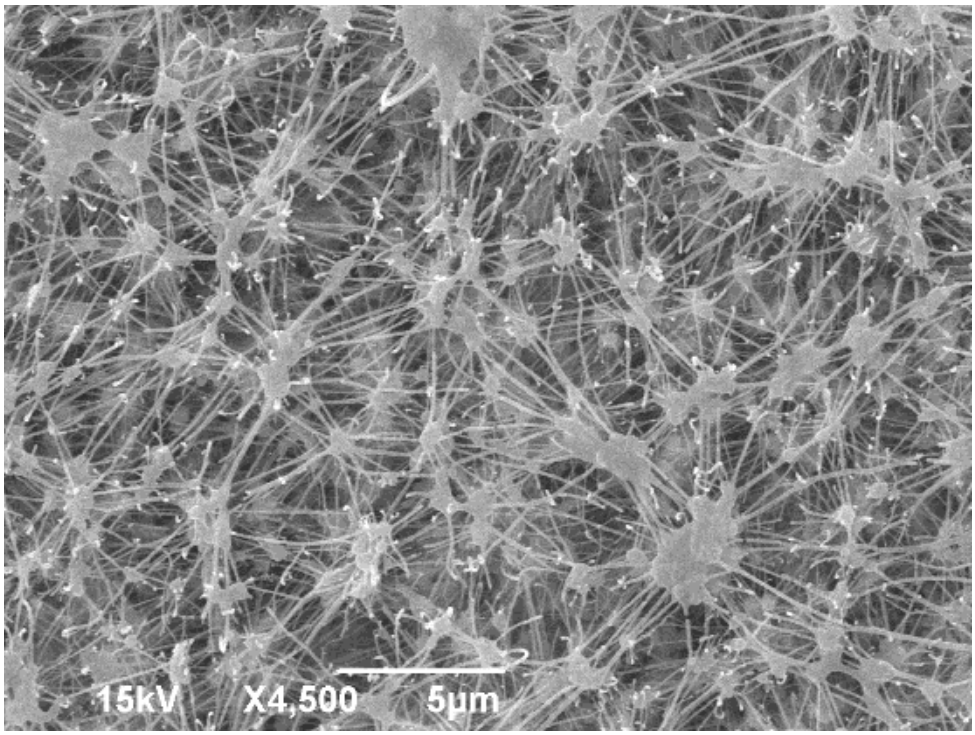

Figure 63: Teflon No PDMS top down view 4500 magnification

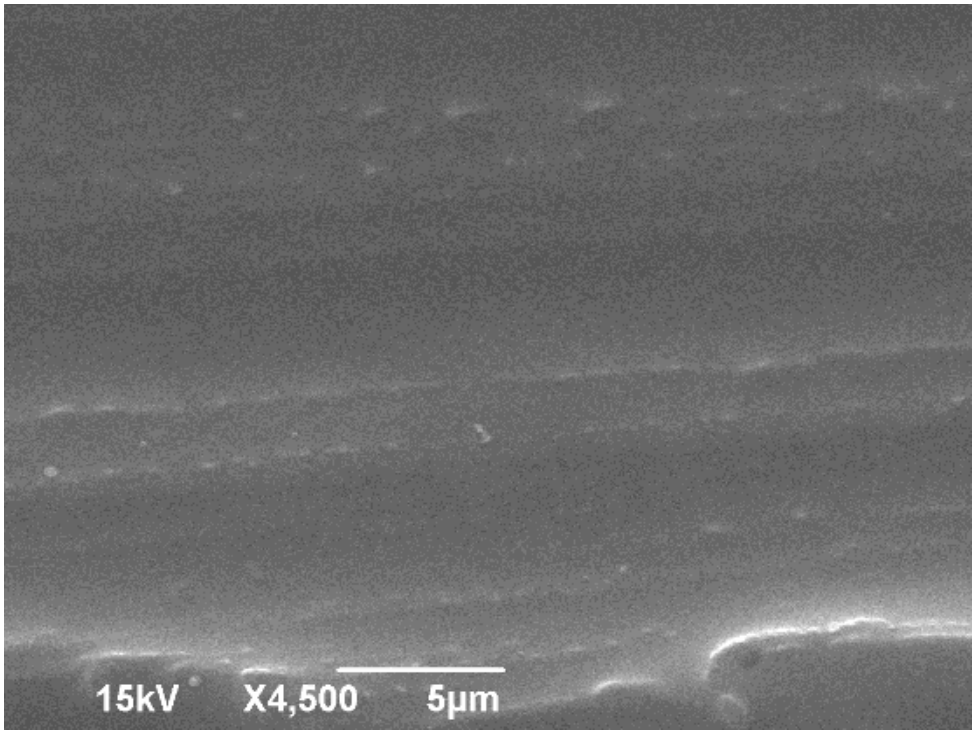

Figure 64: Teflon/10µm PDMS cross section view 4500 magnification

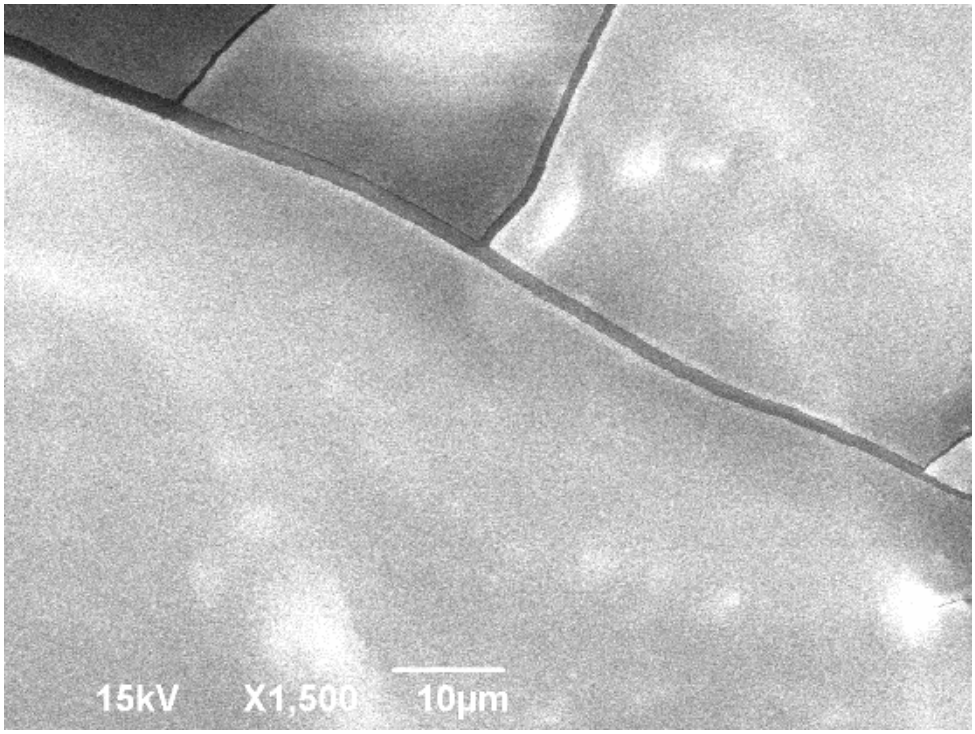

Figure 65: Teflon/10µm PDMS top down view 1500 magnification

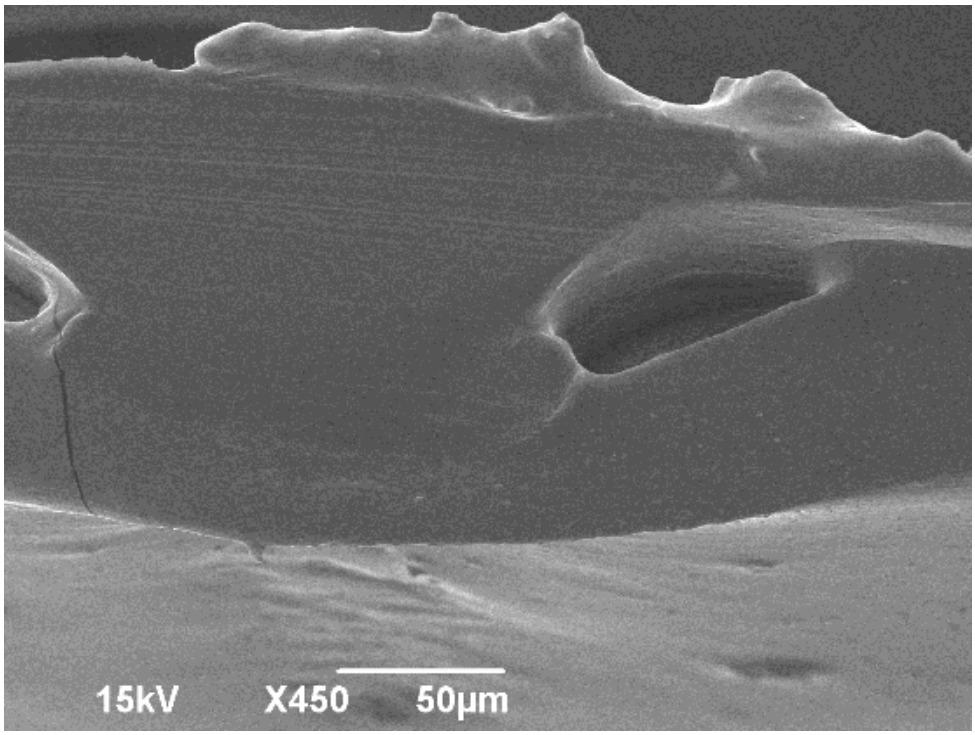

Figure 66: Teflon/20µm PDMS cross section view 450 magnification

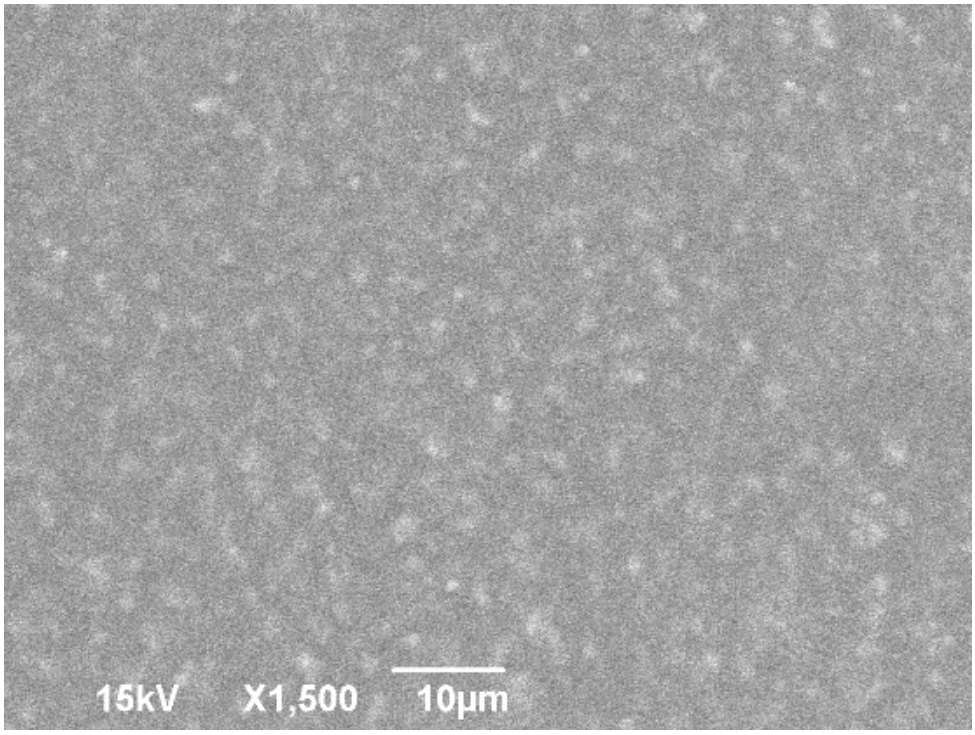

Figure 67: Teflon/20µm PDMS top down view 1500 magnification

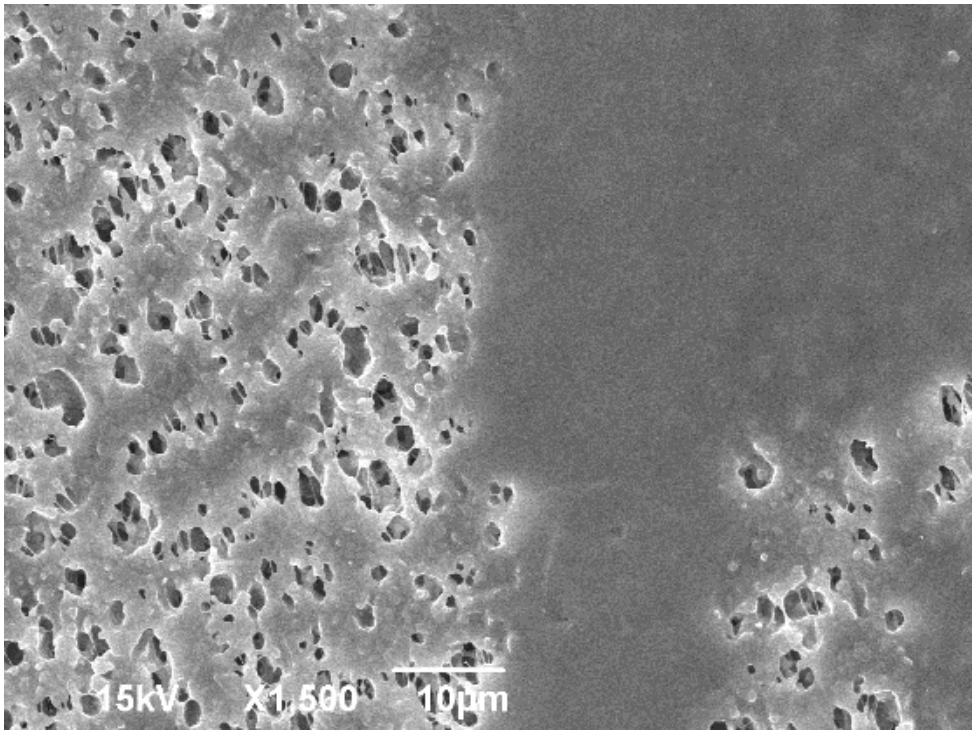

Figure 68: Top down image 1:1 PDMS ratio

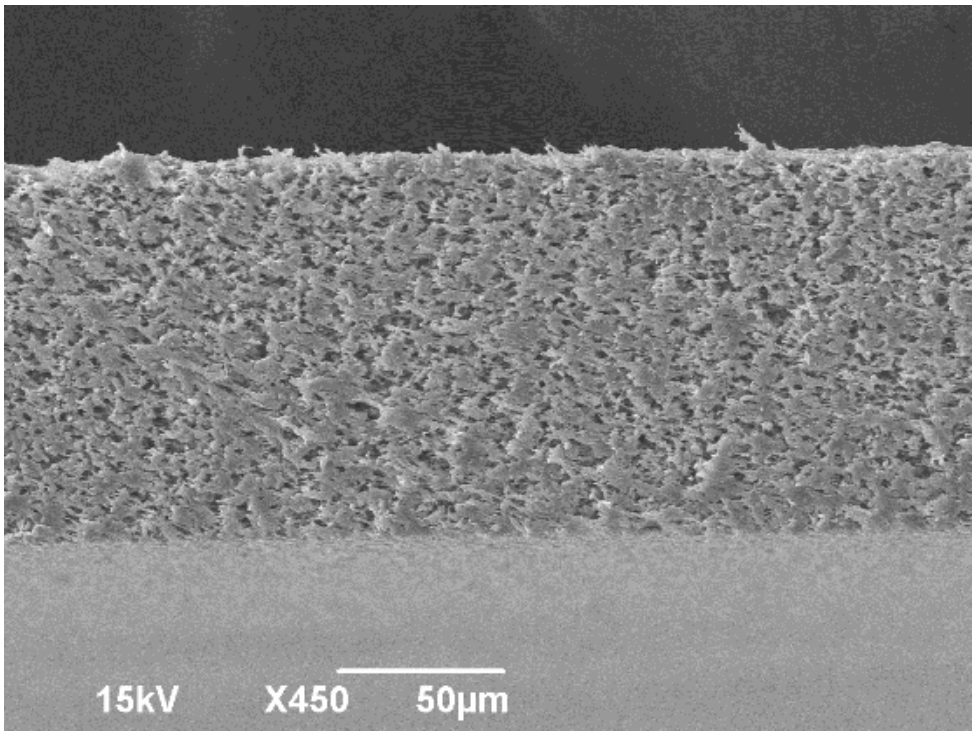

Figure 69: Cross section image 1:1 PDMS ratio

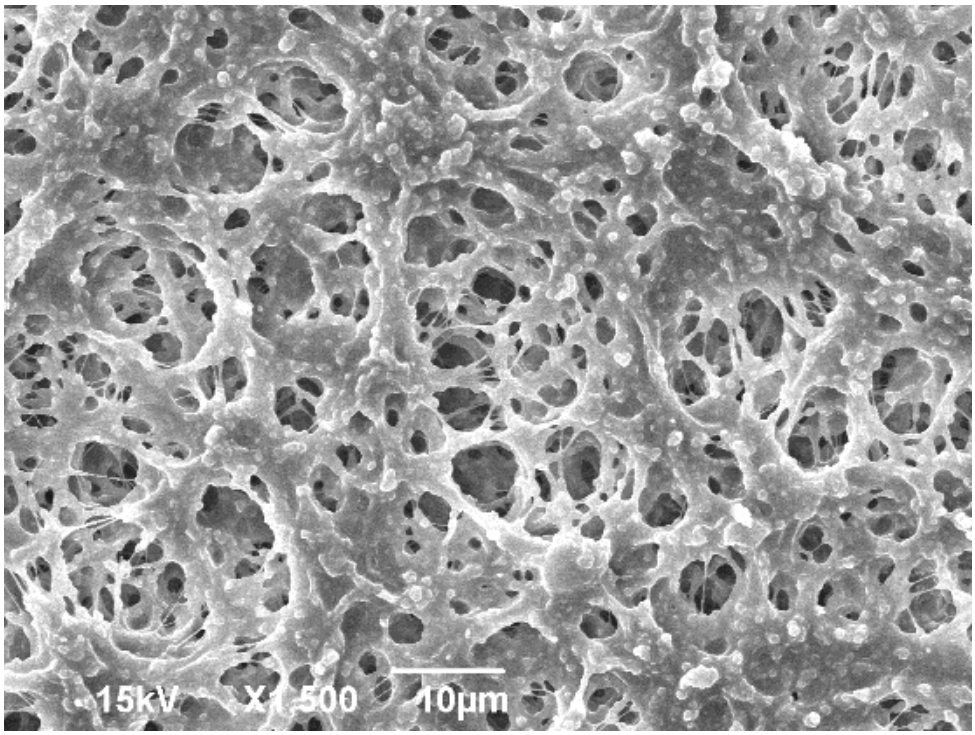

Figure 70: Top down image 1:5 PDMS ratio

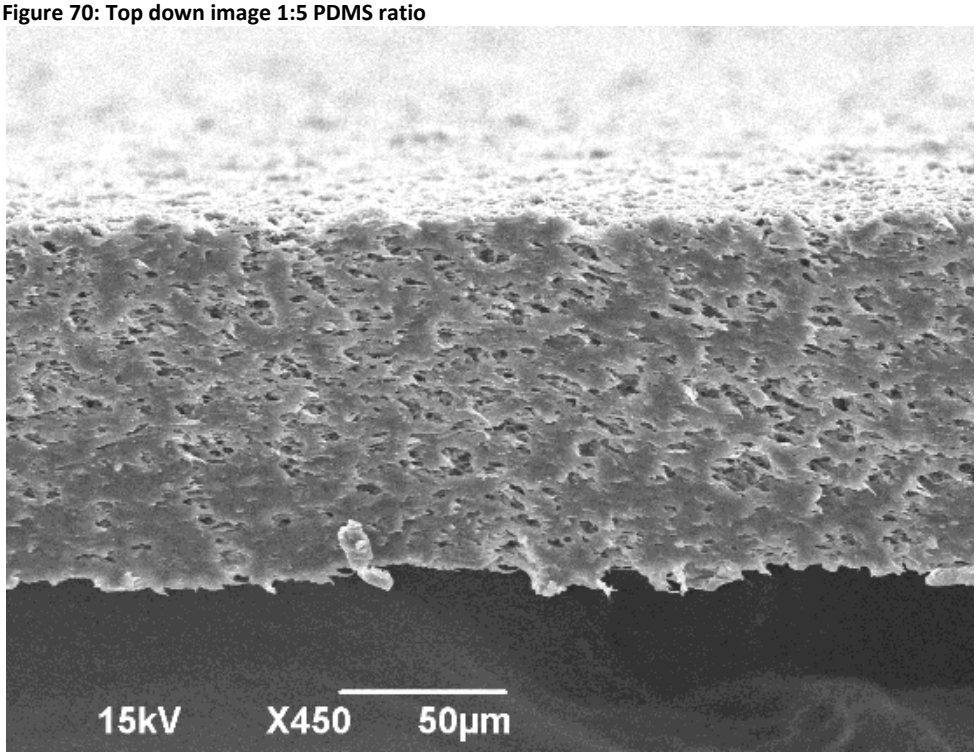

Figure 71: Cross section image 1:5 PDMS ratio

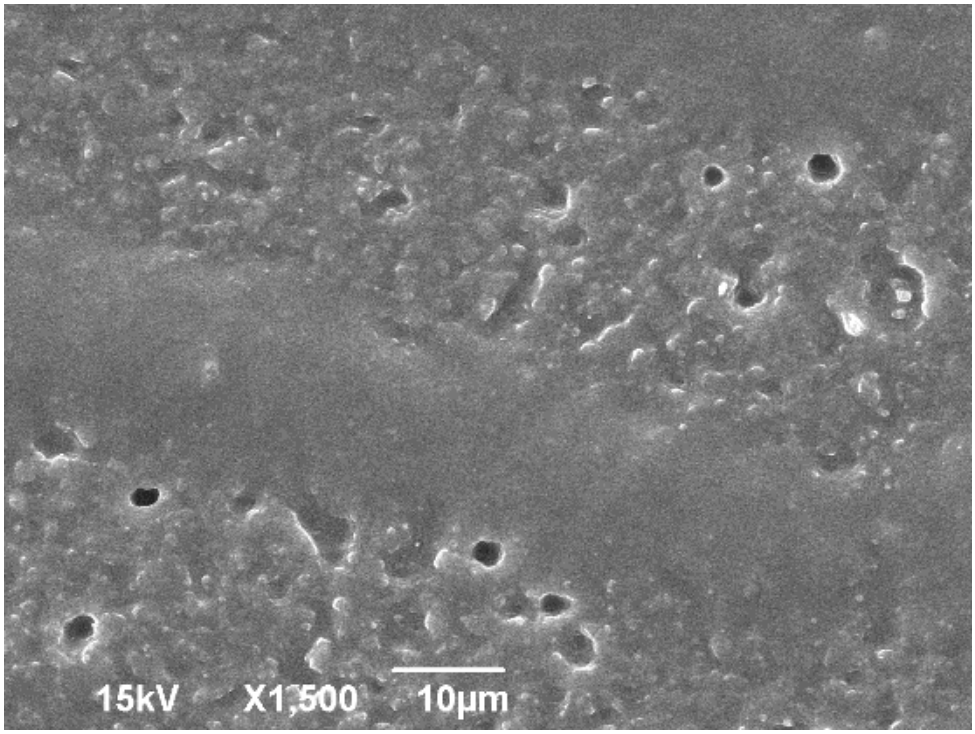

Figure 72: Top down image 1:9 PDMS ratio

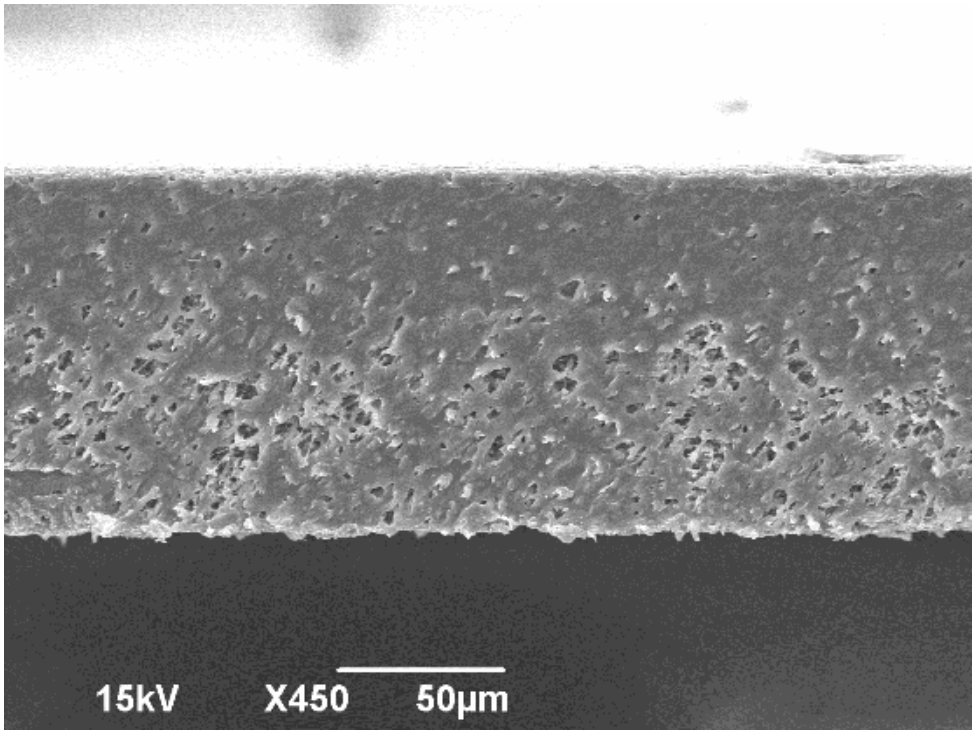

Figure 73: cross section image 1:9 PDMS ratio

Appendix E
Pervaporation Results

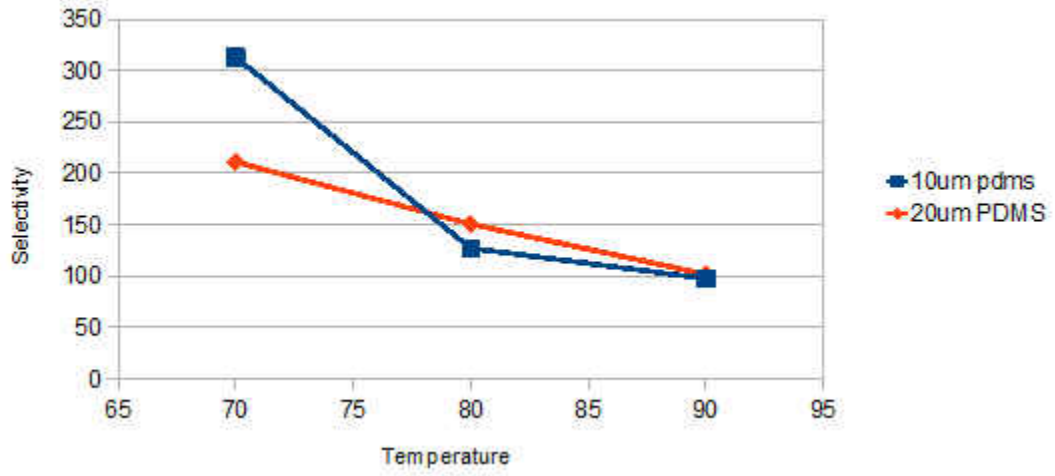

Figure 74: Selectivity vs. Temp for Polyester

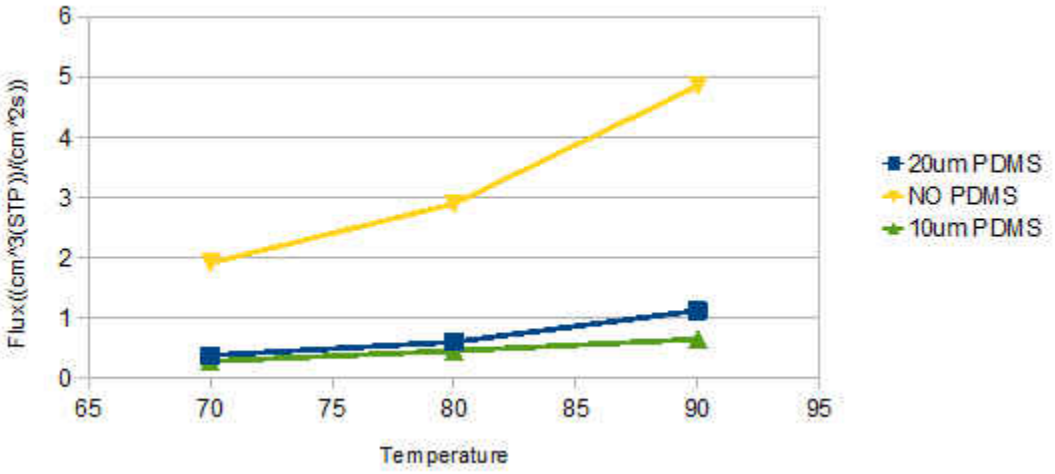

Figure 75: Flux vs. Temperature for Polyester

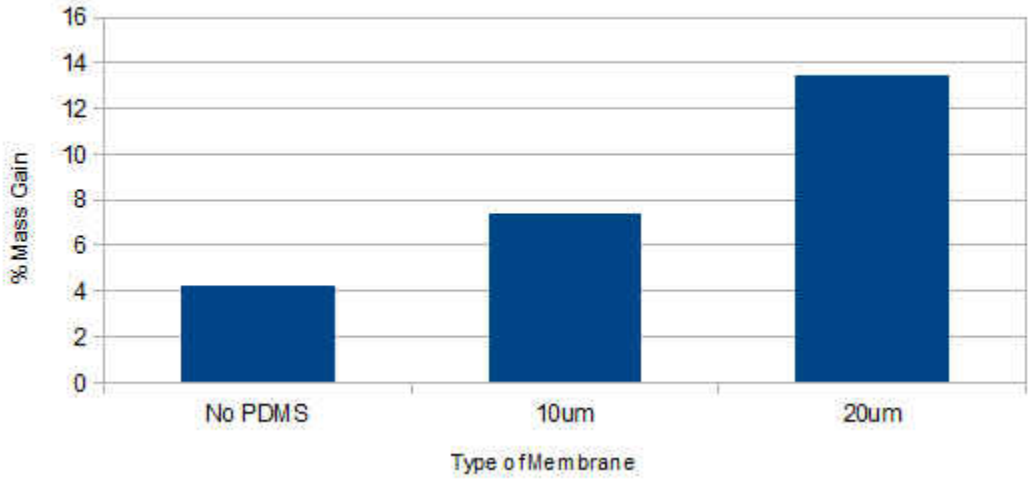

Figure 76: Mass Gain for Polyester Membrane

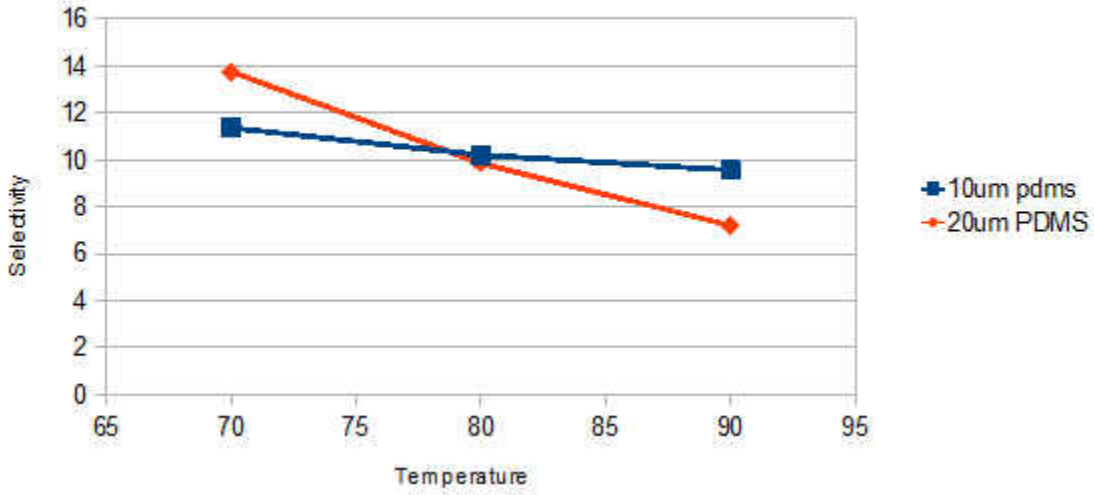

Figure 77: Selectivity vs. Temperature PVDF

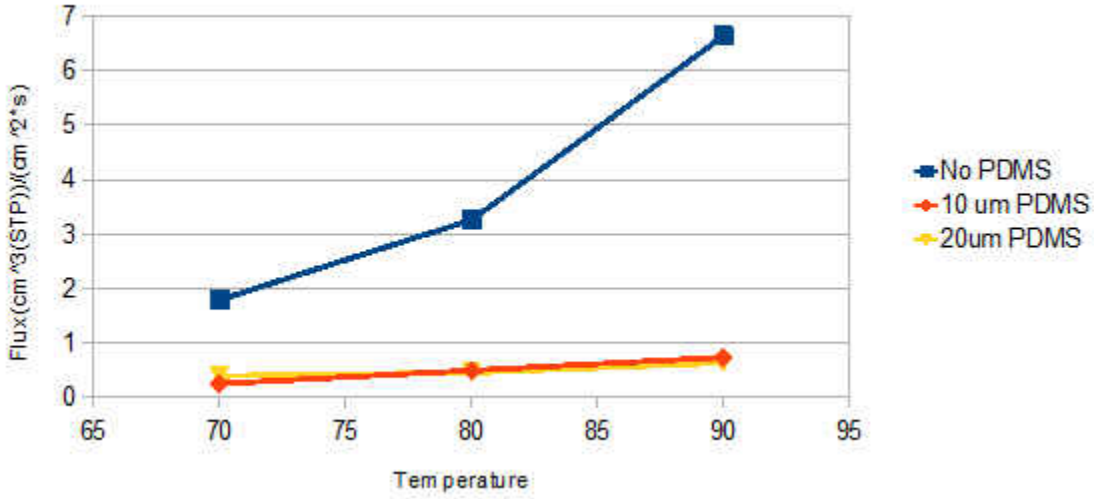

Figure 78: Flux vs. Selectivity for PVDF

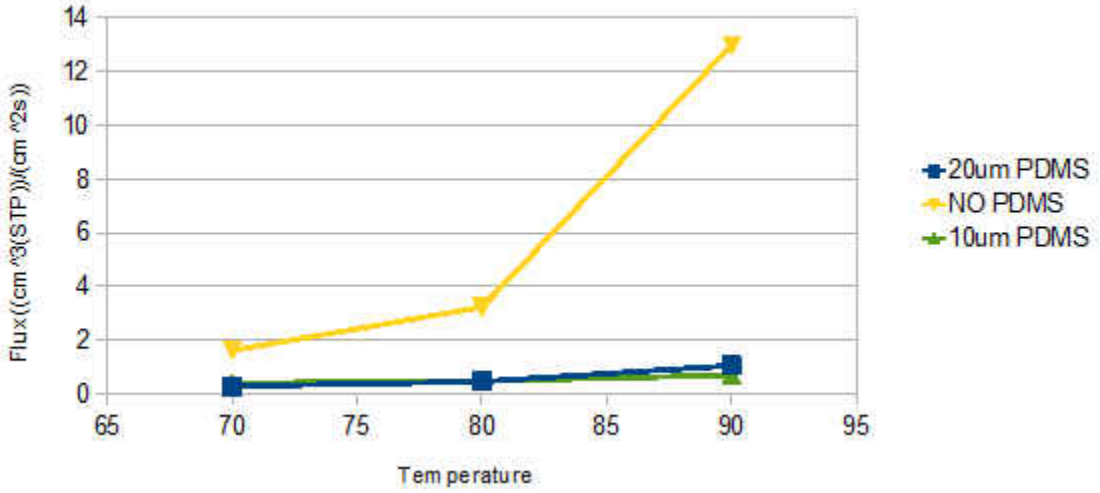

Figure 79: Flux vs. Temp Polyamide

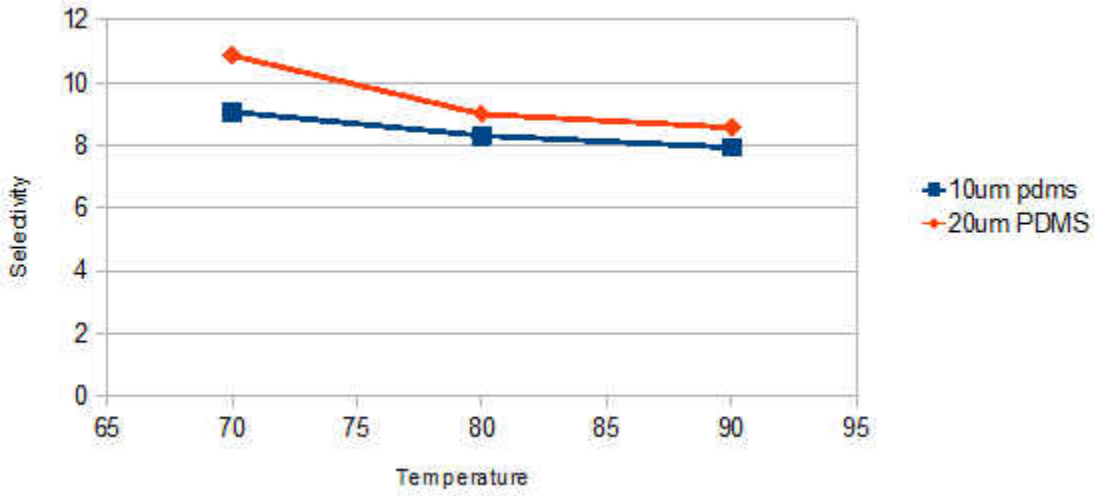

Figure 80: Selectivity vs. Temperature Polyamide

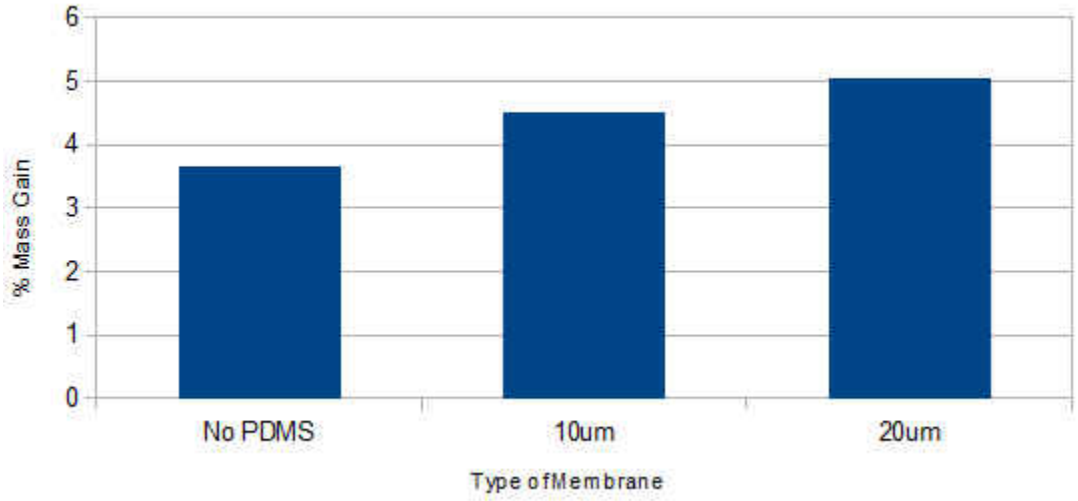

Figure 81: Mass Gain after pervaporation for Polyamide

Appendix F
Pervaporation SEM Images

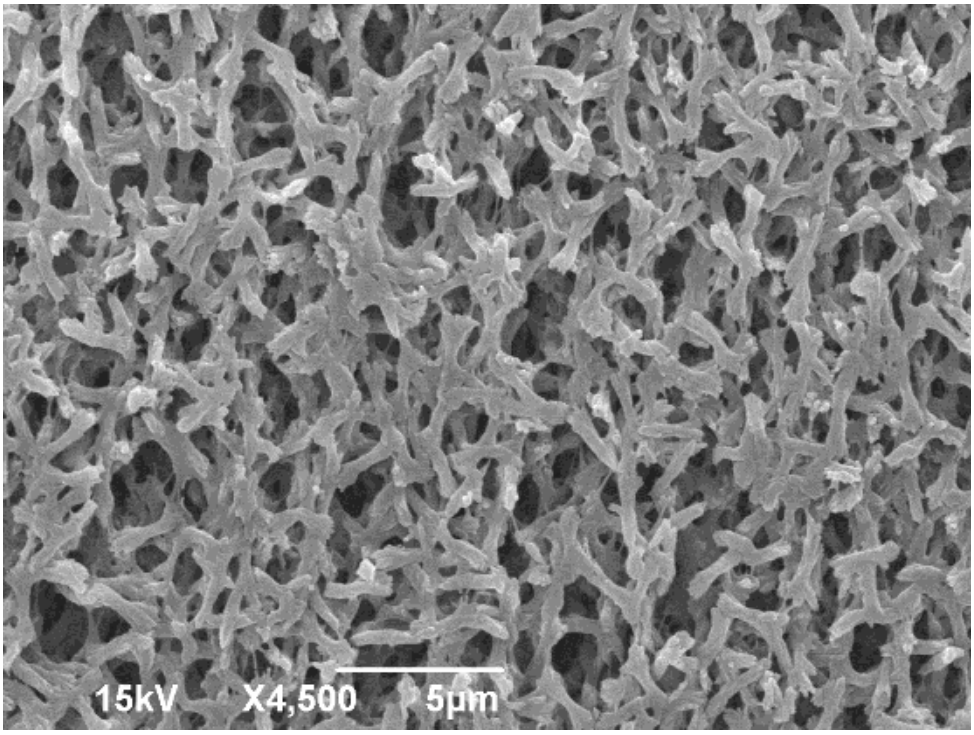

Figure 82: Polyamide pervaporation no PDMS Surface View

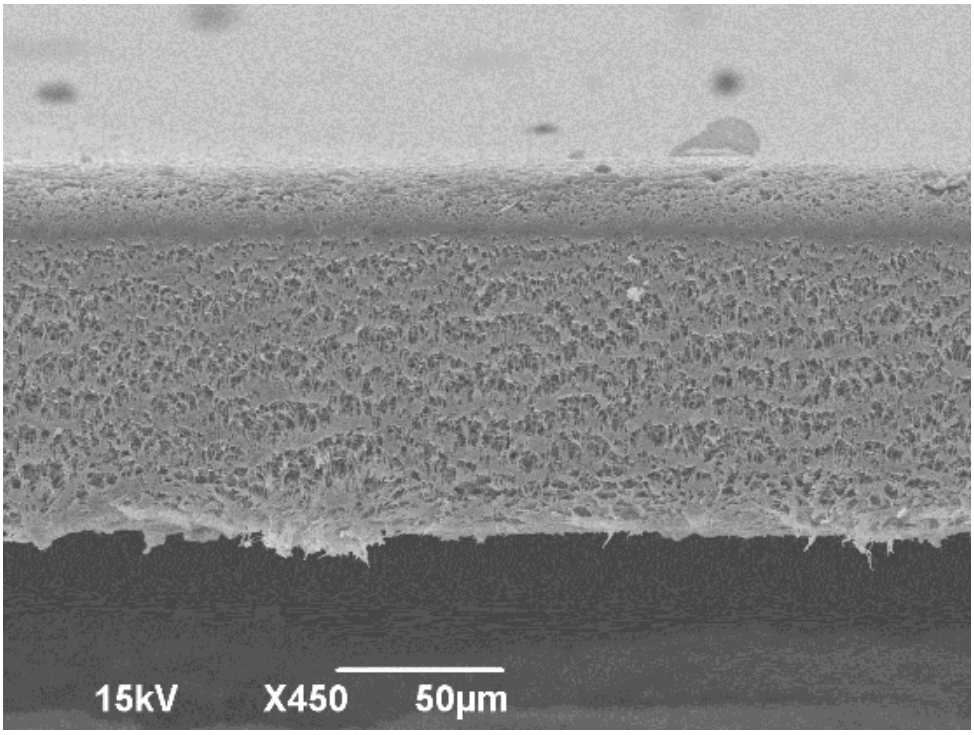

Figure 83: Polyamide pervaporation no PDMS Cross-section View

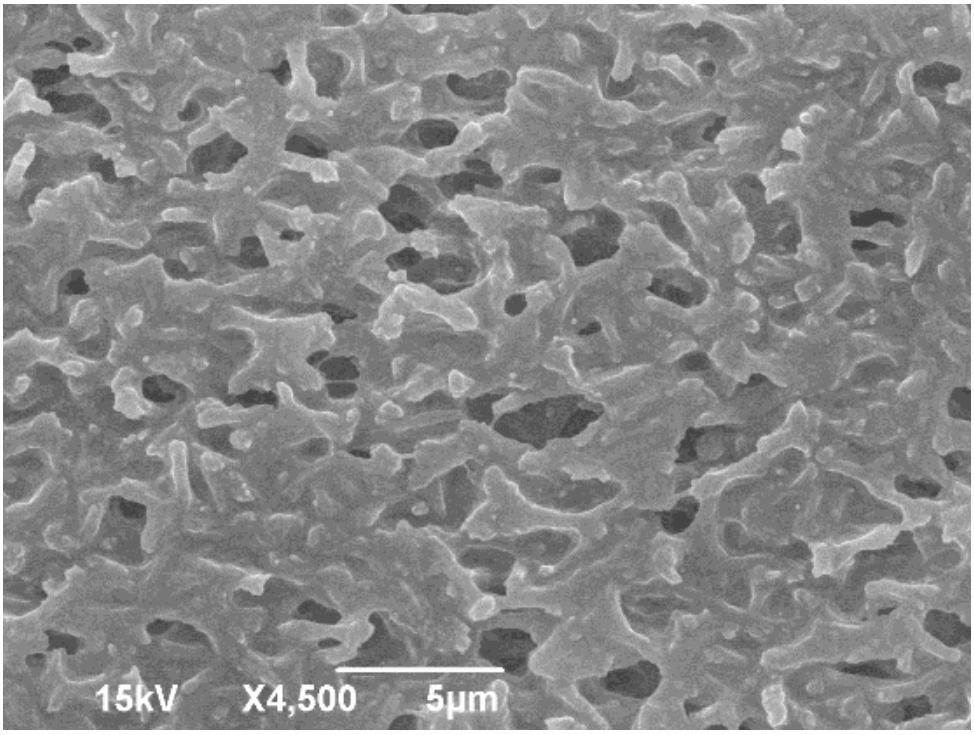

Figure 84: 10µm PDMS/Polyamide surface view after pervaporation

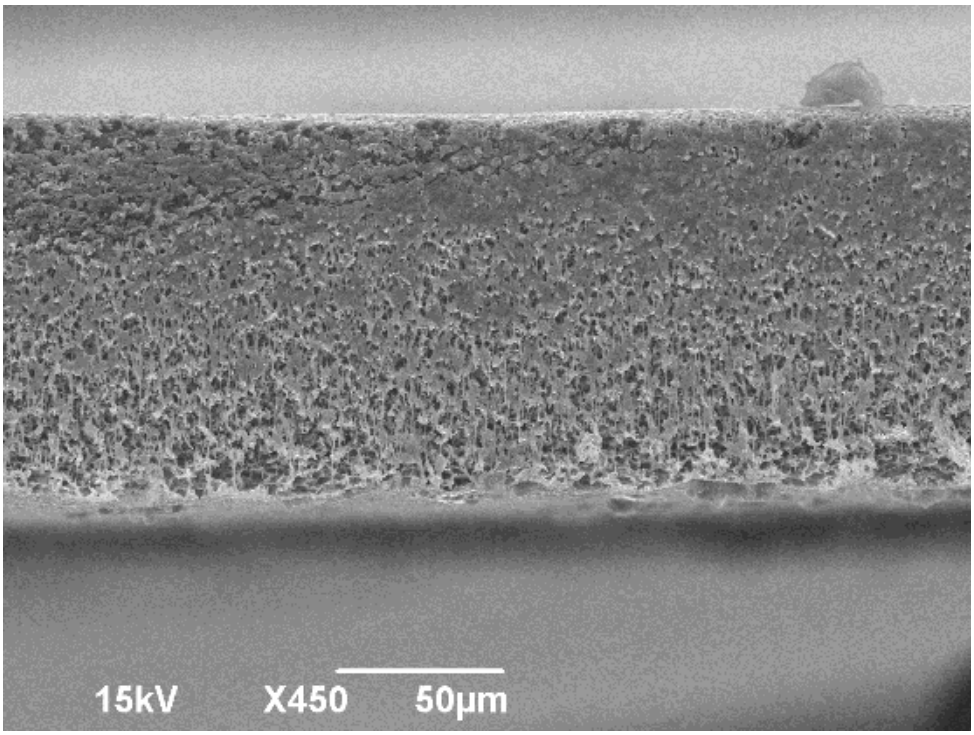

Figure 85: 10µm PDMS/Polyamide Cross-section after pervaporation

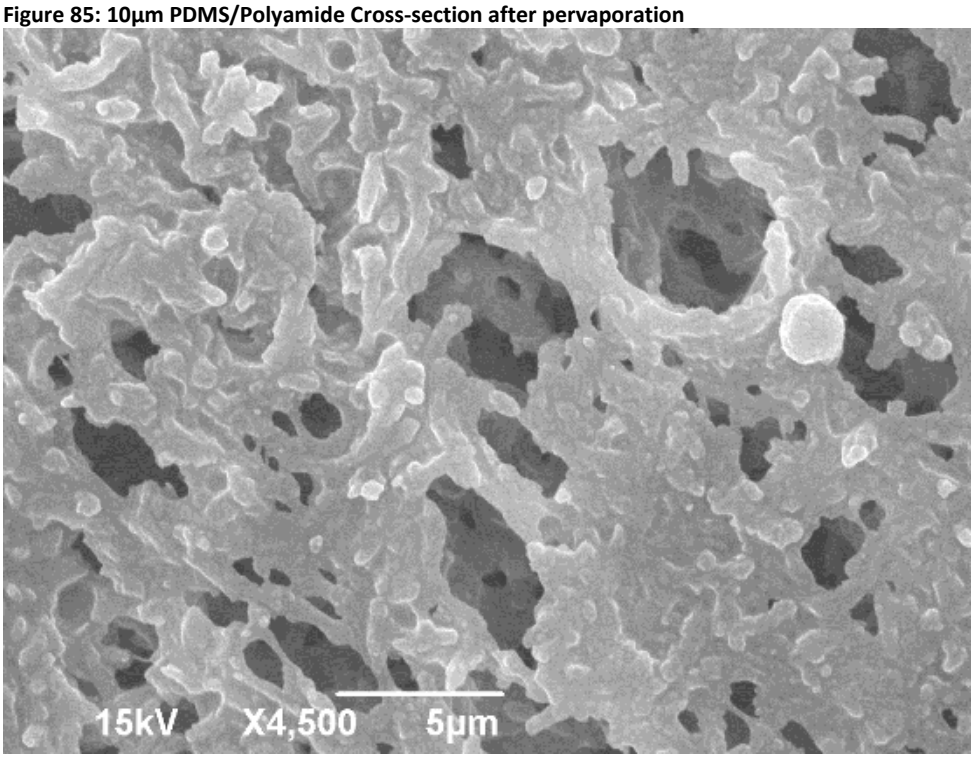

Figure 86: 20µm PDMS/Polyamide after pervaporation surface view

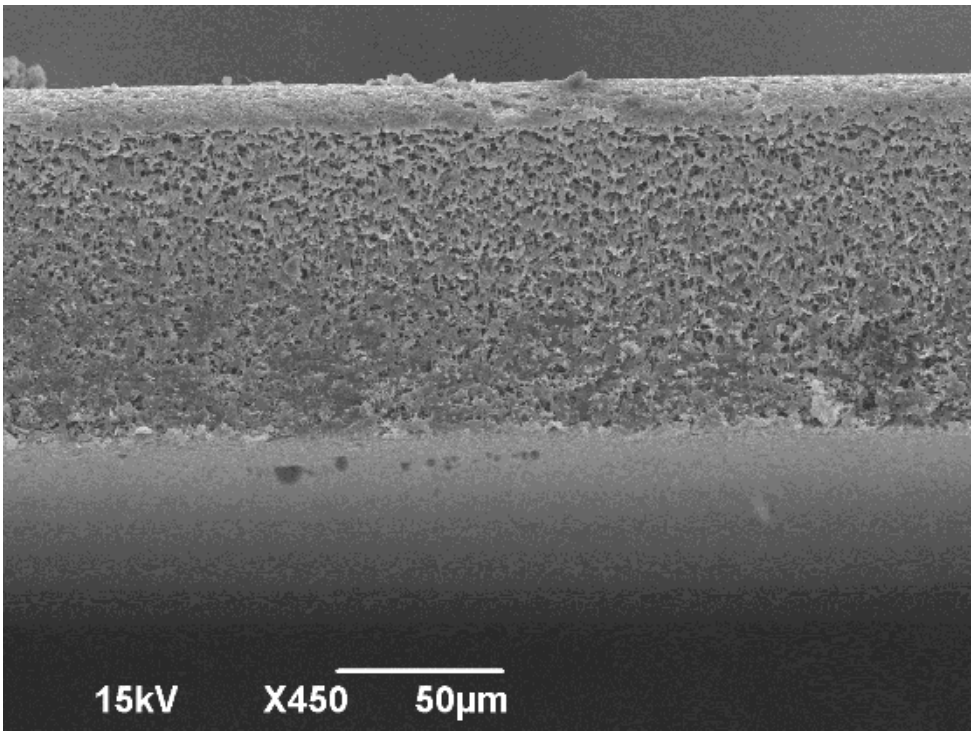

Figure 87: 20µm PDMS/Polyamide after pervaporation surface view

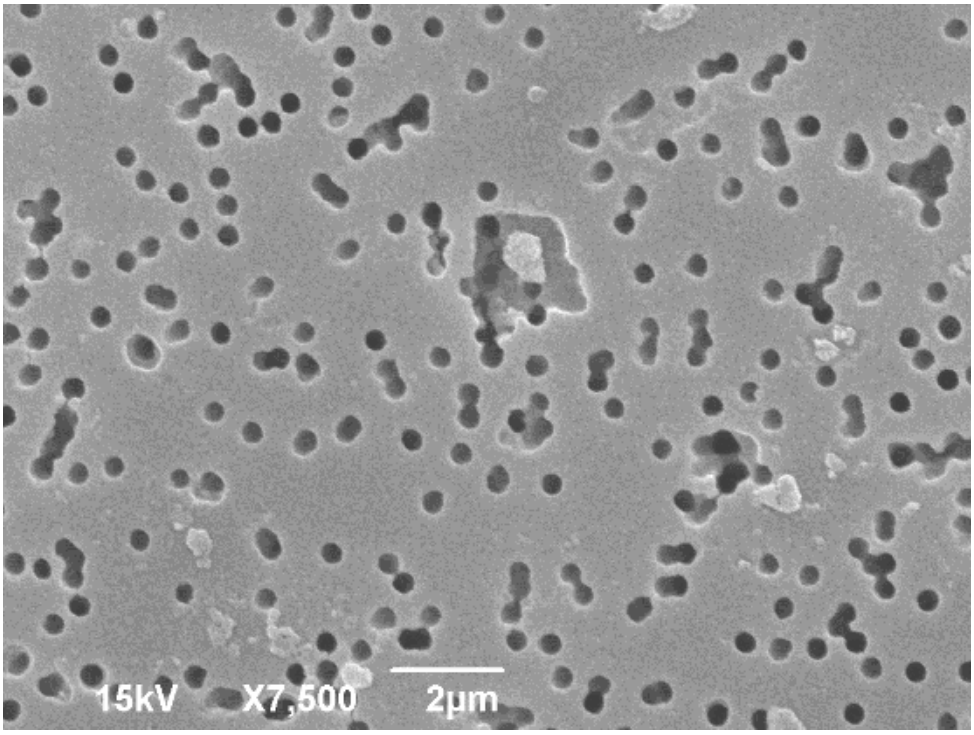

Figure 88: Polyester /No PDMS after pervaporation surface view

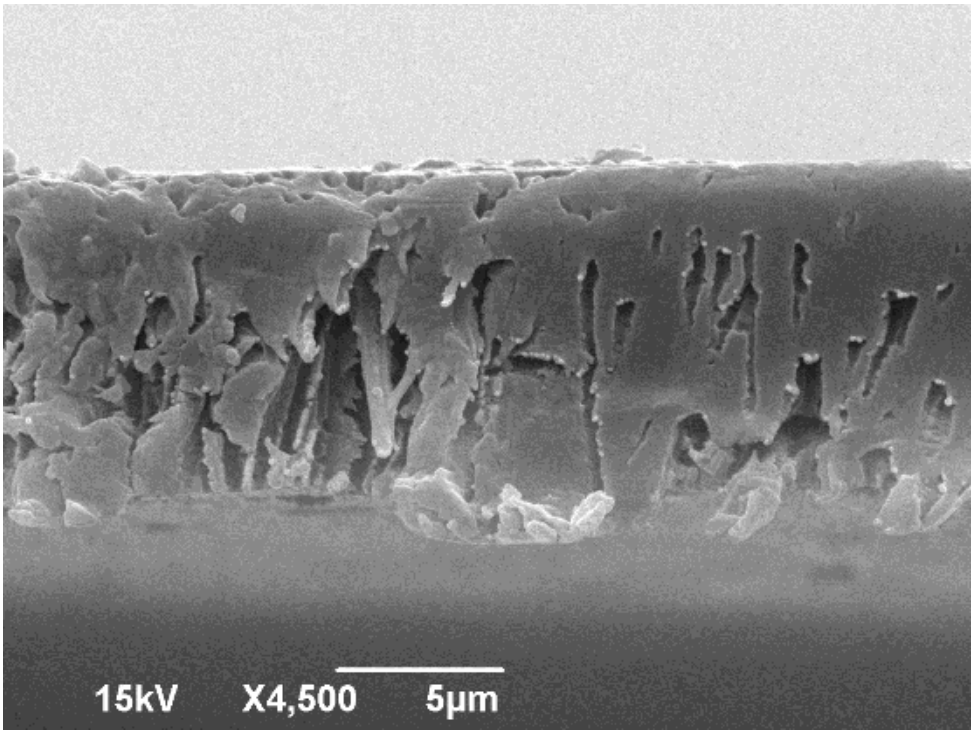

Figure 89: Polyester No PDMS after pervaporation cross-section view

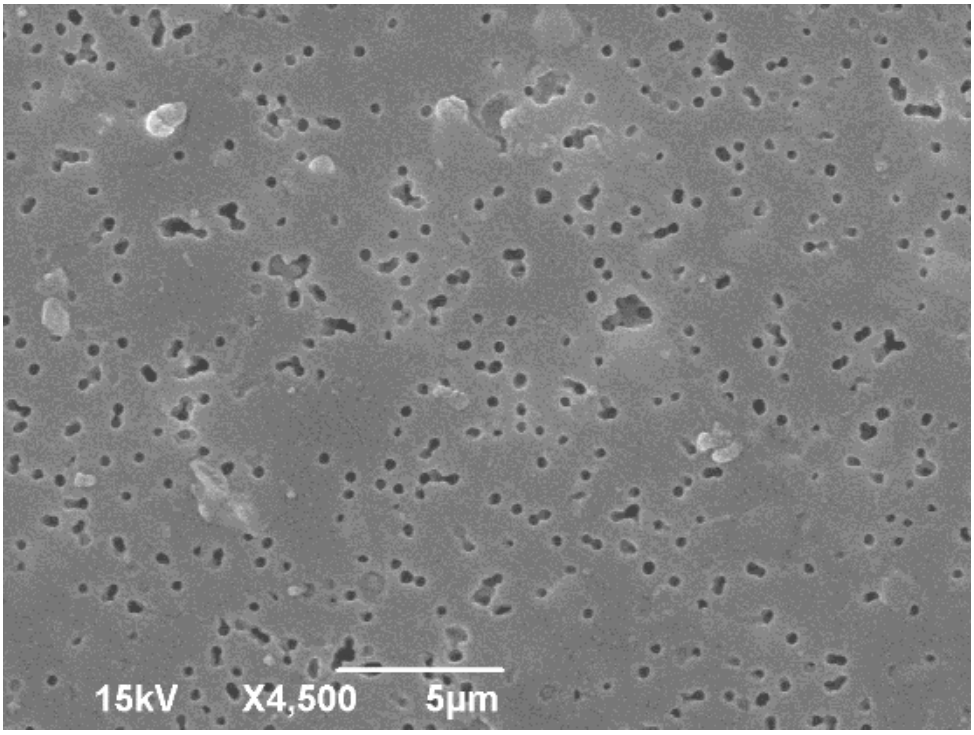

Figure 90: Polyester/10µm PDMS after pervaporation surface view

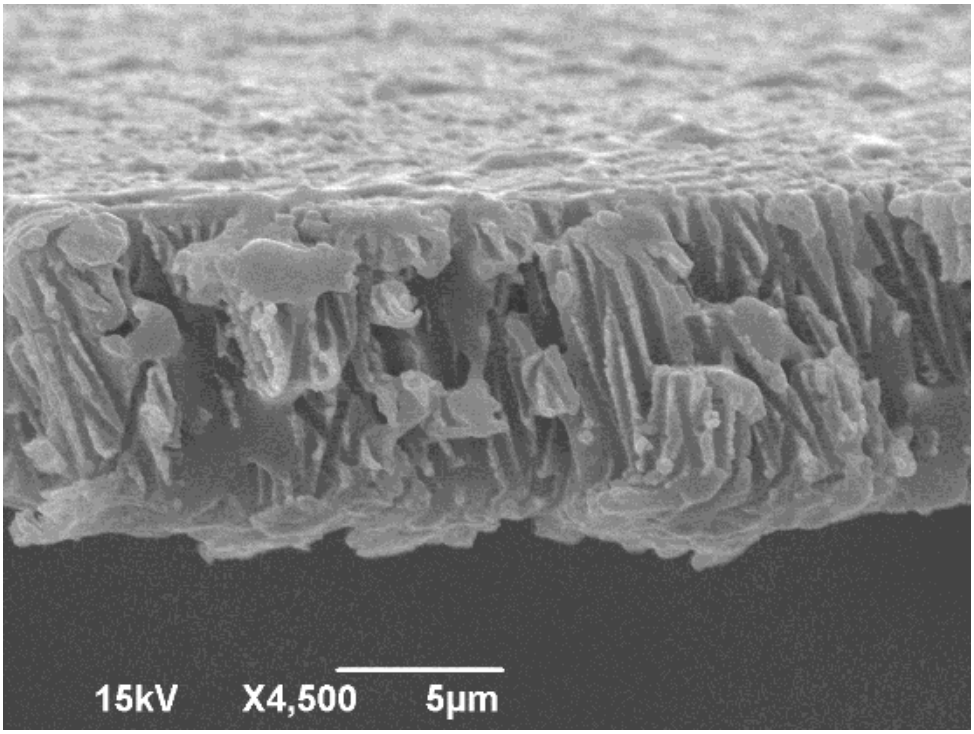

Figure 91: Polyester/10µm PDMS after pervaporation cross section view

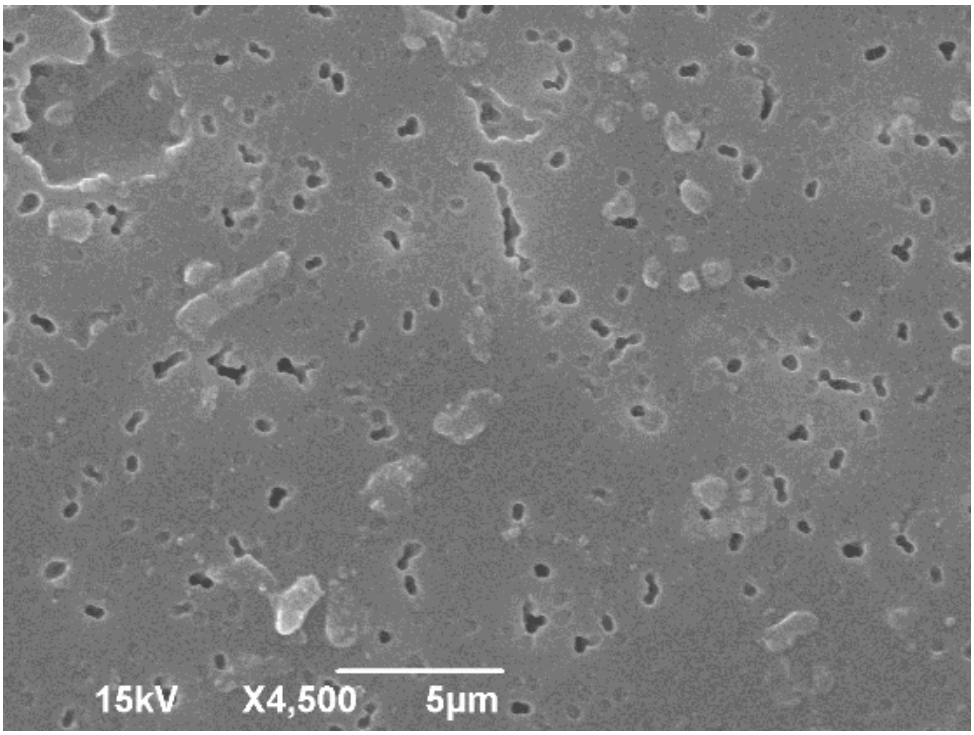

Figure 92: Polyester/20µm PDMS after pervaporation surface view

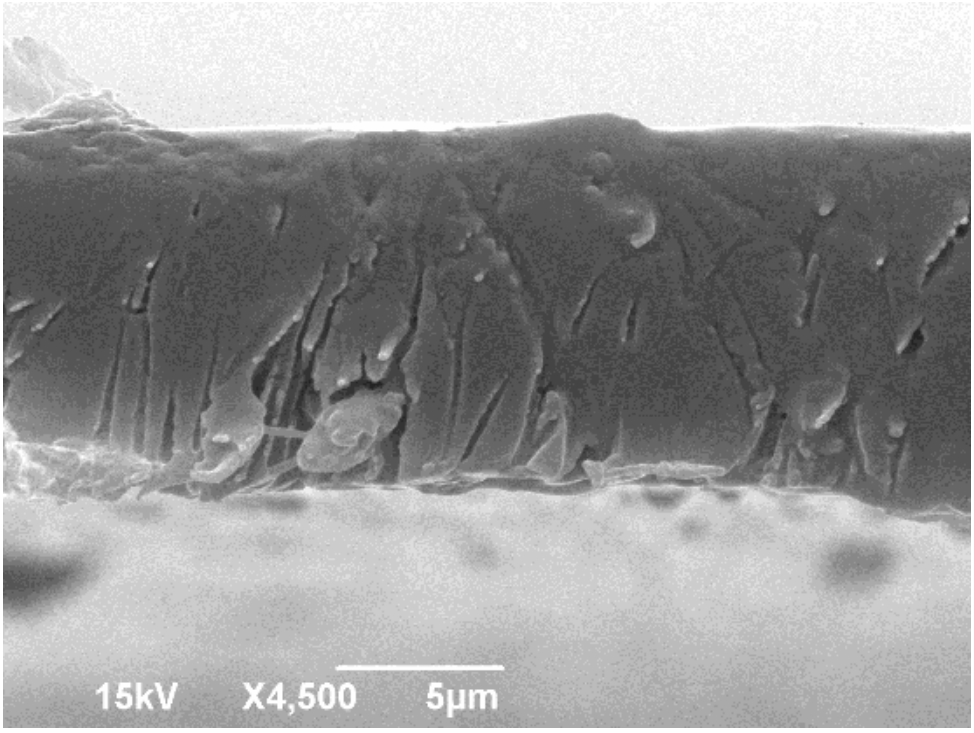

Figure 93: Polyester/20µm PDMS after pervaporation cross-section view

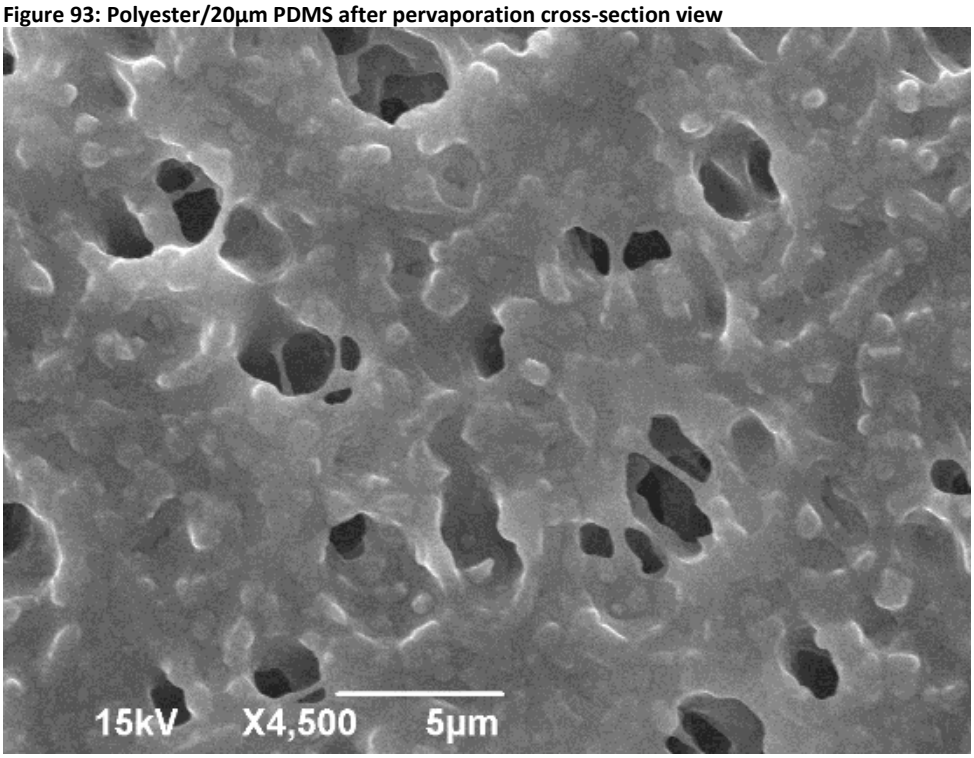

Figure 94: PVDF/10µm PDMS after Pervaporation Surface view

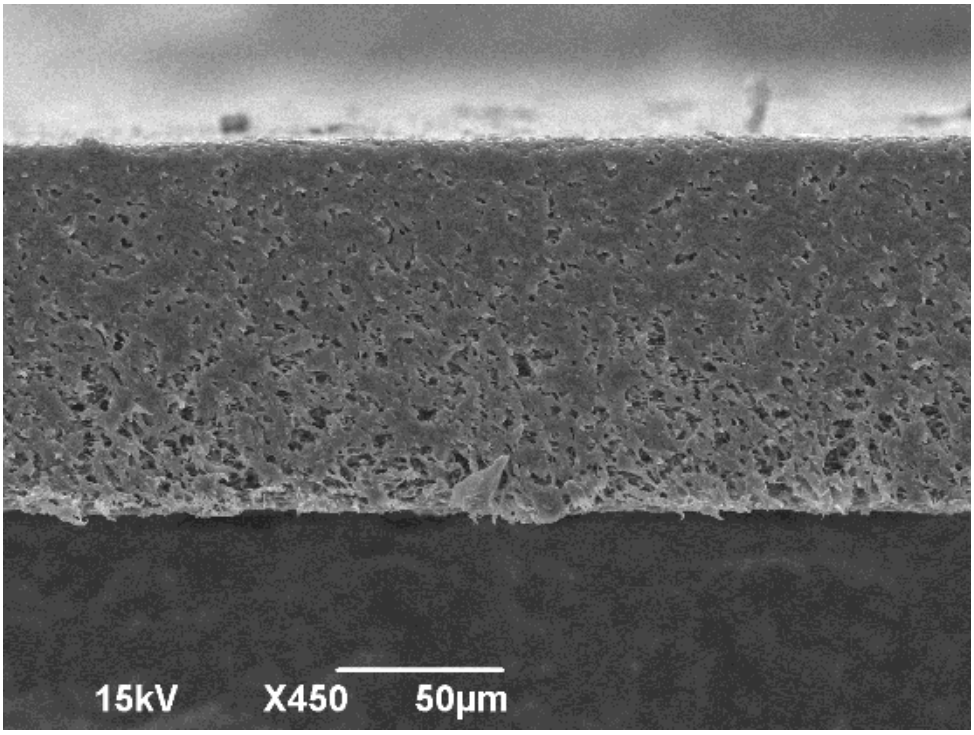

Figure 95: PVDF/10µm PDMS after Pervaporation cross-section view

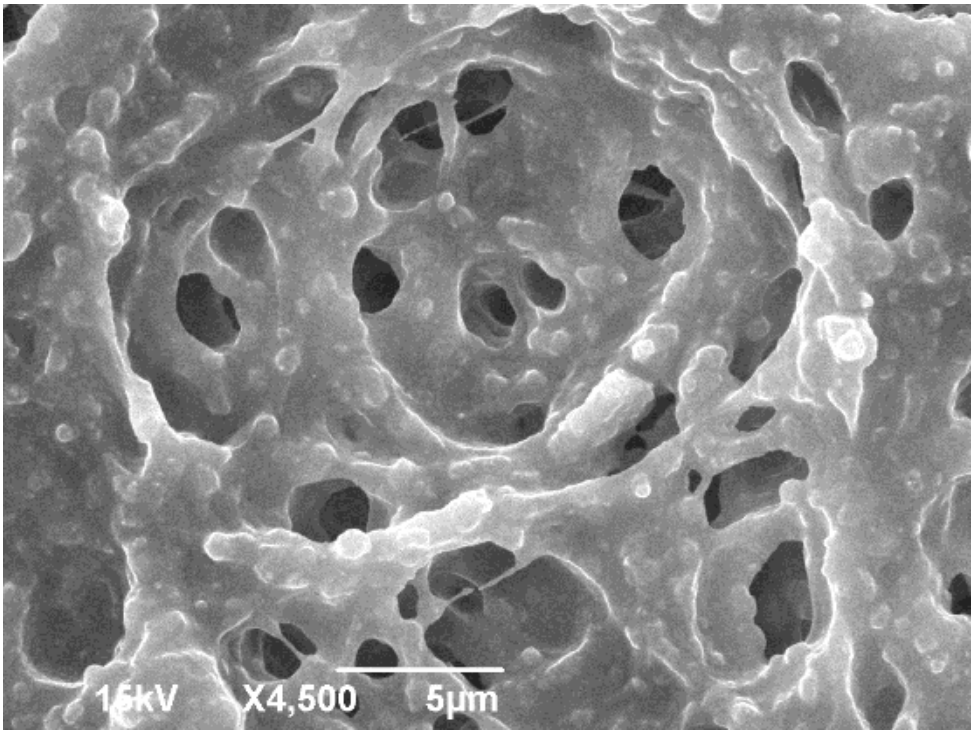

Figure 96: PVDF/20µm PDMS after pervaporation Surface view

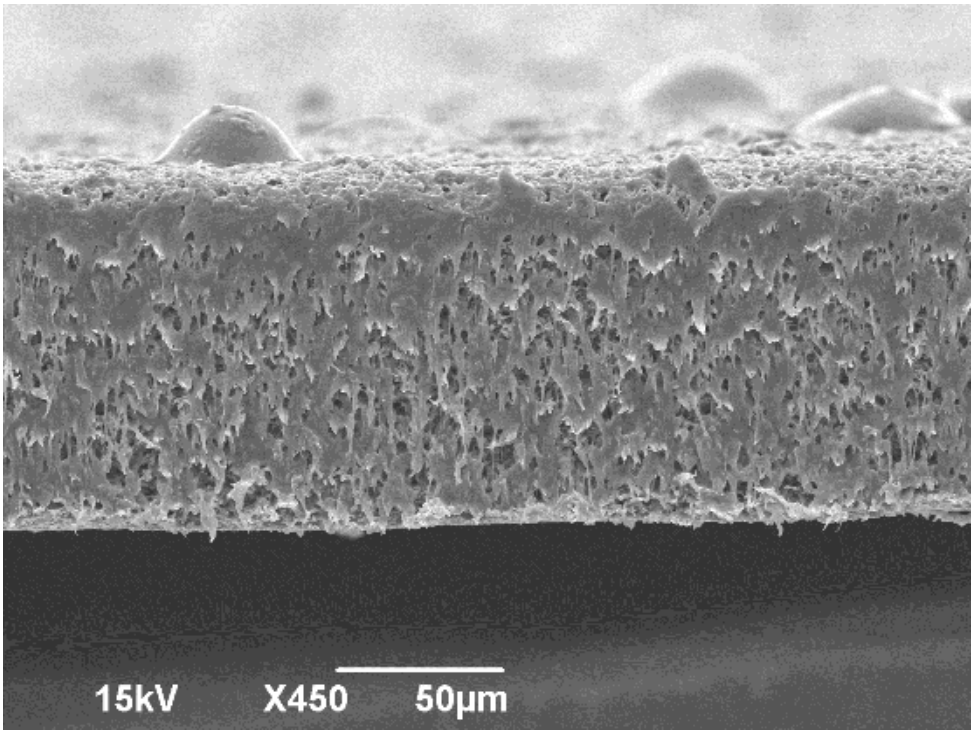

Figure 97: PVDF/20µm PDMS after pervaporation cross section view

Appendix G

Polymer Membrane Candidates list

Rank	Polymer	Name	$P(CO_2)$(barrer)	Tg (C)	Tm(C)
1	poly(1-trimethylsilyl-1-propyne)	PTMSP	3520[2]	262[2]	323[2]
2	polydimethylsiloxane	PDMS	3100[5],4553[7]	-128[4]	-40[3]
3	6FDA-based polyimides	6FDA–durene	456[1], 24.2[5]	300-350[9]	N/A
4	Poly(phenylene oxide)	PDMPO (60.0% brominated)	159.9[1]	184[2]	279-285[2]
5	cis-polyisoprene	cis-PIP	134[5],191[7]	99[2]	156[2]
6	Polycarbonates	TMHFPC	111[1]	217[2]	270[2]
7	Polysulfones	PSF	110[1], 5.6[5]4.6[7]	237[2]186-190[9]	N/A
8	Poly(ether-b-amide)	PEBAX[6]	30-104[15]	-60 to -70[2] -30to 160[9]	120-210[2]
9	Polyarylates	TBHFBPA/tBIA	85.1[1]	N/A	N/A
10	Poly(4-methyl-1-p pentene)	PMP	83[5]	151-162[2]	270[2]
11	Polyester	PE	HDPE 76.4[12] LDPE 13.4[12]	-20[8]	166-249[2]
12	Poly(2,6-dimethyl phenylene oxide)	PPO	61[5]	249-259[2]	282[2]
13	Poly(pyrrolone)	6FDA–TAB	54.0[1]	N/A	273(?)[2]
14	Polypropylene	PP	13.4,34[11]	-10[8]	135-165[8]
15	Poly(arylene ether)	6FPPy–6FBPA	29.46 [1]	N/A	82-96[8]
16	poly(tertbutylacetylene)	PTBA	5.0-27.4[13]	-77[13]	126-204[13]
Rank	Polymer	Name	P(CO2)(barrer)	Tg (C)	Tm(C)
17	Poly(tetrafuoroethylene)	PTFE	21.3[11]	204[2]	316[2]

18	*Polystyrene*	*PS*	*12.4*	*98[8,9]*	
19	*Polyimides*	*PMDA–BAPHF*	*11.8[1]*	*230-330[9]*	*N/A*
20	*Cellulose acetate*	*CA*	*5.5[7]*	*117-245[2]*	*304[2]*
21	*polyethersulfone*	*PES*	*4.2[2]*	*259[2]*	*N/A*
22	*Poly(vinyl acetate)*	*PVAC*	*3.1[10]*	*150[2]34.8[9]*	*231[2]*
23	*Polyamide*	*Nylon Hydrophobic*	*1.5[11]*	*160[2]*	*231-234[2]*
24	*Poly(vinyl chloride)*	*PVC*	*1.3[12]*	*71[9]173-188[2]*	
25	*poly(ethylene terephthalate)*	*PET*	*0.5[12]*	*172-198[2]*	*281[2]*
26	*Polyvinyl fluoride*	*PVF*	*0.06[11]*		
27	*Polyvinylidene fluoride*	*PVDF*	*0.05[14]*	*114[2]*	*227[2] 155-192[8]*
28	*poly(amide-imide)*	*PAI*		*287[2]*	*N/A*
29	*Nitrocellulose*	*cellulose nitrate CN*	*2.1[2]*	*163[2]*	*N/A*
30	*Polyvinylpyrrolidone*	*PVP*		*194-233[2]*	*N/A*
31	*Polyvinyl alcohol*	*PVA*	*161[10]*	*181[2]*	*281[2]*
32	*Poly(acetylene)*	*Poly(trimethyl-prop-1-ynyl-silane)*	*19000 [1]*	*145[2]*	*420[2]*
33	*Poly(ethylene oxide)*	*PEO*	*773[1]*	*70-112[2],-60[6]*	*99-171[2] 60[6]*

WORK CITED

1. Baker R (2000) *Membrane Technology and Application, 2nd addition,* John Wiley & Sons LTD
2. Chu R. (2012) *Examination of Membrane Filtration market,* Frost & Sullivan
3. Parmesan C., Yohe G.(2011) *A globally coherent fingerprint of climate change impacts across natural systems,* Patterson Laboratories, University of Texas
4. Rosenzweig C, Peart R, Glyer D. (2010) *Global climate change and US agriculture* Nature 345, 219-224
5. Rozelle P. (2008) *Carbon Capture and Gasification Technologies* National Energy Technology Laboratory 685, 103-155
6. Ciferno J., Fout T. (2009) *Capturing Carbon from Existing Coal-Fired Power Plants* American Institute of Chemical Engineering 583, 33-41
7. Kanniche M, Jaud P., Bouallou C., (2009) *Pre-combustion, Post-combustion and Oxy-combustion in thermal power plant for CO_2 capture* Applied Thermal Engineering ATE 2806
8. Parchy M. (2007) *Comparative study of Post- and Pre-combustion decarburization* Department of business enterprise and regulatory reform No 314 BERR/PUB URN 08/775
9. Colin F. Alie (2004) *CO_2 Capture with Mea: Integration the absorption process and steam cycle of an existing Coal-Fired Power Plant* Thesis University of Waterloo, Ontario Canada
10. Zhang X (2011) *Efficient Regeneration of Physical and Chemical solvents for CO_2 capture* University of North Dakota progress report
11. Junjun Y., Qin Changlei, An Hui, Wenqiang Liu (2012) *High-temperature pressure swing adsorption process for CO_2 separation* Energy and Fuels, 26 1: 169-175
12. Stephanie Burt, Andrew Baxter, Larry Baxter (2010) *Cryogenic CO_2 capture to control climate change emissions* Sustainable energy solutions *58 2: 85-93*
13. Tuinier M.J., Kramer G.J. Kuipers J.A.M. (2010) *Cryogenic CO_2 capture using dynamically operated packed beds* chemical engineering science 65: 114-119
14. Alizera A (2011) *Efficient Regeneration of Physical sorbent for CO_2 capture* University of North Dakota progress report
15. Suzanne Shelly (2009) *Capturing CO_2: Membrane Systems Move Forward* American Institute of Chemical Engineering 3: 42-47
16. Brunetti A., Scura F. Drioli E. (2010) *Membrane technologies for CO_2 separation* Journal of Membrane Science 359: 115-125
17. Powell C.E., Qjao G.G. (2005) *Polymeric* CO_2/N_2 *separation membranes for the capture of carbon dioxide from power plant flue gases* Journal of Membrane Science 279:1
18. Langsam M. (1996) *Polyimides for gas separation* Plastics Engineering 36: 697
19. Sarma Kovvali, K.K. Sirkar, (2000)*Dendrimer Liquid Membranes: CO_2 separation from gas mixtures,* Ind. Eng. Chem. Res 40(11), pp:2502-2511

20. Kovvali A.S., Chen H., Sirkar K.K. (2001) *Dendrimer membranes: a CO_2 selective molecular gate* Journal of American Chemical Society 122: 7594
21. Kovvali A.S., Sirkar K.K (2001) *Dendrimer liquid membranes: CO_2separation from gas mixtures* Industrial Engineering and Chemistry Research 40: 2502
22. Hu Q., Marand S., Dhingra D., Fritsch J., Wen G. (1997) *Poly(amideimide)/TiO_2 Nano-composite gas separation membranes: fabrication and characterization* Journal of membrane Science 135: 65
23. Zimmerman C.M., Singh A., Koros W.J. (1997) *Tailoring mixed matrix composite membranes for gas separation* Journal of membrane Science 137: 145
24. Mahajan R., Koros W.J. (2000) *Factors controlling successful formation of mixed-matrix gas separation materials* Industrial Engineering and Chemistry Research 39: 2692
25. Hirayama Y., Kase K., Nozomu T., Kusuki K. (1999) *Permeation properties to CO_2 and N_2 of poly(ethylene oxide)-containing and cross-linked polymer films* Journal of Membrane Science 160: 87
26. Lin H., Freeman B.D. (2005) *Membrane Materials to remove co2 from gas mixtures* Journal of Molecular Structure 739: 57
27. Nijimeijer T., Potreck J., Kosinski T., Wessling M. (2009) *Mixed water vapor/gas transport through the rubbery polymer PEBAX* Journal of Membrane Science 338:11
28. Bounaceur R., Lape N., Roizard D., Favre E. (2006) *Membrane processes for post-combustion carbon dioxide capture: a parametric study* Energy 31:2556
29. Baker R.W. (2008) *Recent developments and future directions in membrane modules* Proceedings of 12th Aachener membrane colloquium October 29-30,
30. Konietzny R, Editor (2010), *Pervaporation and Gas Permeation,* Heinrich Heine Universitat Dusseldorf
31. Dawson Robert, Stockel E., Holst James, Cooper Andrew (2011) *Microporous organic polymers for carbon dioxide capture* Energy Environment Science 4: 4239-4245
32. Chern, R. T., W. J. Koros, H. B. Hopfenberg and V. T. Stannett, (1985) *Material selection for gas separations using membranes*, ACS Symposium Series No. 269: Materials Science of Synthetic Membranes, Ed. by D. R. Lloyd, American Chemical Society, Washington DC, Chapter 2
33. Shairvnatar M., (2010) *Membrane Separation and technology, Research Reviews* Technology & Media Vol 13 pp.: 265-631
34. J.A. Nollet, Hippolyte-Louis Guerin and Louis-Francios Delatour, (1748) *Lecons de physique experimentale*, Paris
35. Nollet J.A., (1779) *Recherches sur les causes du bouillonnement des liquides*, Histoire de l'Académie Royale des Sciences, Paris, pp.: 57–104
36. Ruckstuhl, A. (1951) *Thomas Graham's study of the diffusion of gases*, Journal of Chemical Education, pp: 594-596
37. Frommer, M.A., (1972) *Reverse Osmosis Membrane Research*, Lonsdale, H.K. and Podall, H.E., EDs., Plenum Press, New York, pp.85-110

38. Mulder, M. (1991). *Basic Pinciples of Membrane Technology,* Dordrecht: Kluwer Academic Publisher Group.
39. Frommer, M.A., (1972) *Reverse Osmosis Membrane Research*, Lonsdale, H.K. and Podall, H.E., EDs., Plenum Press, New York, pp.85-110
40. Kammermeyer K., (1957) *Silicone rubber as a selective barrier*, Ind Eng. Chem 49 pp: 1685.
41. Frommer, M.A., (1972) *Reverse Osmosis Membrane Research*, Lonsdale, H.K. and Podall, H.E., EDs., Plenum Press, New York, pp.85-110
42. Koltuniewicz Andrzej (2008) *The History and state of art in membrane Technologies* Wroclaw University of Technology
43. Lipnizki F., Hausmanns G., (2000) *Hybrid Processes in Biotechnology Chemical Engineering Technology 23, 7: 569-577*
44. J.G. Wijmans , R.W. Baker (1995) *The solution-diffusion model: a review*, Journal of Membrane, Science Vol 107, pp1-21
45. K. W. Boddeker, Editor, (1995) *The early History of Membrane Science: Selected papers*, Journal of Membrane Science, 100, 1
46. Konietzny Roman (2010) Image of Solution-Diffusion Model Institut Fur Organische Chemie Und Makromolekulare Chemie
47. Mulder, M. (1991). *Basic Pinciples of Membrane Technology,* Dordrecht: Kluwer Academic Publisher Group.
48. Rik van der Lingen, (2006) Dendrimers and application in future membrane devices" Journal of Membrane Vol 54., pp: 326-335
49. Scheibert Emery (2010) Image of PAMAM Dendritech Inc.
50. Esfand Roseita, Tomalia Donald (2001)*Poly(amidoamine) (PAMAM) dendrimers: from biomimicry to drug delivery and biomedical applications* Drug Discovery Today 6,8: 427-436
51. Hartmut, Bruschke, (1995) *Industrial application of membrane separation processes,* Vol 67 issue 6 pp:993-1002
52. K.W. Boddeker and G. Bengston, (2008) *Pervaporation membranes separation processes,* Ed. By R.Y M. Hang. Elsevier, Amsterdam 437 – 460, 1991.
53. V.Y. Dindore, D.W.F. Brilman, F.H Geuzebroek, G.F. Versteeg, (2004) *Membrane-Solvent selection for CO2 removal using gas-liquid contactors*, Separation and Purification Technology 40(2), pp: 133-145
54. Zhan Xia, Li Ji-ding, Huang Jun-qi, Chen Cui-xian (2010) *Pervaporation properties of PDMS membranes cured with different cross-linking reagents for ethanol concentrations from aqueous solutions* Chinese Journal of Polymer Science 24, 4: 533-542
55. Senthilkumar U., Reddy B.S.R. (2007) *Polysiloxanes with pendent bulky groups having amino-hydroxyl functionality: Structure-permeability correlation* Journal of Membrane science 292: 72-79
56. Ashworth A.J., Brisdon B.J., England R., Hodson A.G.W., Watts A.R. (1995) *The permeability of carbon dioxide and methane in poly(organosiloxane) membranes*

containing mono- and di-ester functionalities Journal of Membrane Science 101: 109-115
57. Jiang D.D. (2000) *Cross-linker effects on PDMS Permeability* Polymer Degradation and Stability 68:75-82
58. Senthilkumar U., Reddy B.S.R. (2003) *Structure-gas separation property relationships of non-ionic and cationic amino-hydroxyl functionalized poly(dimethylsiloxane) membranes* Journal of Membrane Science 232: 73-83
59. Prado L.A., Sforca M., Oliveira Adriana. (2008) P*oly(dimethylsiloxane)networks modified with poly(phenylsilsequioxane)s: Synthesis, structural characterization and evaluation of the thermal stability and gas permeability* European Polymer Journal 44: 3080-3086
60. Kosaraju P., Kovvali A.S., Korikov A., Sirkar K.K., (2005) *Hollow Fiber Membrane contactor based on* CO_2 *absorption-stripping using novel solvents and membranes* Industrial Engineering Chemistry 44: 1250-1258
61. Mitsui Chemicals Inc. *Polyethersulfone(PES) Technical Literature 2004*
62. R Bounaceur, N Lape, D Roizard, C Vallieres, E Favre, (2005) *Biogas, membranes and carbon dioxide capture, Journal of Membrane Science Vol 328, Issue 1-2 pp:11-14*
63. Rik van der Lingen, (2006) Dendrimers and application in future membrane devices" Journal of Membrane Vol 54., pp: 326-335
64. Jianhua F., Kidetoshit K., Ken-ichi O., (2001) *Gas permeation properties of hyperbranched polyimide membranes,* Journal of Membrane Science, Vol 182 pp:245-256
65. Jianhua F., Kidetoshit K., Ken-ichi O., (2001) *Gas permeation properties of hyperbranched polyimide membranes,* Journal of Membrane Science, Vol 182 pp:245-256
66. Sarma Kovvali, K.K. Sirkar, *Dendrimer Liquid Membranes: CO2 separation from gas mixtures,* Ind. Eng. Chem. Res 40(11), pp:2502-2511
67. Junichiro Hayashi, Masatake Yamamoto, Katsuki Kusakae, Sigeharu Morooka, (1995), *Simultaneous Improvement of Permeance and Per selectivity of 3,3,4,4,-Biphenyltetracarboxylic Dianhydride-44-Oxydianiline polyimide membrane by carbonization*, Ind. Eng. Chem. Res, 34, pp: 4364-4370
68. Liguang Wu, Jiangnan Shen, Congjie Gao, (2008), *Permeation of CO2 and CH4 through a 2-(N,N-dimethyl amino) ethyl methacrylate and acrylonitrile copolymer membrane*, Desalination 223, pp: 410–416
69. K Kamalesh, G Lewandowski, D Knox, L Axe, R Luo "*Immobilized liquid membranes for facilitated transport and gas separation"* Dissertation